PREDICTING THERMAL DEFORMATIONS DURING ROLL FORMING OF THERMOPLASTIC MATRIX COMPOSITES

by

Corey Lynam

A THESIS SUBMITTED IN PARTIAL FULFILLMENT OF
THE REQUIREMENTS FOR THE DEGREE OF

MASTER OF APPLIED SCIENCE

in

The College of Graduate Studies

(Mechanical Engineering)

THE UNIVERSITY OF BRITISH COLUMBIA
(Okanagan)

April 2011

Abstract

Thermal deformations that occur during the manufacturing processes of long fibre reinforced composite have been a continued challenge for manufacturers. These deformations can be difficult to predict due to the complex thermal and mechanical behaviour of composite laminates. This thesis examines the fundamental mechanisms that lead to a final part shape to be different from the original mould shape. While the discussion is framed around a comingled polypropylene and E-glass thermoplastic matrix composite as well as a roll forming manufacturing process, it is also relevant to the wider group of thermoplastic matrix composites and their manufacturing methods. A methodology is developed that can be used to characterize the thermal mechanical behaviour of the laminate, optimize the manufacturing process controls and predict the magnitude of thermal deformations. It was found that, for the case of roll forming of comingled polypropylene and E-glass laminates, process controls should be optimized first so that crystallization of the matrix material occurs at the ideal position along the forming line. Once the process is optimized, thermoelastic modeling methods should give an adequate prediction of the thermal deformations. However, for other manufacturing processes and for other materials, a complete thermoviscoelastic process model may be required in order to yield accurate predictions. Ultimately, the methodology presented in this study can be used by thermoplastic matrix composite manufacturers to reduce the time and cost associated with developing the manufacturing process of a new component by reducing the need for trial and error iterations of process controls and tooling geometries.

Table of Contents

List of Tables

List of Figures

Acknowledgements

I would like to begin by expressing my sincere gratitude to my supervisor Dr. Abbas Milani for his guidance, support and encouragement throughout my thesis project. Dr. Milani's genuine enthusiasm and dedication to my work has been inspirational and his constant support has been greatly appreciated.

There are several people who contributed to this research and components of my thesis who I would like to extend my thanks: I am grateful for the insight, guidance and technical advice from Dr. David Trudel-Boucher at NRC-IMI in Boucherville, QC. I would also like to acknowledge Dr. Martin Bureau for providing me with the facilities to conduct material testing as well as Ms. Manon Plourde for her guidance using the test frames at NRC-IMI. In addition, I would like to express my thanks to Mr. Hossein Borazghi for providing test material as well as access and insight into his manufacturing facility at AS Composites Inc in Pointe-Claire, QC. I would also like to sincerely thank Mr. Borazghi for contributing to my financial support by sponsoring my industrial NSERC-MITACS scholarship. Furthermore, I would like to thank the members of the composites group at UBC in Vancouver for their technical advice and also for providing stress relaxation tests.

Finally, this thesis would not have been possible without the financial assistance I received from the Natural Sciences and Engineering Research Council of Canada (NSERC) and from Mathematics of Information Technology and Complex Systems (MITACS) through their industrial post graduate scholarship program.

Dedication

I dedicate this thesis wholeheartedly to my wife Bri Howard. She is my greatest inspiration in all of my life's endeavours. I am so grateful for her incredible love, guidance and support. I am very lucky to be able to share the rest of my life with her.

1 Introduction

Thermoplastic matrix composites have attracted an increasing market share in a number of applications in leading industries such as aerospace, automotive and construction. Developments in fabricating new composite architectures as well as new, rapid forming processes have allowed thermoplastic matrix composites to be competitive alternatives to thermoset composites. Commercial materials, such as Twintex®, are designed to overcome the relatively high viscosity of thermoplastic polymers at processing temperatures. In its initial fabric form, continuous glass fibres are commingled with continuous polypropylene (PP) fibres in bundles, which are then woven into a fabric. By commingling the polypropylene and glass fibres in each yarn, diffusion distances of the matrix are reduced and, therefore, lower cycle times and pressure can be used. New composite manufacturing processes have also been developed that take advantage of these types of materials. Among others, roll forming is a continuous manufacturing process which has been recently implemented in industrial settings. In roll forming, unconsolidated laminates of a thermoplastic composite (here Twintex®) are continuously passed through an oven and a series of compaction rollers. The oven heats the material above the melting temperature of polypropylene, then several pairs of rollers compact the laminate and distribute the melted polypropylene throughout the fabric. As the material cools below the crystallization temperature of the matrix, it consolidates into its final hard form. This thermoplastic matrix composite material and roll forming manufacturing process combination can demonstrate several advantages over traditional thermoset matrix composites. These include higher production rates, process automation, lower costs, higher impact toughness and simpler manufacturing processes. There are also reduced health and safety concerns when forming thermoplastic composite materials, since there is no release of volatile organic compounds.

Thermal deformations can occur during the manufacturing process of thermoplastic matrix composites where the final part shape is different than the original tool shape (in the case of roll forming, different than the shape of the final set of rollers). Typically, these deformations are in the form of 'spring-in', where the included angle between two surfaces on the part is smaller than the angle of the tool. These deformations can be significant for large components, in assemblies and/or when strict dimensional tolerances are required. Spring-in is primarily due to the anisotropic thermal properties of the composite and the thermal cycle during the manufacturing process. The current practice in industry is to use "rule of thumb" compensations on the mould (tool) shapes based on previous experience. Typical compensations range from 1º – 2.5º. As a result, several iterations of tooling geometries are needed before a final part can be produced within acceptable tolerances. In turn, these tooling iterations can add a significant cost to the process development phase of a new product and/or prevent it from being financially feasible. The ultimate goal of the present study is to create a predictive model of the spring-in for a roll forming process so that few, if any, trial and error iterations of tooling are needed.

This study begins in Chapter 2 with a detailed description of thermoplastic composite materials and their manufacturing methods as well as a comprehensive overview of the mechanisms that lead to spring-in. Chapter 3 provides a literature review of currently published work in the field of thermoplastic spring-in modeling. Chapter 4 presents the results of material property testing conducted within this study. Chapter 5 describes an example case of a roll forming process and presents the results of spring-in angle measurements. Chapter 6 describes the finite element modeling technique used in this study and discusses the significance of the model results. Finally, Chapter 6 summarizes all of the results and recommendations.

2 Background

2.1 Thermoplastic Matrix Composite Materials

Continuous fibre reinforced polymer (CFRP) composite materials can be categorized in two groups based on the matrix material. The first group is thermoset matrix composites, which is comprised of thermosetting polymers as the matrix material. The matrix is formed during the manufacturing process of the end use component by an irreversible chemical curing reaction of two parts: a resin and a hardener. The advantage of this group is that the resin and hardener have a relatively low viscosity in their un-reacted liquid state; it is relatively easy for the resin and hardener mixture to diffuse into a fabric of reinforcement material. In addition, since the cure reaction takes an appreciable amount of time after mixing and is typically thermally activated, there is sufficient time to assemble the part before cure. During cure, the glass transition temperature of the matrix material evolves from a very low value to a high value so that the final material is in a solid glassy state. One advantage of a high glass transition temperature after cure is that thermoset matrix composite materials can often be used at temperatures above their cure temperature in service.

The second group of CFRP is the thermoplastic matrix composites, comprising of thermoplastic polymers as the matrix material. The thermoplastic polymer material is formed in a step prior to the end use component manufacturing step and can typically take the form of a solid sheet, tape or fibres. A thermoplastic polymer will soften and melt with the application of heat, then crystallize and harden when cooled. When processing a thermoplastic composite material, the matrix is heated above its melting temperature, allowed to diffuse into the reinforcement and

then cooled below its crystallization temperature. The challenge in processing thermoplastic composite parts is that the matrix material has a much higher viscosity in its melted state than a pre-cure thermoset matrix. It typically requires higher pressure and higher temperature to process a thermoplastic matrix composite material. In service, the composite cannot be used at temperatures that approach the processing temperature since the matrix will soften and re-melt. However, there are reduced health and safety concerns when forming thermoplastic composite materials, since there is no chemical cure and therefore no release of volatile organic compounds.

The most common reinforcement materials for both thermoplastic matrix and thermo set matrix materials are: glass fibres, carbon fibres and aramid fibres. Given any of these reinforcement materials, a thermoplastic matrix composite will typically a have higher toughness and higher impact resistance while a thermoset matrix composite will have a higher maximum operating temperature, as well as a small strength and stiffness benefit. Traditionally, thermoset matrix materials have dominated CFRP composite industries due to their relative ease in manufacturing. However, with improvements in the manufacturing techniques of thermoplastic matrix composites, an increasing number of industries have been adopting thermoplastic matrix composites as an alternative.

2.1.1 Twintex®

The material used in this study is a thermoplastic matrix composite with the trade name Twintex®, commercialized by St. Gobain Vetrotex. It is a continuous fibre composite with constituents of a polypropylene matrix (40%) and E-glass fibre reinforcements (60%). It is produced in a woven fabric form with a balanced 2 X 2 Twill weave pattern, has a specific

weight of 1492 g/m^2 (44 oz/yd^2) and a nominal thickness of 1mm (0.04in) per lamina after consolidation. In order to overcome the manufacturing challenge as described above (namely the high viscosity of the melted matrix during processing) the polypropylene is initially in fibre form and is comingled with the glass fibres in every fibre bundle (yarn). Figure 2-1 shows how this pre-comingling of the two composite constituents reduces the diffusion distances for the melted matrix and helps the matrix penetrate each bundle and surround the glass fibre strands. With reduced diffusion distances, lower pressure is required to produce a composite part with a low void content (Borazghi, Boucher, Denault, & Fisa, 2008).

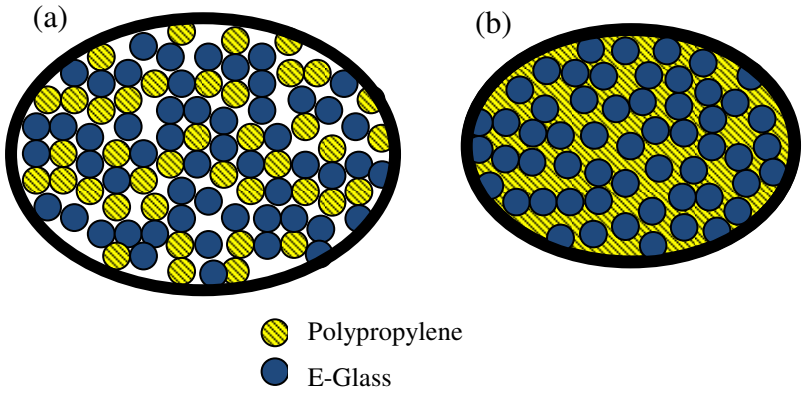

Figure 2-1 Schematic of a cross section of a pre-consolidated (a) and consolidated (b) Twintex® bundle

The glass transition temperature of the polypropylene in Twintex® is around -15^{o}C and the melting temperature is around 163^{o}C (see DSC results in Section 4.3). Since the glass transition temperature is below room temperature, the material will show viscoelastic behaviour even at room temperature. With a melting temperature of 163^{o}C, the applications of Twintex® are limited to lower temperatures. However, being based on E-glass and the commodity polymer polypropylene, Twintex® has a very low material cost and is generally very competitive for low, room and modest temperature applications. Some of these applications include: vehicle door

panels, helmets and protective armour, small wind turbine blades, as well as residential building materials. For higher temperatures and more demanding applications there are other thermoplastic polymers that can be substituted for polypropylene usually at an increased material cost.

2.1.2 Crystallization in Polypropylene

Fundamental to any manufacturing process model of Twintex® is an understanding of the crystallization process of the polypropylene matrix material. The isotactic polypropylene in Twintex® is a linear polymer, such that propylene monomers (C_3H_6) are linked in long chains through covalent bonds. At temperatures above the melting temperature, these chains are arranged in an irregular amorphous structure. If the polymer is cooled very quickly, the amorphous arrangement of molecular chains can be frozen in place due to van der Waals' forces. However, at slower cooling rates, the molecules will align themselves into their lowest energy state, which is a regular crystal formation. This crystallization process in thermoplastics occurs by repeated stacking of individual molecular chains. A single molecular chain can fold back onto itself many times within a crystal or extend between two adjacent crystals. Crystallization can occur to various degrees such that the microstructure is a certain combination of amorphous and crystalline zones. The polypropylene in Twintex® is typically described as a semi-crystalline material.

Crystals form in a radial direction from a central nucleus such that the microstructure contains an array of spherulites as shown in Figure 2-2. Nucleation of stable spherulites is a diffusion-based process, as it requires the displacement of polymer chains. Thus, the nucleation

process takes a certain amount of time before free growth of the crystals can begin. Free growth of the crystals will continue until the spherulites impinge on one another. Secondary crystallization process can then occur at sites other than those originating at the nuclei. However, secondary crystallization is slower and occurs at lower temperatures. Due to the nucleation and growth process, the crystallization kinetics and the degree of crystallinity will depend strongly upon the rate of cooling. Even after secondary crystallization, the final microstructure will always contain some amorphous zones. It is, therefore, not possible to have a 100% crystalline microstructure.

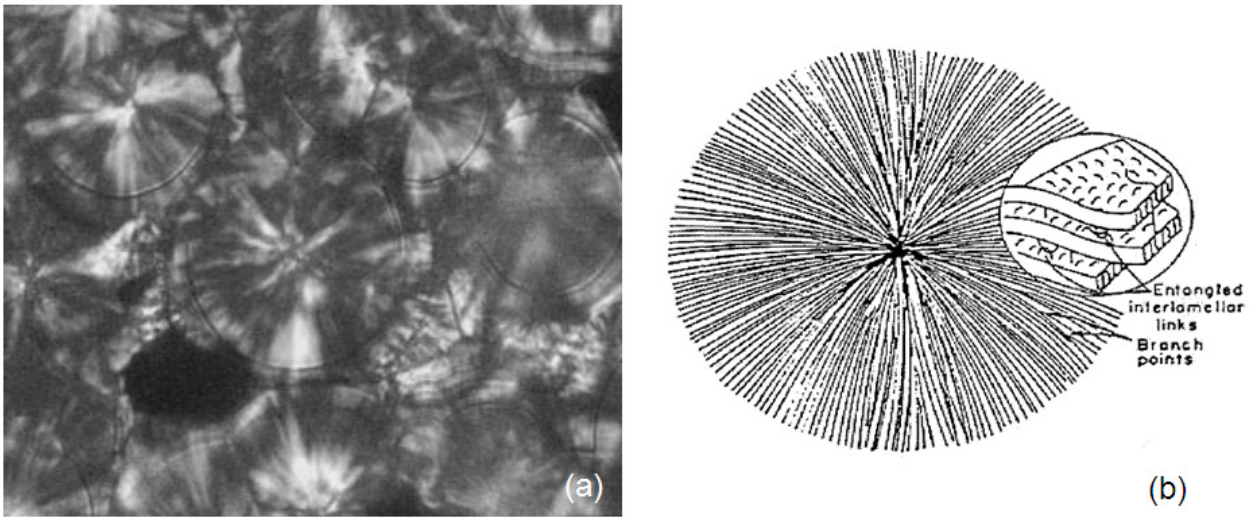

Figure 2-2 (a) Micrograph of polypropylene (Tian, Yu, & Zhou, 2007) and (b) Scematic of a spherulite (Advani & Sozer, 2003)

2.2 Thermoplastic Matrix Composite Manufacturing Methods

In order to transform a pre-consolidated fabric of Twintex® into a rigid part, the laminate must be heated above the matrix material's melting temperature then cooled below its crystallization temperature. To reduce void content and to form the laminate to a desired shape, this thermal cycle is done along with the application of pressure. There are several

manufacturing methods that can be applied to Twintex®. The most common processes are compression moulding, vacuum bag and autoclave, roll forming and stamp forming. Each of these methods are described in the following sections.

2.2.1 Compression Moulding

The most commonly used manufacturing process for thermoplastic matrix materials is the compression moulding process. In compression moulding, the composite laminate is compressed between a male and female mould pair. The moulds are pre-heated to a temperature above the melting temperature of the matrix material by circulating oil or electrically, as shown in Figure 2-3. The laminate is loaded in to the mould cavity and the mould pair is closed. Pressure is applied with a hydraulic or pneumatic piston and held for a specified amount of time. The entire assembly then cools to room temperature together. Compression moulding tooling can be expensive due to the required heating channels, but is generally more cost effective than using an autoclave to reach high pressures. Process times are typically greater than half an hour depending on the laminate thickness. Sufficient time must be given for voids and air pockets to diffuse to the edges of the laminate. The surface finish on both sides of the laminate is very good due to the prolonged contact with the mould surfaces.

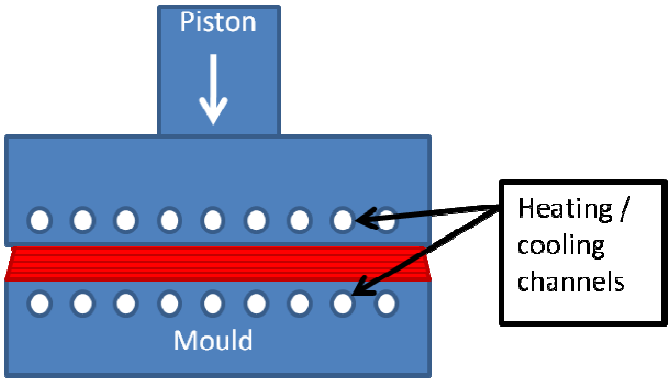

Figure 2-3 A schematic of a compression moulding forming press

2.2.2 Vacuum Bag and Autoclave

Thermoplastic matrix composites can also be processed with a vacuum bag and autoclave technique. In this technique, the laminate is pre-formed over the mould using a vacuum bag and the assembly is processed inside an autoclave. The autoclave increases the applied pressure and cycles the temperature through the matrix melt region. Figure 2-4 shows an example of a female mould, where the laminate would be vacuum bagged to the mould. A typical thermal cycle within the autoclave is shown in Figure 2-5.

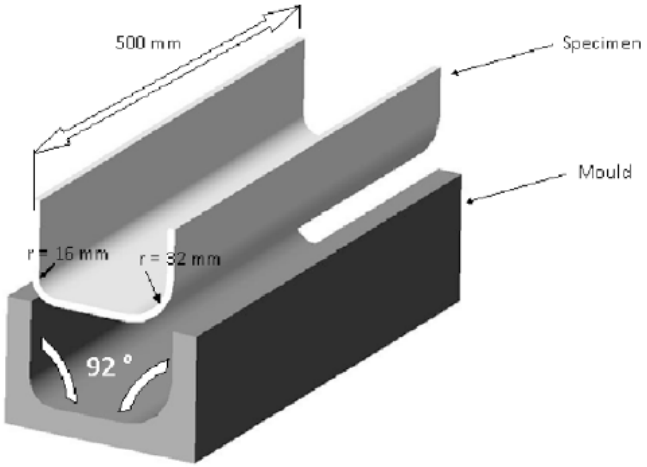

Figure 2-4 Compression moulding geometry of a U-shaped part (Salomi, Garstka, Potter, Greco, & Maffezzoli, 2008)

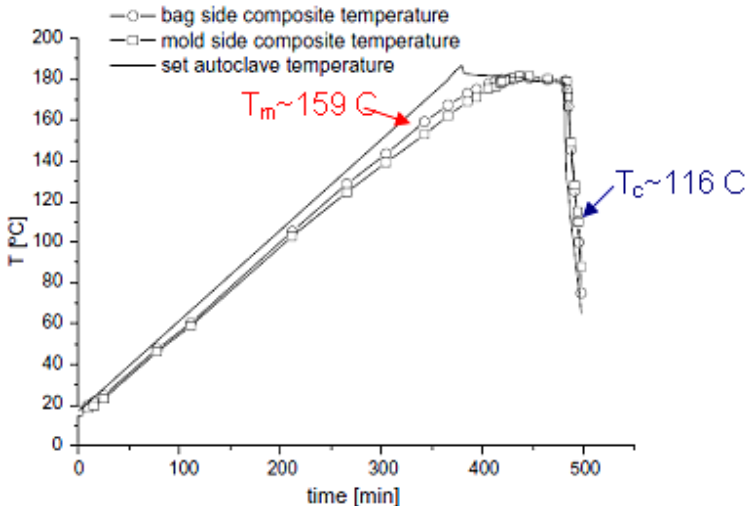

Figure 2-5 Compression moulding thermal cycle (Salomi, Garstka, Potter, Greco, & Maffezzoli, 2008)

The relatively long time scale for the thermal cycle in Figure 2-5 is a result of the high viscosity of the melted matrix material. Voids and air pockets that are trapped in the laminate during bagging must be given sufficient time to diffuse to the edges of the mould or the vacuum bag valves during this process. This required hold time at high temperature leads to a relatively low part production rate. While this may be the case, the material quality (based on a low void content, high strength and high stiffness) is very good with a vacuum bag and autoclave technique. Note that the surface finish on the mould side is better than on the bag side.

2.2.3 Roll Forming

Roll forming is a continuous manufacturing process that can be used with the Twintex® material to achieve very high production rates. In this process, unconsolidated laminas of Twintex® are continuously passed through an oven and a series of compaction rollers. Figure 2-6 shows the arrangement of a typical roll forming machine where two layers of Twintex® are being laminated. Depending on the desired process thermal cycle, small convection ovens can be placed between pairs of rollers. The temperature of the rollers can also be controlled with circulating oil or radiant heaters, which heat each roll pair directly. The geometry of components is limited to those with consistent cross sections in the longitudinal direction of the process, although the dimension in that direction is almost unlimited.

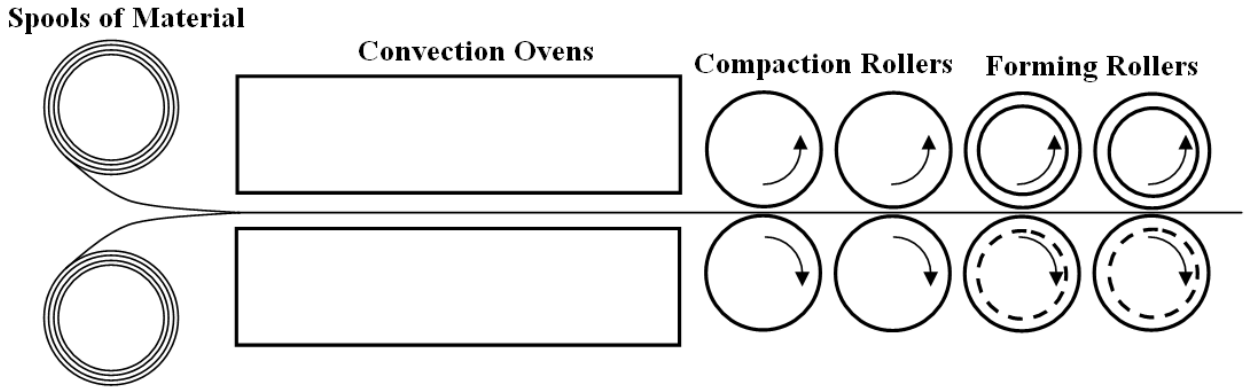

Figure 2-6 A schematic of a typical roll forming machine set up

Figure 2-7 shows a typical roll forming thermal cycle in terms of time and distance along the machine. This represents the temperature of a cross section of the laminate as it passes through the machine. The cycle is valid once the process has reached a constant line speed of 0.5 m/min and steady state temperatures. A significant advantage of the roll forming method is the reduction in the production cycle time. The thermal cycle in Figure 2-5, for an autoclave, is on the order of hundreds of minutes and leads to a production rate around 1 part per 8 hours. The thermal cycle in Figure 2-7, for roll forming, is on the order of minutes and if we assume a part size of one meter, a line speed of 0.5 m/min will lead to a production rate of 1 part every two minutes, which is a significant improvement over an autoclave. This reduction is attributed to the directional squeeze out of voids in the laminate. Unlike autoclaves, which apply uniform pressure and rely on self diffusion of voids to the edges of the laminate, the roll forming process drives voids out of the laminate in a directional manner. When the laminate is subjected to high pressure as it passes under a pair of rollers, there are pressure free zones immediately adjacent to the rollers. It is this pressure gradient that drives voids into the low pressure zone behind the compaction rollers. The primary roll of each of the compaction rollers is to sequentially reduce

the percent void content so that, at the last roller stage, crystallization can occur with as few voids as possible.

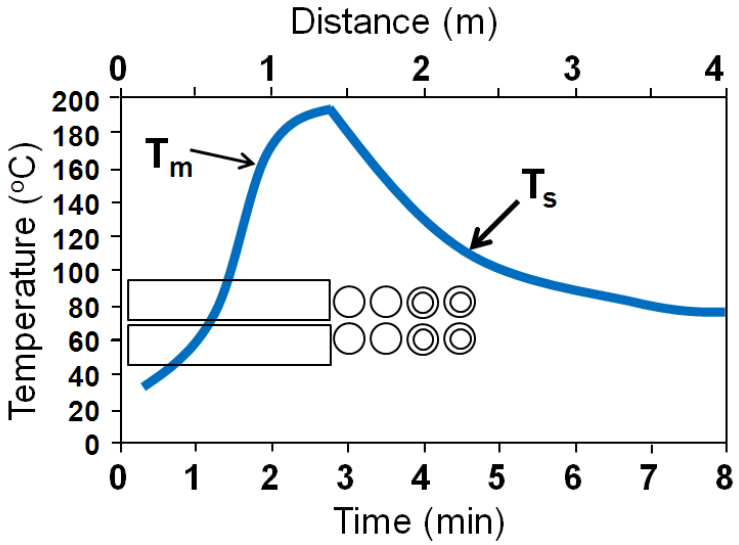

Figure 2-7 A typical roll forming thermal cycle (at 50 mm/min)

In roll forming, the laminate is only under pressure as it passes through a pair of compaction rollers. If the geometry of the compaction roller and laminate are taken as in Figure 2-8 with an initial laminate thickness of 'h_i', roller radius 'R', roller gap 'g' and line speed '*v*', the length of contact can be calculated using the following:

$$L_C = \sqrt{R^2 - \left(R - \frac{h_i - g}{2}\right)^2} \qquad \text{Equation 2-1}$$

The amount of time of compaction (t_c) can be found by:

$$t_c = {}^{L_C}/_{v} \qquad \text{Equation 2-2}$$

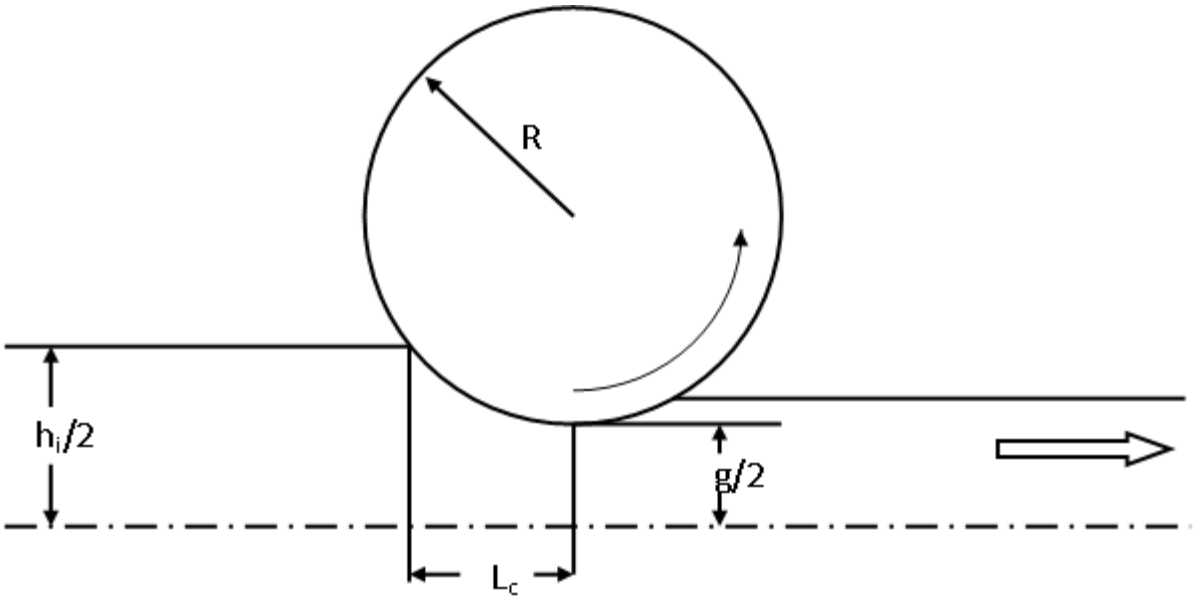

Figure 2-8 Geometry of compaction roller (Borazghi, Boucher, Denault, & Fisa, 2008)

Borazghi, Boucher, Denault, & Fisa, 2008, investigated the consolidation and void content of flat plates of Twintex® produced by the roll forming method. They found that an optimal roll gap sequence should start at 50% of the unconsolidated laminate thickness and subsequent gaps should not be so small that there is lateral squeeze out of the resin. Smaller roll gaps lead to squeeze flow of the resin which can detrimentally alter the fibre structure. They also found that slower line speeds and higher oven temperatures lead to a lower final void content. This is due to a lower matrix viscosity and longer times in contact with the rollers. Table 2-1 shows the compaction at each of the four stages of the roll forming process used in the investigation where a final void content of less than 4% was achieved. For the process considered in Table 2-1, four layers of 44 oz/yd^2 Twintex® were laminated.

Table 2-1 Optimized roll forming stage gaps for 4 layers of 44oz/yd^2 Twintex®, using a line speed of 0.5 m/min and an inlet temperature of 195 ^oC
(Borazghi, Boucher, Denault, & Fisa, 2008)

Process Stage	1st rollers	2nd rollers	3rd rollers	4th rollers
Roll Gap – g (mm)	4.50	4.10	3.85	3.85
Sample Thickness – h (mm)	6.30	4.97	3.96	3.92
Void Content (%)	29.0	11.5	5.3	3.9
Compression Length – L_c (mm)	2.6	1.8	1.3	0.4
Compaction Time – t_c (s)	3.2	2.2	1.6	0.5

The majority of current applications of roll forming in industry are limited to the fabrication of flat plates and sandwich structures. However, the roll forming method can be applied to produce non flat cross sections if the final two stages of rollers are replaced with forming rollers, as shown in Figure 2-6. The forming rollers should be the final roller stage since crystallization of the matrix occurs as the material passes the last roller. The same optimized roll forming cycle and process controls developed by Borazghi, Boucher, Denault, & Fisa, 2008, for a low void content can be used when forming non flat cross sections.

Dykes, Mander, & Bhattachatyya, 2000, have performed experimental analyses into the roll forming of non flat sections. They used a five stage roll forming machine to produce U-channel sections and characterized the deformed shape of the laminate as it enters the forming roller stage. Figure 2-9 and Figure 2-10 show the characteristic shape adopted by the laminate. The shape is divided into three regions: region A, where the laminate is undeformed; region B, where the laminate is deformed, but not in contact with the roller; and region C, where the laminate deforms while in contact with the roller. It was found that at forming temperatures above the melting temperature of the matrix, virtually no transverse bending takes place until the

sheet comes into contact with the first forming roller stage. When in contact with the roller, the sheet deforms in a trellis shear like manner.

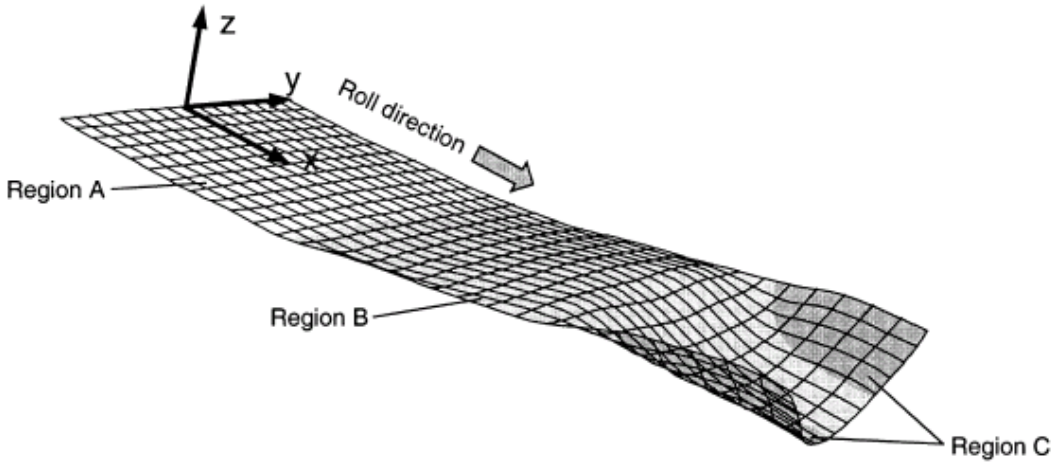

Figure 2-9 Characteristic shape of a laminate before entering the first stage forming rolls (Dykes, Mander, & Bhattacharyya, 2000)

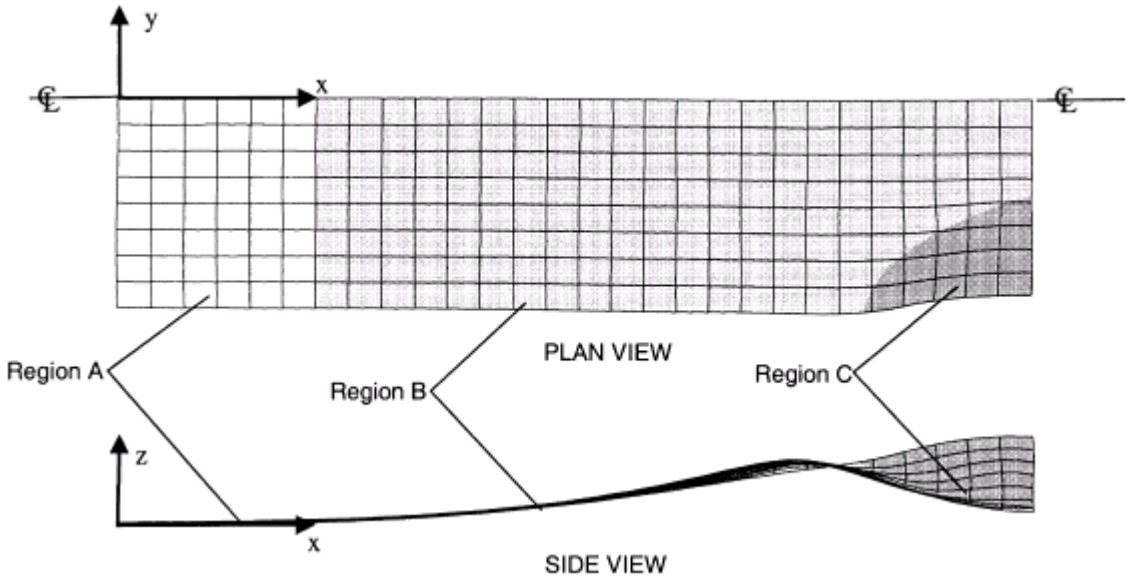

Figure 2-10 Characteristic shape of a laminate before entering the first stage forming rolls, plane and side view (Dykes, Mander, & Bhattacharyya, 2000)

2.2.4 Stamp Forming

Stamp forming is a manufacturing process that is often used with Twintex® when low costs and high production rates are required. In this process, a pre-consolidated flat sheet of Twintex® (which can be mass produced by roll-forming in an earlier step) is heated above the matrix melting temperature in an oven and quickly transferred to a pair of cold, usually room temperature, moulds. The moulds close on to the laminate while it is still at elevated temperature to form it to the desired shape. The stamping moulds are held until the laminate cools below the matrix crystallization temperature and then released off the laminate. Figure 2-11 shows typical displacement and force curves over time for the process. In a stamping press there are two stages in the process: a closing stage and a compression stage. In the closing stage, the moulds are closed onto the hot laminate rapidly until the gap distance is approximately equal to the initial (uncompressed) thickness of the laminate. In this step, the load builds gradually as the laminate conforms to the mould shape. Once the predetermined 'switch on' load is reached, the compression step of the process begins. In this step, the desired stamping pressure is built up slowly (typically over 3 to 5 seconds) and held for a hold period (typically 20 to 60 seconds) before releasing.

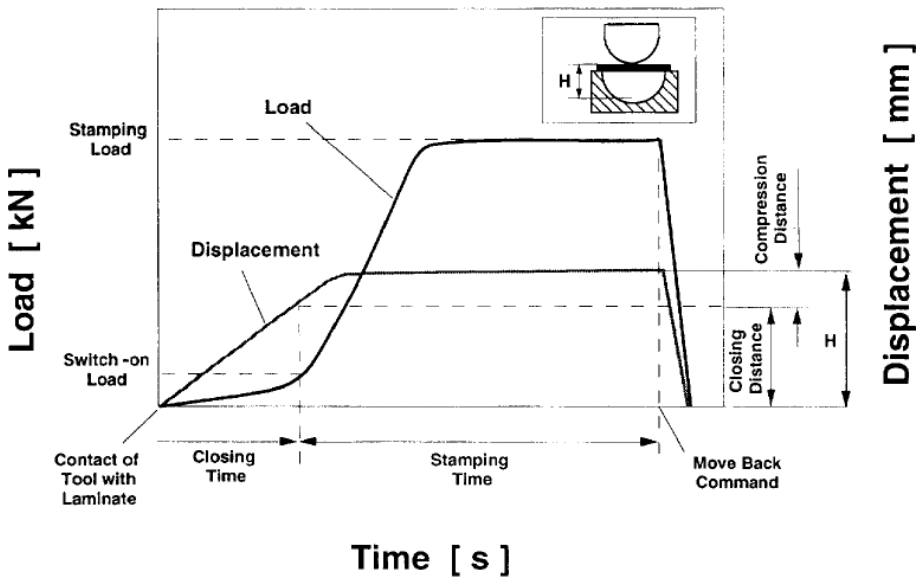

Figure 2-11 Typical load and displacement values in a stamp forming process (Friedrich & Hou, 1998)

There are notable similarities between the stamp forming process and the roll forming process. If a cross section of the laminate is followed as it passes through a roll forming process with an oven and a single forming stage, the treatment of the material will be very similar to that which is produced by the stamp forming process. In both processes, the laminate is heated above the matrix melting temperature in an oven before being quickly passed to the forming moulds. The close and open action of stamping a laminate is very similar to that of a laminate passing through a pair of rollers. In both methods, the process parameters are selected so that the material cools as it comes into contact with the forming moulds and crystallization occurs before it is released from the mould. In this way, stamp forming is often used as a test case for defining and optimizing a roll forming manufacturing process. Stamp forming moulds are less expensive to fabricate and easier to re-machine for dimensional corrections than forming rollers.

2.3 Spring-in

Spring-in of a composite laminate during its manufacturing process refers to distortions of the final part geometry when compared with the original mould shape. The term is derived from "spring-back" in sheet metal forming where an over compensation of desired bending angles are used to account for the elastic return of the material. In composites, the final part shape will contain smaller angles than the original mould shape, as shown in Figure 2-12, leading to the term: "spring-in". This spring-in is primarily due to the anisotropic thermal properties of the composite and the thermal cycle during the manufacturing process. The current practice in industry is to use "rule of thumb" compensations based on previous experience. Typical compensations range from 1 – 2.5^{o}. These deformations can be significant for large components, in assemblies or when strict dimensional tolerances are required.

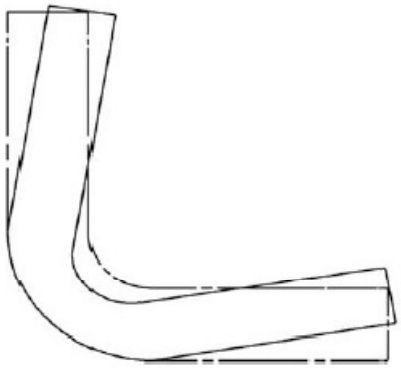

Figure 2-12 Spring-in after cooling a L-section composite (Salomi, Garstka, Potter, Greco, & Maffezzoli, 2008)

2.3.1 Spring-in Mechanisms

The primary mechanism that leads to the spring-in of composite materials during their manufacturing process is the anisotropy of thermal properties, as well as, the thermal cycle that they are subjected to. This mechanism for spring-in of thermoplastic composites was first described by O'Neil & Spencer in 1988. However, in 1991, Barnes, Byerly, LeBouton, & Zahlan identified up to six second order mechanisms that also contribute to deformation of the laminate and affect the final spring-in angle. Each of these mechanisms contributes to the final part shape being different from the original mould shape. These mechanisms are applicable to any manufacturing process for thermoplastic composites, although some mechanisms can have more or less dominance for certain manufacturing methods. The following is a summary of the current understanding of the mechanisms that lead to spring-in of thermoplastic composites:

2.3.1.1 Anisotropic Thermal Properties

The effect of anisotropy of thermal properties on spring-in was first described by O'Neil, Rogers & Spencer in 1988. This mechanism is the dominant driving force for the spring-in of composite materials during manufacturing. The mechanism is based on the anisotropy of thermal expansion in a composite laminate. Due to the architecture of a continuous fibre reinforced composite, the thermal expansion in either of the fibre directions will be dominated by the thermal expansion of the reinforcement material. Similarly, the thermal expansion in the through thickness direction will be dominated by the thermal expansion of the matrix material. For Twintex®, the coefficient of thermal expansion in the fibre plane is typically 1.79×10^{-6} mm/mm·^{o}C and the coefficient of thermal expansion in the through thickness direction is

typically 1.92×10^{-4} mm/mm·°C (Saint-Gobain-Vetrotex, 2005). There is a two order of magnitude difference between the coefficients of thermal expansion in the fibre plane and through the thickness of the material.

During the manufacturing process of a thermoplastic composite, the thermal history of the matrix material starts at the crystallization point. As it cools to room temperature there is an anisotropic volume change according to the thermal expansion values given above. For a flat sheet, this anisotropic volume change will not lead to any deformation since the laminate is able to contract independently in each direction and the difference of expansion in each direction has no effect. However, when the laminate is formed into a curved shape and is cooled to room temperature, the anisotropic thermal expansions will lead to an additional dimensional distortion. Given orthotropic expansion properties, O'Neil presented the following equation to predict the amount of deformation (O'Neill, Rogers, & Spencer, 1988):

$$\Delta\theta = \theta_0(\alpha_t - \alpha_p)(T_s - T) \qquad \text{Equation 2-3}$$

Where $\Delta\theta$ is the difference between the mould shape and the part shape (spring-in angle), θ_o is the initial angle (mould shape), α_t and α_p are the through thickness and in plane coefficients of linear thermal expansion respectively, T_s is the crystallization temperature (or "start temperature") and T is the current temperature (taken as room temperature to find the final shape).

Equation 2-3 is valid for an orthotropic material that is cooling without physical constraints from a high to low temperature and is accurate in that case. In industry, however, this equation does not accurately represent what is seen from the majority of manufacturing

processes. There are many factors that are present in a composite manufacturing process that are not considered in Equation 2-3, which is based solely on orthotropic thermal properties. For example, it does not include interactions between the material and surrounding tooling or allow for a temperature gradient in the material. It also assumes an instantaneous crystallization temperature and uses linear coefficients of thermal expansion through the entire temperature range. For these reasons, Equation 2-3 has not been generally accepted in the thermoplastic composites industry as a sufficient prediction of spring-in angle. The anisotropy of thermal properties remains the primary driving force for spring-in. However, for real processes, Equation 2-3 can be an oversimplification of the complex thermal and mechanical influences on the final part shape.

2.3.1.2 Asymmetric Thermal Gradients Through the Thickness

Thermal stress gradients through the thickness of the laminate that are present during the manufacturing process of a composite material can lead to a deformation of the final laminate. This mechanism is applicable to both flat and curved section parts and is due to asymmetric cooling of the laminate. In vacuum bagging, for example, when the laminate is moulded to a single sided steel tool, there will be different cooling rates for the laminate near the nylon bag as opposed to the laminate near the steel tool. Since the tool has a higher thermal capacity than the circulating air near the nylon bag, the matrix material near the bag will cool faster and crystallize first. On the tool side, the matrix material will cool slower and crystallize last. At the point in time when the tool side of the laminate crystallizes, the material near the nylon bag will be at a lower temperature and have already thermally contracted to some extent. The remaining thermal contraction to room temperature on the bag side will be less than that on the tool side. This will

lead to a mismatch of the thermal strains through the thickness of the laminate at room temperature. When constrained in the vacuum bag, tensile stresses develop near the tool side and compressive stresses develop near the bag side. Figure 2-13 shows the stress distribution in the laminate after cooling to room temperature, but before removing the vacuum bag. After removal from the bag and mould, the laminate will deform by bending towards what was the tool side. For non-flat tools, symmetric cooling will lead to spring-back on a female tool and spring-in on a male tool.

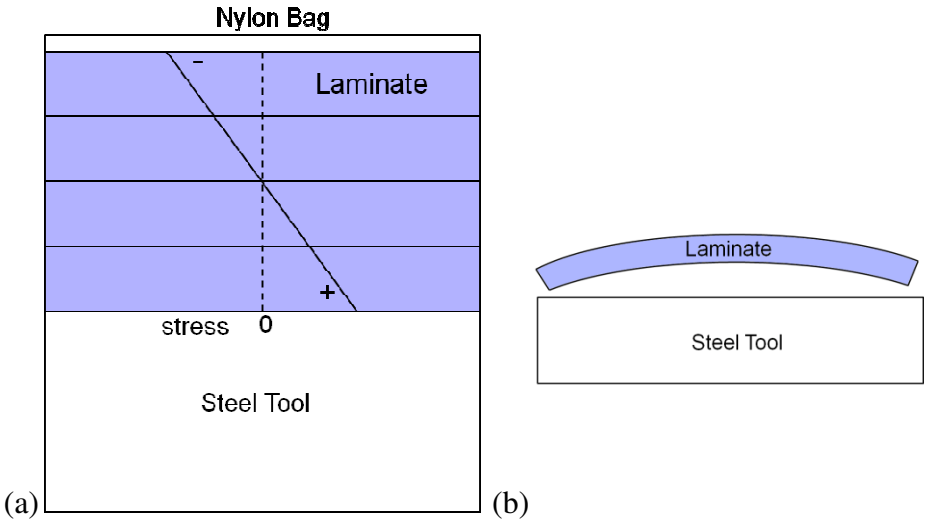

Figure 2-13 (a) Stress distribution and (b) deformation due to asymmetric cooling

It should be noted that the deformation due to a thermal stress gradient is only present when there is asymmetric cooling. If both the top and bottom moulds are made of the same material and the cooling is symmetric, there will be no deformation from this mechanism. In the case of roll forming, where both the upper and lower rollers are made of the same material and have the same temperature, this mechanism should not contribute to the deformation. In practice, the manufacturer will continually adjust processing parameters to avoid any curvature in what are intended to be straight sections.

2.3.1.3 Local Matrix Rich Regions

One of the challenges in producing complex shapes in thermoplastic matrix composites is to avoid local matrix pooling in the corner sections of the part. Processing parameters should be optimized by the manufacturer to ensure an even distribution of the matrix in the composite. A resin rich region in the corner of a thermoplastic laminate will change the local material properties and increase the thermal expansion through the thickness. Figure 2-14 shows micrographs of a resin rich corner section and the increase in spring-in angle.

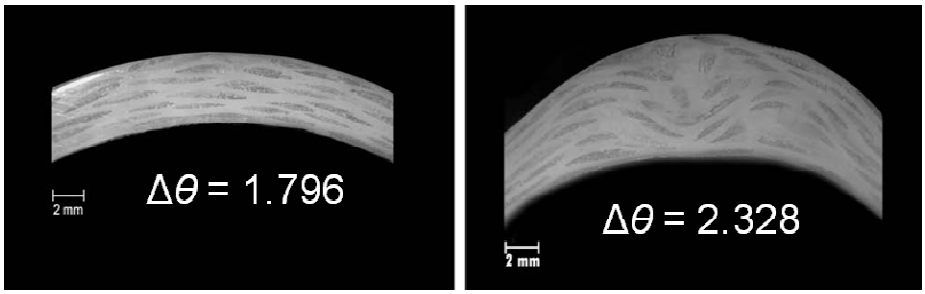

Figure 2-14 Spring-in angle of a matrix rich corner section (Salomi, Garstka, Potter, Greco, & Maffezzoli, 2008)

2.3.1.4 Pre-Crystallization Modulus Development

The polypropylene used in Twintex® is a semi-crystalline material such that the microstructure contains regions of both crystalline and amorphous polypropylene. When heated above its melting temperature, the polypropylene will have a completely amorphous, melted microstructure. As the material cools below its melting temperature the microstructure of the supercooled polypropylene remains amorphous until the beginning of the crystallization process (nucleation). The majority of thermoplastic composite process models assume that prior to crystallization, there is no modulus development and that the crystallization point represents the

point at which the material can begin to develop a thermal mechanical stress history. It is, however, possible for a semi-crystalline material such as Twintex® that the pre-crystallization, supercooled, amorphous material may begin to develop a modulus. In this temperature range (between the melting temperature and the crystallization temperature), any internal stresses that develop will likely be relaxed quickly due to viscous flow. Nonetheless, it is possible that a pre-crystallization modulus development can have a small impact on the final spring-in angle.

2.3.1.5 Crystallization Shrinkage

Typically in thermoset composite process modeling, the spring-in angle is attributed to a combination of anisotropic thermal properties (similar to Section 2.3.1.1) and cure shrinkage. For thermoplastic matrix composites it is intuitive to consider crystallization shrinkage in the place of cure shrinkage. However, thermoplastic composite process models typically ignore the effects of crystallization shrinkage due to the high viscosity of the matrix during crystallization. For thermoset materials, there is a change of the glass transition temperature during cure. It will evolve from a very low temperature to a temperature often above the processing temperature. As a result, the post-cure material is in a glassy state with a high elastic modulus. For thermoplastic materials, there is no cure reaction and there is no change to the glass transition temperature. As such, the material is always well above its glass transition temperature during processing. For the polypropylene in Twintex®, the glass transition temperature is around -15ºC (Saint-Gobain-Vetrotex, 2005). It is often argued that at processing temperatures well above the glass transition temperature, the material behaviour will be very viscous and any stresses that may develop due to crystallization shrinkage will be relaxed almost instantaneously (Sunderland, Yu, & Manson, 2001). For the purpose of this study, crystallization shrinkage is not considered. However, some

recent stress relaxation testing (shown in Section 4.5) has revealed the possibility of a pre-crystallization modulus development which could have an elastic component, albeit very small. It will be part of future work within the composites group at UBC to further investigate the modulus development and the duration of stress relaxation around the crystallization point.

2.3.1.6 Stress Relaxation of Constrained Components

As described above, thermoplastic composite materials will behave viscoelastically during their manufacturing process. When the thermoplastic matrix material is raised above its softening and melting temperature, there is a large amount of viscous flow. As the material crystallizes and cools, it will continue to behave viscoelastically until it reaches a temperature below its glass transition temperature, after which it can be considered elastic. With a glass transition temperature around -15º, it is expected that Twintex® will behave viscoelastically at all processing temperatures even as the material cools to room temperature.

There are two primary sources of stress in the composite material during the manufacturing process: one is due to the constraint of the laminate with the tool and the other is due to the mismatch of thermal properties between the composites matrix and reinforcement constituents. Both sources will contribute to viscoelastic changes of the stress and strain state over time.

In any manufacturing processes for thermoplastic composites, the laminate is constrained over the mould for a certain amount of time. In compression moulding and vacuum bagging, the laminate is constrained by the vacuum bag or the pair of moulds for the entire thermal cycle until

it is disassembled. In roll forming and stamp forming, the laminate is only constrained for a short period of time while either the rollers or the stamp moulds are in contact with the material. This constraint of the laminate will lead to internal stress development since anisotropic thermal properties of the composite laminate provide a driving force for spring-in deformation. Figure 2-15 shows the stress distribution of a U-shaped composite formed on a male tool. Compressive stresses develop in the inner radius and tensile stresses develop on the outer radius of the corner sections.

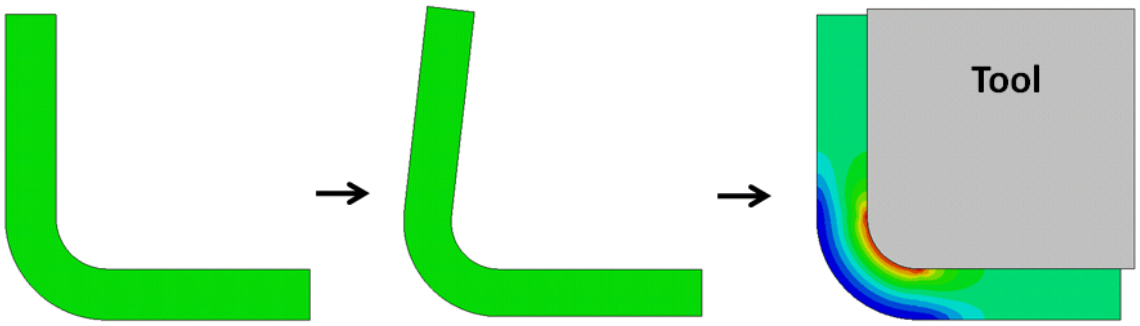

Figure 2-15 Internal stress developent due to constraint with tooling (Lynam & Milani, 2010)

The stresses shown in Figure 2-15 will relax viscoelastically depending on the viscoelastic properties of the matrix material and the amount of time that the laminate is in contact with the tool. This stress relaxation should reduce the amount of spring-in compared to the unconstrained or elastic case. This mechanism causes the spring-in angle to depend upon the cooling rate in the process, as well as the amount of time that the laminate is constrained by the tool. For compression moulding and vacuum bagging, the cooling rate is relatively slow and the laminate is in contact with the tool for a long time period. As such, this mechanism is expected to have a large impact during compression moulding or vacuum bagging of Twintex®. For roll forming and stamp forming, the cooling rate is very fast and the laminate is in contact with the

tool for a short time. This mechanism is not expected to have a large impact during roll forming or stamp forming.

2.3.1.7 Viscoelastic Relaxation of Internal Stresses

The second source of internal stress in the composite laminate during the manufacturing process comes from the mismatch of thermal properties of the matrix and reinforcement constituents. This mismatch leads to the development of internal residual stresses as the component cools from the process temperature to room temperature. This mechanism accounts for a viscoelastic stress relaxation in the matrix constituent.

Figure 2-16 shows a schematic of the effect of the mismatch of thermal properties of the composite constituents as it cools from the processing temperature. Upon cooling from the consolidation temperature, the matrix and the reinforcement must deform together despite coefficients of linear thermal expansion that can be two orders of magnitude apart. Irrespective of the geometry, this creates tensile stress in the matrix and compressive stress in the fibres. The equilibrium condition is held since the stress in the matrix and the fibres are equal with opposite signs. If we then consider a viscoelastic stress relaxation of the matrix material, the stress in both the matrix and the fibre will reduce (approach to zero) together. Despite the fact that the reinforcement material is elastic in this temperature range, it will undergo a stress reduction as a result of the condition of equilibrium with the matrix. This stress reduction in the reinforcement causes a slight extension of the fibres since all surfaces are free to deform after removal from the mould. An extension of the fibres around a corner radius will lead to a small increase in the spring-in angle.

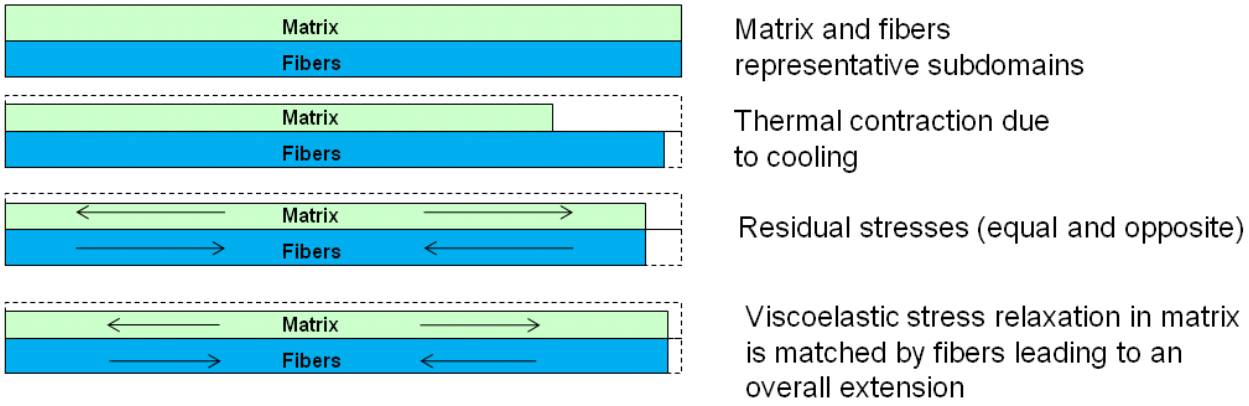

Figure 2-16 Schematic of viscoelastic stress relaxations of the matrix leading to an overall elongation of a composite (Lynam & Milani, 2010)

3 Literature Review

3.1 Thermoplastic Spring-in Modeling

The first description of spring-in deformations in thermoplastic matrix composites was done by O'Neill, Rogers and Spencer in 1988. They derived an equation to predict the distortions produced in the moulding of laminated channel sections as they cool (Equation 2-3:$\Delta\theta = \theta_0(\alpha_t - \alpha_p)(T_s - T)$). This equation was developed by solving the stress-strain equations of elasticity for an orthotropic, linear thermoelastic solid in conjunction with appropriate boundary conditions for a curved section that is free to deform (zero stress solution). It gives the change in the angle between any two cross sectional normals (centre line of the laminate) as a function of: the original angle, the in-plane and through thickness coefficients of thermal expansion, and the change in temperature. Equation 2-3 is significant in that it gives the primary driving force from spring-in. Note that Equation 2-3 is independent of the laminate thickness and the corner radius. It can, therefore, be applied to any pair of surfaces on a complex shaped part.

In 1991 Barnes, Byerly, LeBouton and Zehlan noted that with the development of manufacturing processes with higher forming and cooling rates, such as stamping, the induced distortions do not necessarily follow the simple form as described by O'Neill, Rogers and Spencer. They investigated the effects of different cooling rates and asymmetric thermal distributions on the final spring-in deformations and identified the presence of residual stresses. Most significantly, Barnes, Byerly, LeBouton and Zehlan discuss a number of second order mechanisms that can lead to the final part shape being different than what is predicted by Equation 2-3. These second order mechanisms ware described in the following sections: Section

2.3.1.2 Asymmetric Thermal Gradients Through the Thickness, Section 2.3.1.3 Local Matrix Rich Regions, and Section 2.3.1.6 Stress Relaxation of Constrained Components. While these mechanisms were recognised in the literature, a model had not yet been proposed to improve on Equation 2-3.

Equation 2-3 is very similar to the Radford model (Radford & Rennick, 2000), which is commonly used in predicting spring-in angles for thermoset matrix composites. The Radford model assumes that spring-in is only due to the anisotropic thermal properties and the matrix cure shrinkage. In the case of thermoplastic matrix composites, since there is no curing reaction, crystallization shrinkage would take the place of cure shrinkage. However, since thermoplastics behave much more viscously at processing temperatures, crystallization shrinkage is often neglected from spring-in angle predictions (Sunderland, Yu, & Manson, 2001).

Salomi, et al. 2008, expanded Equation 2-3 by including non-linear (or temperature dependant) thermal expansion. They assumed a linear dependence of the through thickness coefficient of thermal expansion on temperature such that:

$$\alpha = A + B(T - T_g) \qquad \text{Equation 3-1}$$

Where A and B are coefficients found by linear regression of experimental thermal expansion data. The in-plane coefficient of thermal expansion is assumed to be zero, since it is two orders of magnitude smaller than the through thickness coefficient. The derived equation with temperature dependant thermal expansion is as follows:

$$\Delta\theta = \theta_0\left(1 - \exp\left[\left(A - BT_g\right)\left(T - T_s\right) + \frac{B}{2}\left(T^2 - T_s^2\right)\right]\right) \qquad \text{Equation 3-2}$$

However, in order to achieve acceptable agreement between the predicted spring-in angle and measured experimental values, Salomi, Garstka, et al. 2008, had to add a correction term (α_c) to Equation 3-2 as follows:

$$\Delta\theta = \theta_0\left(1-\exp\left[\left(A-BT_g-\alpha_c\right)\left(T-T_s\right)+\frac{B}{2}\left(T^2-T_s^2\right)\right]\right) \qquad \text{Equation 3-3}$$

The need for this correction term underscores the fact that a complete predictive model for spring-in must include the second order mechanisms.

Recent efforts in the field of thermoplastic process modeling have been to build computational finite element (FE) models that can incorporate more of the second order mechanisms. The advantage of a finite element based model over closed form equations is that they can capture more completely the effect of anisotropic thermal properties, asymmetric thermal gradients, temperature dependant thermal expansion properties, as well as tool and part interactions. There have been several efforts to define finite element models which can capture the effect of stress relaxation in the laminate due to constraints with the tooling. This includes: Sunderland, Yu and Manson in 2001 and Kim, Bernet, et al. in 2002. These models use a fully coupled thermo-viscoelastic constitutive material model to track the viscoelastic stress relaxation processes. The finite element code modeled the intermediate part of the cooling cycle when the laminate is constrained in the mould, as a thermoviscoelastic material. The final part of the cooling cycle, when the mould constraint is removed, is modeled as a thermoelastic material. Kim, Bernet, et al. 2002, found that with fast cooling rates, the thermoviscoelastic model gives a similar prediction to Equation 2-3. At slower cooling rates, however, Sunderland, Yu and Manson 2001, showed that the stress relaxation mechanism becomes more significant.

4 Material Property Testing

Material property testing was performed on coupon sized samples at the National Research Council, Industrial Materials Institute (NRC-IMI) in Boucherville, Quebec. The performed tests included: uniaxial extension, thermal mechanical analysis (TMA), differential scanning calorimetry (DSC) and dynamic mechanical analysis (DMA). A set of stress relaxation tests using a DMA machine was performed by the composites group at UBC Vancouver. The purpose of the testing was to characterise the thermal and mechanical behaviour of Twintex® under the process conditions seen in roll forming. The results from each set of tests are summarised in the following sections.

4.1 Uniaxial Extension

Uniaxial extension tests were performed with an Instron 5582 tensile frame equipped with an oven chamber and 100kN load cell. Samples were cut in both the warp and weft directions (longitudinal and transverse directions) from a roll formed sheet of Twintex® made from 2 layers at 44 oz/yd^2 each. Sample geometry was the ASTM D3039 standard for balanced and symmetric composites, a rectangular 25mm x 222.3mm sample. Table 4-1 shows the test matrix. Tests were performed at room temperature, 80^{o}C and 120^{o}C. Above this temperature the matrix material becomes too soft for the sample to be held by the tensile grips without the fibres slipping and pulling out. Two repeats of each test were performed and two different stain rates were tested: 2mm/min and 100mm/min.

Table 4-1 Uniaxial extension test matrix

Material Direction	Temperature	Strain Rate	Number of Repeats	Total
Warp	20ºC	2 mm/min	2	12
		10 mm/min	2	
	80ºC	2 mm/min	2	
		10 mm/min	2	
	120ºC	2 mm/min	2	
		10 mm/min	2	
Weft	20ºC	2 mm/min	2	12
		10 mm/min	2	
	80ºC	2 mm/min	2	
		10 mm/min	2	
	120ºC	2 mm/min	2	
		10 mm/min	2	

The response of Twintex® to uniaxial extension tests in the warp and weft directions is dominated by the properties of the reinforcing fibres. No strain rate dependence was observed in the uniaxial extension tests, since E-glass is not rate dependant at this temperature range. A linear elastic response was observed with all of the uniaxial extension tests up until the point of failure. Figure 4-1 shows a group of failed samples with the dominating failure mode of fibre breakage in the gauge length. Table 4-2 and Figure 4-2 summarize the uniaxial extension results fit to a linear Young's modulus. At room temperature, both the modulus and the ultimate strength of the roll formed Twintex® show decreased values when compared to the typical compression moulded value. The latter values are given by the Twintex® supplier (Saint-Gobain-Vetrotex, 2005). There is also a difference in the modulus and ultimate strengths between the two material directions. The warp direction is the longitudinal direction in the roll forming process. The reduction in strength in the warp direction suggests that there is some amount of pre-loading applied to the material as a result of the directional nature of the roll forming process. Finally, temperature dependence is also apparent with a reduction of properties as temperature increases.

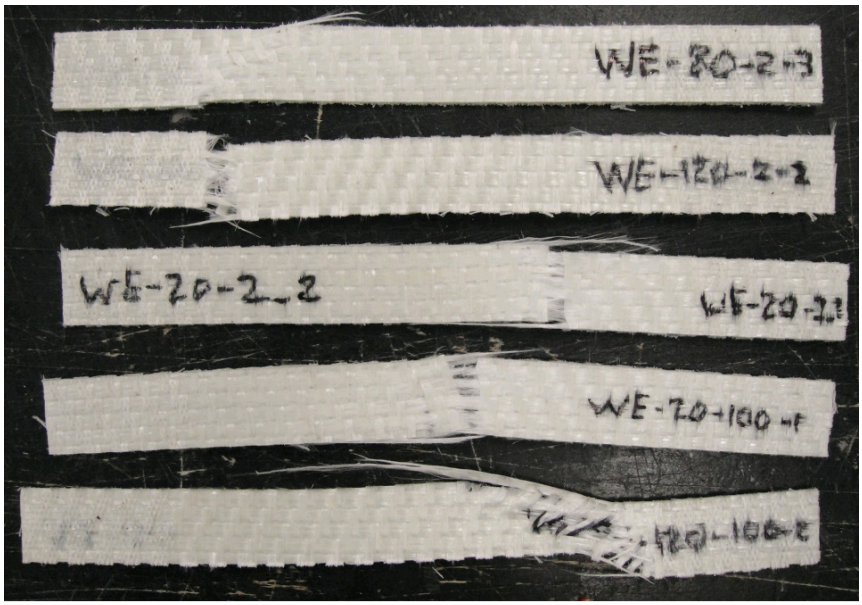

Figure 4-1 Uniaxial extension samples after failure

Table 4-2 Uniaxail extension results of roll formed samples compared to typical compression moulded samples ([1]Saint-Gobain-Vetrotex, 2005)

	Warp		Weft		Compression Moulded[1]	
Temperature (ºC)	**Modulus (MPa)**	**UTS (MPa)**	**Modulus (MPa)**	**UTS (MPa)**	**Modulus (MPa)**	**UTS (MPa)**
20	8638.41	184.47	10075.42	250.22	13380.00	287.62
80	7970.18	137.58	9730.42	240.58	-	-
120	5510.7	118.28	8740.22	209.78	-	-

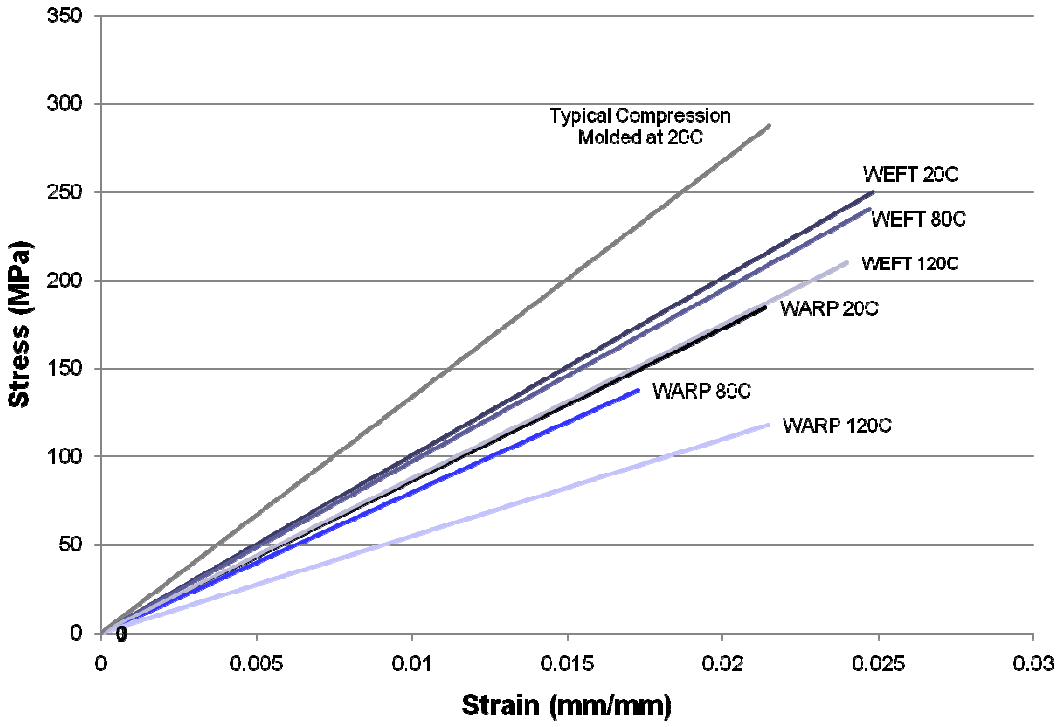

Figure 4-2 Uniaxial extension results of roll formed samples compared to typical compression moulded samples (Saint-Gobain-Vetrotex, 2005)

4.2 Thermal Mechanical Analysis (TMA)

The difference between the through thickness thermal expansion and the in-plane thermal expansion is the primary driving force for spring-in. In order to create a spring-in prediction model, accurate measurement of the thermal expansion properties is required. A Perkin Elmer TMA7 Thermal Mechanical Analyser (TMA) was used to measure the through thickness thermal expansion of roll formed Twintex® samples. The TMA machine measures the displacement of a probe on the surface of the sample across a temperature sweep. Figure 4-3 shows the probe displacement vs. temperature results of each of the three samples and Figure 4-4 shows the average coefficient of thermal expansion as a function of temperature. The TMA test was limited to a maximum temperature of about 135^{o}C. Above this temperature, softening of the matrix

material prevented accurate displacement measurements from the probe. Similarly, due to the softening of the material, TMA tests cannot be performed for the cool down cycle after melting. However, the proposed model will only use thermal expansion data from these TMA tests after the material cools below its crystallization point. After crystallization, the thermal expansion behaviour upon cooling is expected to be similar to the tested values upon heating. For the purpose of inputting to a user subroutine, a second order polynomial was fit to the average TMA results:

$$\alpha_t = -1.4459\text{x}10^{-08}\ T^2 + 5.0639\text{x}10^{-06}\ T - 5.5624\text{x}10^{-05} \qquad \text{Equation 4-1}$$

where α_t is the through thickness coefficient of thermal expansion and T in the temperature.

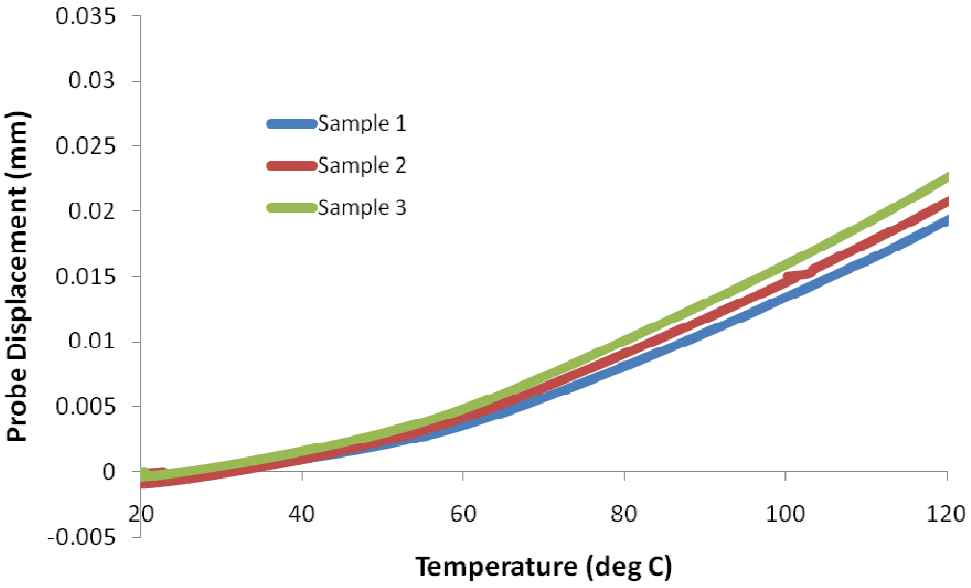

Figure 4-3 Through thickness thermal expansion of Twintex®

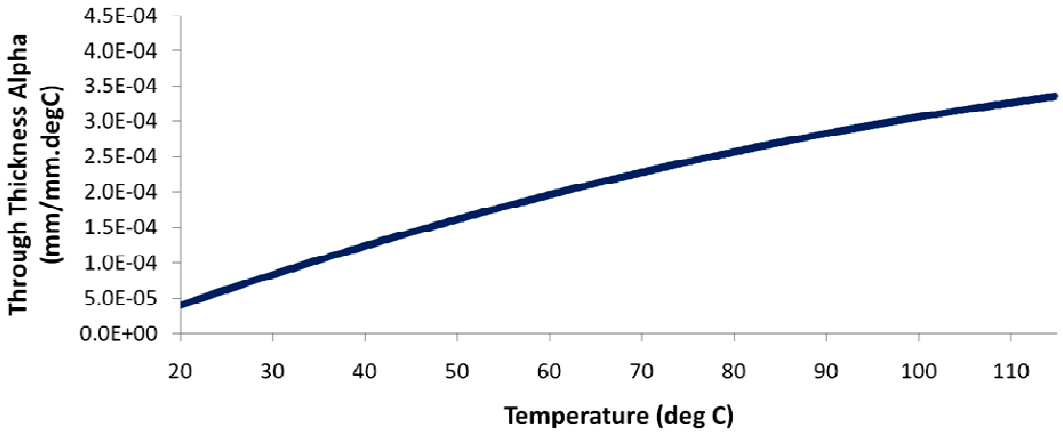

Figure 4-4 Coefficient of thermal expansion (alpha) in the through thickness direction of Twintex®

4.3 Differential Scanning Calorimetry (DSC)

Differential Scanning Calorimetry (DSC) is used to characterize the change of the microstructure of the matrix material during the manufacturing process. In the finite element model, the material properties will be defined uniquely for when the matrix material structure is amorphous and semi-crystalline. DSC results were used to measure the transition of the polypropylene from an amorphous melted structure to a semi crystalline structure. This transition defines when the material begins to be able to build up a thermal and mechanical history and is the start of spring-in development.

DSC is defined by ASTM E473 as a technique in which the heat flow rate difference into a substance and a reference is measured as a function of temperature, while the substance and the reference are subjected to a controlled temperature program. A reference must be used because the heat flow into or out of a sample cannot be measured directly. The sample and the reference are heated and/or cooled such that the sample follows a predefined temperature cycle. Then

based on the difference in temperature between the reference and the sample and known thermal properties of the reference, the heat flow into or out of the sample can be found indirectly.

DSC is commonly used to measure first and second order thermodynamic transitions. A transition is called first or second order when the first or second partial derivative of the free energy with respect to temperature or pressure shows a discontinuity. In polymers, first order transitions are: melting, crystal to crystal transitions (such as glass transition) and crystallization (Menczel & Prime, 2009). We can measure the changing structure of the matrix material by observing the crystallization process in the DSC. Crystallization will be measured by the amount of discontinuity of the first derivative of free energy with respect to temperature. In other words, in the case of DSC testing, crystallization appears as a deviation in a heat flow vs. temperature plot from a constant slope (see Figure 4-5).

Crystallization of a polymer consists of two steps: crystal nucleation and crystal growth. Crystal nucleation is the formation of stable embryonic crystallites of a minimum size where the crystal formation can begin to grow. Crystal growth is the subsequent increase in the crystallite size. Crystal nucleation is not an instantaneous process due to the required mobility of polymer chains and results in the phenomenon of supercooling. Figure 4-5 shows how the supercooling effect is observed with a DSC. There is an offset between the melting temperature upon heating and the crystallization temperature upon cooling when the test is done at a given heating and cooling rate. The crystallization point will change depending on the cooling rate. Theoretically, at very slow cooling rates, crystallization would occur at the same temperature as melting. As the cooling rate increases, crystallization occurs at lower temperatures than melting. Figure 4-6

shows the effect of different cooling rates on the DSC results for unreinforced polypropylene (Tian, Yu, & Zhou, 2007).

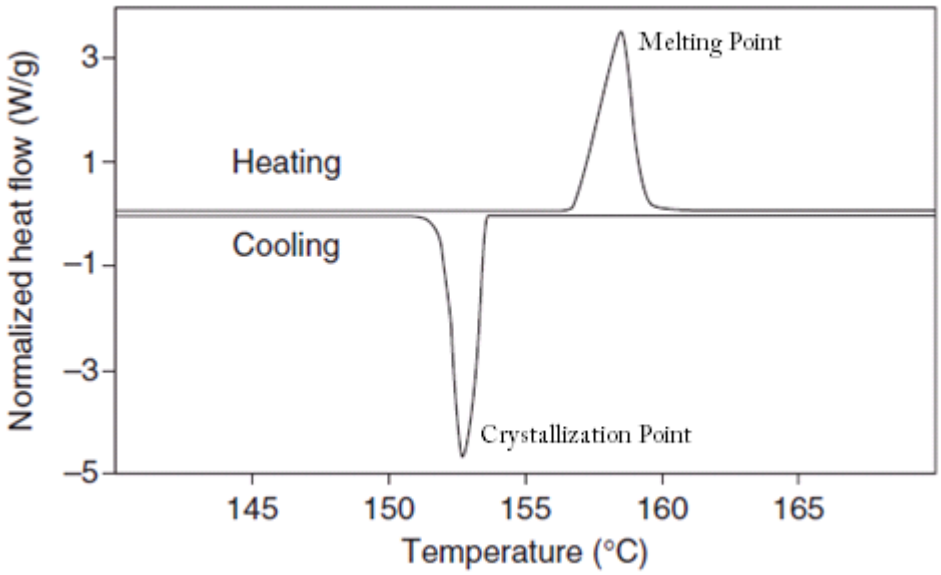

Figure 4-5 Typical DSC results at a heating and cooling rate of 10°C/min showing melting and crystalization points with supercooling (Menczel & Prime, 2009)

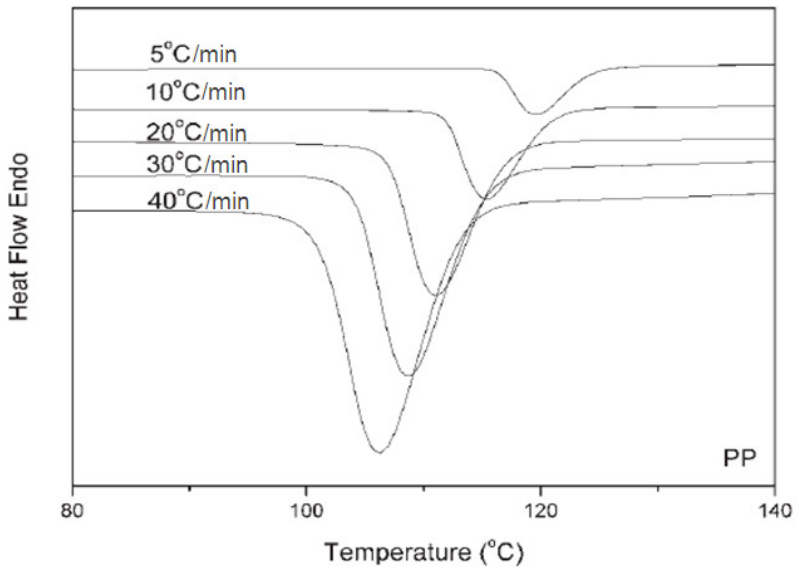

Figure 4-6 Typical DSC results for unreinforced polypropylene (Tian, Yu, & Zhou, 2007)

DSC tests were performed with a Perkin Elmer Pyris 1 machine on samples of Twintex® produced by the roll forming process. A complete characterization of the crystallization kinetics of Twintex® can be done by following the Avrami evaluation (Menczel & Prime, 2009). The Avrami evaluation requires a large number of DSC tests to be performed at a variety of linear cooling rates. A crystallization kinetics model can then be developed, which would describe crystallization of the polypropylene in Twintex® subjected to any arbitrary thermal cycle. Instead of performing multiple tests, which are required to build a crystallization kinetics model, a smaller number of DSC tests were performed on the actual, non linear, thermal cycle that is used in the roll forming process. Figure 2-7 shows the non-linear cooling cycle during roll forming. In this way, the results of the DSC tests are directly applicable to our application of interest and the crystallization point for the roll forming process can be found with confidence. The results, however, are only applicable to the specific material, manufacturing process and thermal cycle used in this project. Future work is planned to complete the characterization of crystallization of the polypropylene in Twintex® so that the approach developed here can be applied to a broader set of processing conditions. The thermal cycle used for the DSC tests is given in Table 4-3 and shown in Figure 4-7. Nine sections of linear, constant cooling rates are used to mimic a smooth cycle as required by the input of the DSC machine.

Table 4-3 Thermal cycle for DSC testing of roll formed Twintex®

Temperature Range	Rate (degC/min)
20-185	20
185-170	-21
170-160	-20
160-150	-19
150-140	-18
140-130	-17
130-120	-16
120-110	-10
110-90	-8
90-45	-6
45-20	-4

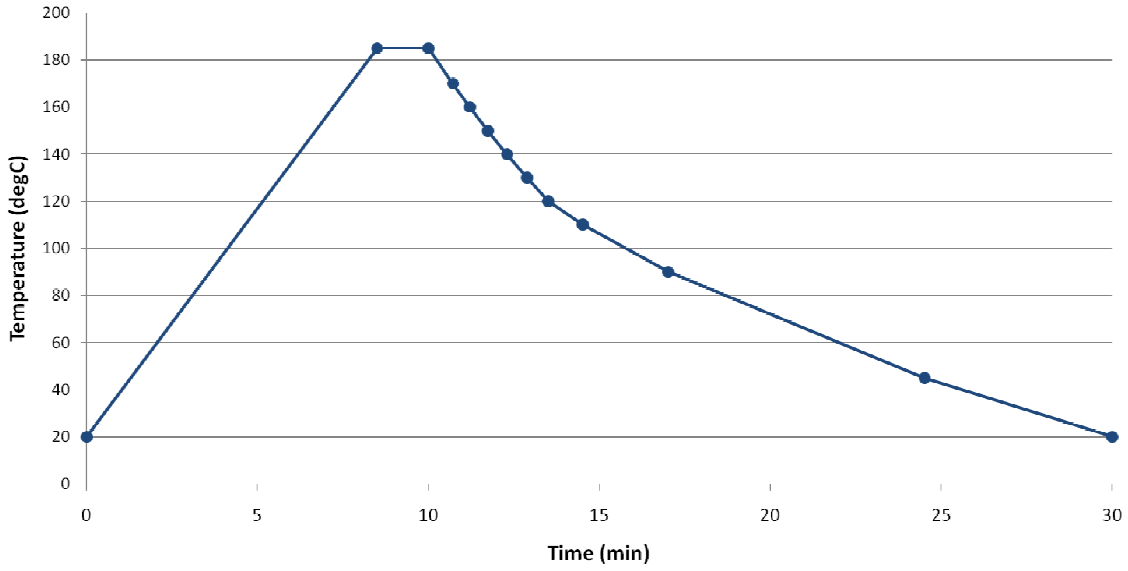

Figure 4-7 Thermal cycle for DSC testing of roll formed Twintex®

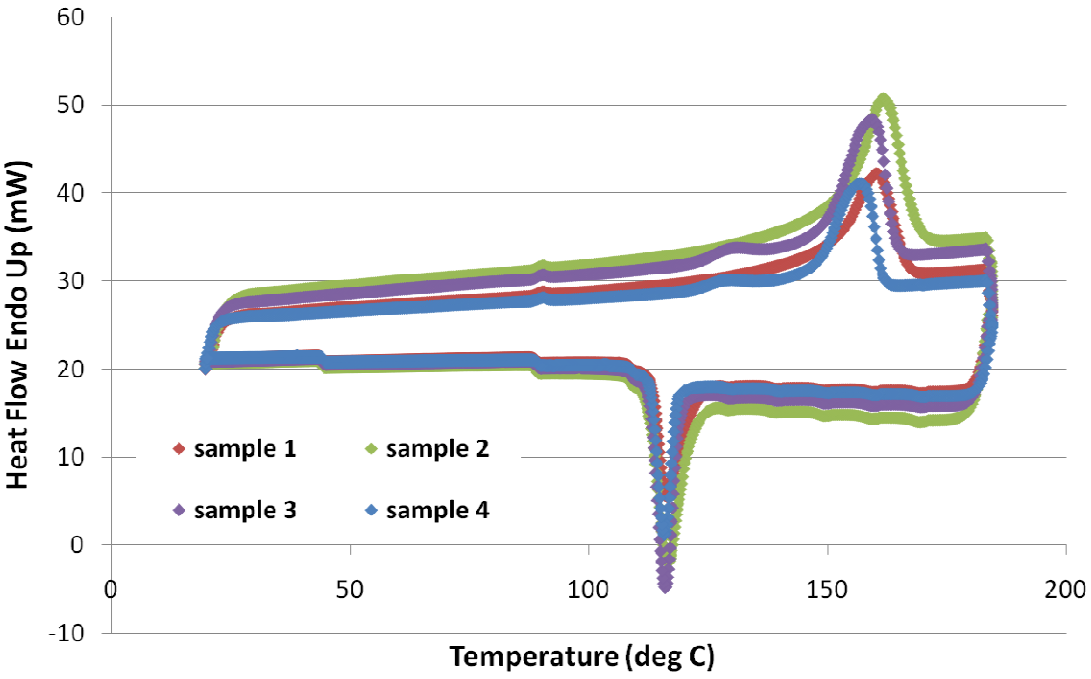

Figure 4-8 DSC results from four samples of Twintex®

Four samples were tested using the thermal cycle in Figure 4-7. Figure 4-8 shows the results from the DSC tests where the offset of the crystallization temperature due to supercooling is approximately 40°C. In the temperature range of the test (20°C to 180°C), polypropylene will undergo two first order thermodynamic transitions: melting upon heating and crystallization upon cooling. There is excellent repeatability of the four samples for the crystallization point. The average of the four samples is shown in Figure 4-9 for the crystallization peak only. Typically, the onset of crystallization is taken at the point shown in Figure 4-9. This onset temperature in Figure 4-9 would be taken as the start temperature (T_s) in Equation 2-3. However, for a more complete description of the crystallization kinetics, including how they develop over time and temperature, we define a new state variable for the relative crystallinity. The relative crystallinity is defined as equal to 0 when the matrix material is melted and the structure is amorphous (on the right hand side of Figure 4-9) and equal to 1 when the matrix material has

completed its transition to a semi-crystalline structure (on the left hand side of Figure 4-9). The transition from a relative crystallinity of 0 to 1 is then mapped using the deviation of the crystallization peak from a constant slope line (shown in Figure 4-9). The curve in Figure 4-10 is found by integrating the heat flow over temperature and then dividing it by the total integration. Therefore, the transition from an amorphous to a semi-crystalline matrix structure (relative crystallinity 0 to 1) in Figure 4-10 is developed based on the discontinuity of the first derivative of the heat flow with respect to temperature. It should be noted that a relative crystallinity of 1 does not imply a fully crystalline structure. Rather, it refers to the degree of crystallization reaching its maximum at the end of the first order transition. Later, second order transitions can also affect the degree of crystallization but in the context of spring-in, we are interested in when the matrix starts to be able to develop a significant stress history.

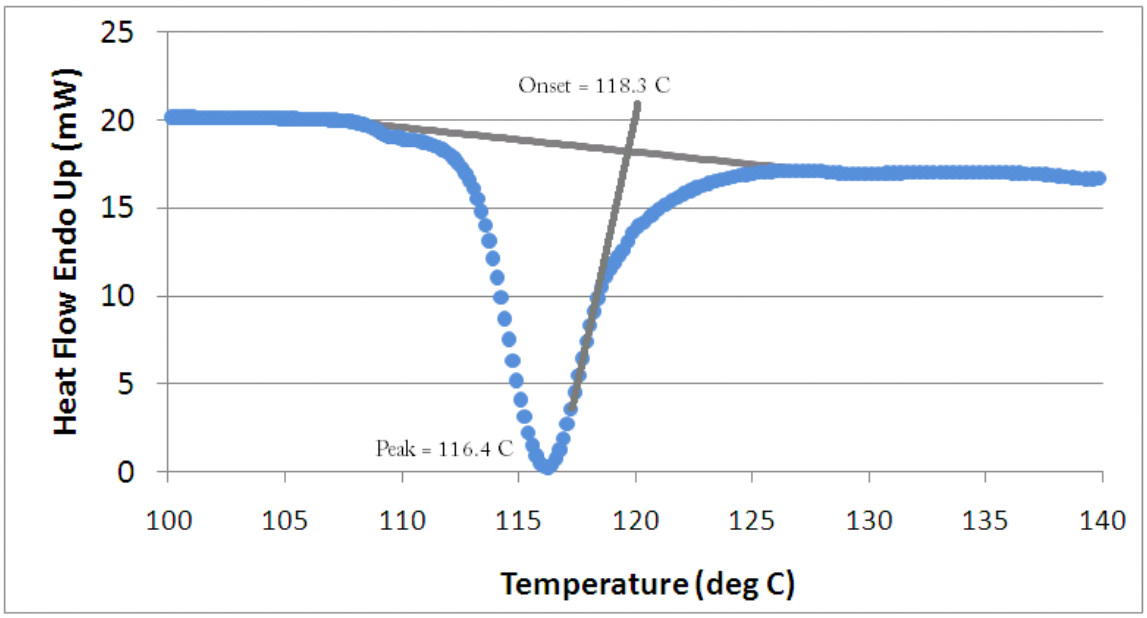

Figure 4-9 Average crystallization peak for Twintex® under the roll forming thermal cycle

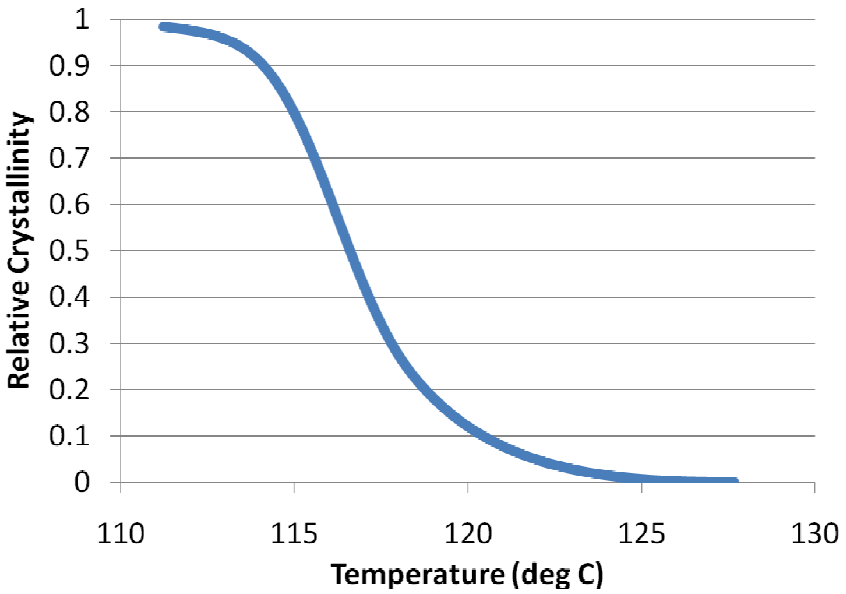

Figure 4-10 Relative crystallinity curve for Twintex® under the roll forming thermal cycle

4.4 Dynamic Mechanical Analysis (DMA)

Dynamic Mechanical Analysis (DMA) can be used to test the viscoelastic behaviour of the laminate. There are a wide range of tests that can be conducted within the DMA family. For the purpose of this study, three-point bending tests on samples of roll formed Twintex® are most appropriate. Three-point bending of a plate sample is the closest loading condition to the bending stresses that develop in the corner section of the V-shaped roll formed sample. The fixture and sample are shown in Figure 4-11.

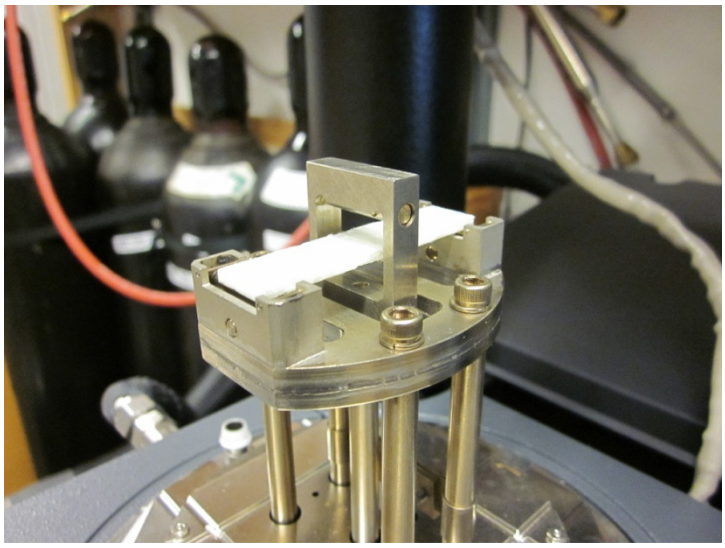

Figure 4-11 Three point bending fixture and Twintex® sample for DMA anlysis

DMA testing involves imposing a sinusoidal strain on a sample and measure the resultant sinusoidal stress. Equivalently, a sinusoidal stress can be imposed and the resulting sinusoidal strain can be measured. For a perfectly elastic material and for small deformations the sinusoidal stress and strain curves would be perfectly in phase, such that there are no losses. Since there is a direct proportionality between stress and strain through Hooke's law, the ratio of the stress and strain amplitudes will be equal to the flexural modulus. For an ideal liquid with an applied sinusoidal shear strain, the sinusoidal stress response will be 90^{o} out of phase since the stress is proportional to the strain rate. For viscoelastic materials, which exhibit intermediate behaviour between that of a perfectly elastic and ideal liquid material, the sinusoidal stress (or strain) response will have some phase shift to the sinusoidal strain (or stress) input. Figure 4-12 shows the typical input and response. This phase shift, sometimes called a lag angle, is a measure of the viscous character of the viscoelastic material, where 0^{o} represents an ideal elastic solid and 90^{o} represents an ideal viscous liquid.

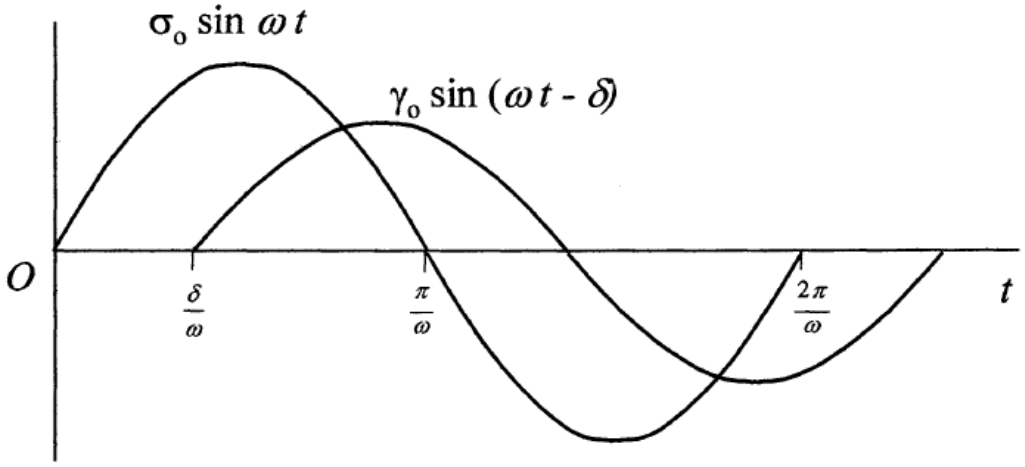

Figure 4-12 Sinusoidal stress and strain input and response curves for a viscoelastic material showing a phase lag (Mase & Mase, 1999)

From the sinusoidal response we can define the storage modulus (E') and loss modulus (E''). The storage modulus represents the elastic character of the material where there are no losses and is given in Equation 4-2. The loss modulus represents the viscous character of the material and is given in Equation 4-3. Figure 4-13 shows, in vector form, how the storage modulus is based the component of the stress response in phase with the strain input. Similarly, the loss modulus is based on the component of the stress response that is 90^{o} out of phase with the strain input. The phase lag (δ) can be calculated using Equation 4-4. In addition, the storage and loss moduluses can be expressed in complex form, where the storage modulus exists in real space and the loss modulus exists in imaginary space, as shown in Equation 4-5.

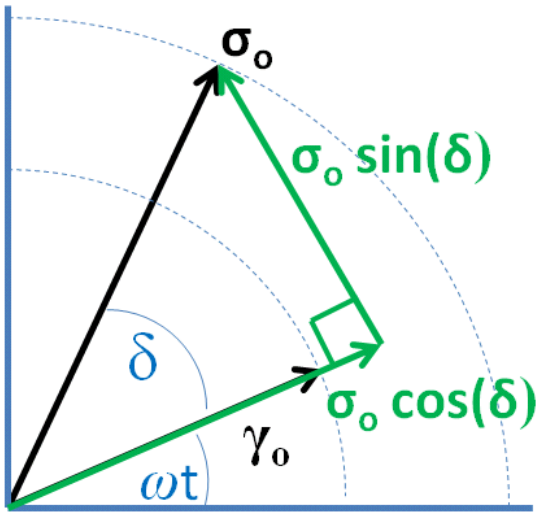

Figure 4-13 Sinusoidal stress and strain in vector form

$$E' = \frac{\sigma_o \cos(\delta)}{\gamma_0}$$ Equation 4-2

$$E'' = \frac{\sigma_o \sin(\delta)}{\gamma_0}$$ Equation 4-3

$$\tan(\delta) = \frac{\sigma_o \sin(\delta)}{\sigma_o \cos(\delta)} = \frac{E''}{E'}$$ Equation 4-4

$$E^* = E' + iE'' = \frac{\sigma_o}{\lambda_o}[\cos(\delta) + i\sin(\delta)] = \frac{\sigma_o}{\lambda_o} e^{i\delta}$$ Equation 4-5

A Rheometric Scientific Model DMTA MKA machine was used to perform DMA tests of roll formed Twintex® samples. Three point bending tests were conducted on samples of two layer, 44oz/yd^{2,} Twintex® produced by roll forming. The tests were done at a constant frequency of 1Hz while the temperature was swept from room temperature to the melting temperature of Twintex®. The results from two samples are shown in Figure 4-14. It can be observed that the

storage modulus and loss modulus are quite constant over the temperature range. Additionally, the phase shift is small, less than 6°, until the temperature approaches the melting point of the material and it begins to soften. A small phase shift suggests that within the range between crystallization and room temperature, the Twintex® laminate behaves much closer to an ideal elastic solid than an ideal viscous liquid.

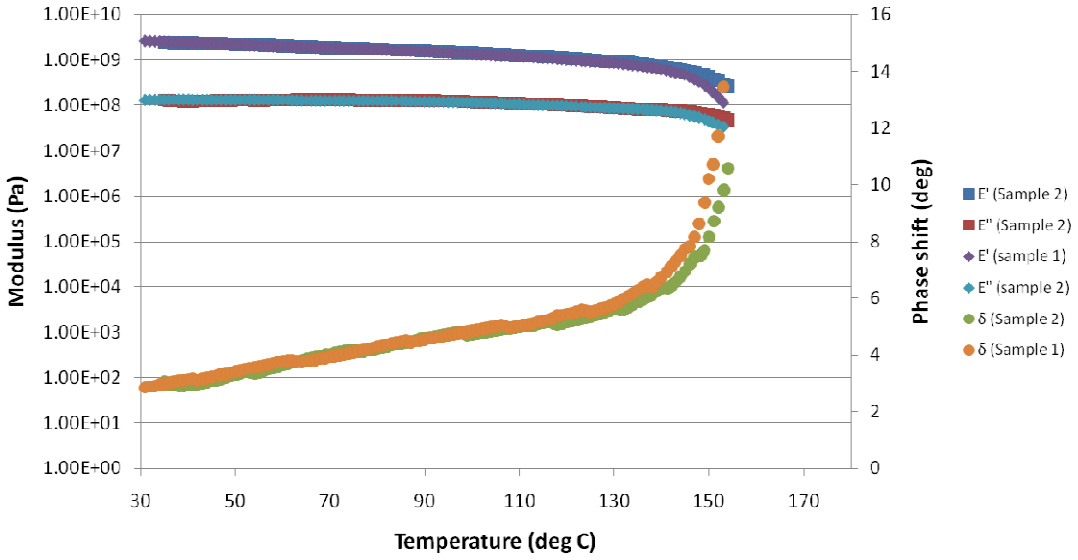

Figure 4-14 DMA results: three point bending, increasing temperature sweep at 1 Hz

4.5 Stress Relaxation

In the context of process modeling, we are interested to know the thermal mechanical behaviour of the laminate during the cool down cycle. It is very challenging to perform DMA testing with a cool down thermal cycle due to the difficulty in holding the sample at temperatures above the melting temperature. Furthermore, above the melting temperature, the laminate tends to delaminate and deconsolidate so that if the cooling cycle is performed while the laminate is not under pressure, the sample may develop a higher void content and lower consolidation compared to the real process. To address these challenges, three point bending stress relaxation

tests were performed with a TA-Q800 DMA by the composites group at UBC Vancouver. During testing, the Twintex® samples were heated to 168ºC and held for 5 minutes before cooling. Based upon the DSC results, at this temperature and hold time, the samples should be uniformly above the melting temperature while the amount of deconsolidation or delamination of the sample is minimized. While performing these tests are challenging, they provide insight into the thermal mechanical behaviour of Twintex® on a decreasing temperature cycle.

In the stress relaxation tests, a small, near instantaneous strain is applied to the sample and resulting force values are recorded so that the change in the modulus can be measured with time. The procedure for the experiment involved:

- Loading the sample in to the fixture
- Bringing sample temperature to 30ºC and hold for 5 minutes
- Apply a center piston displacement of 680μm, hold for 30 minutes and record load
- Raise the temperature to the following inclement and hold for 5 minutes to equalize
- Repeat the two steps above until the melting temperature of the matrix is reached

Stress relaxation tests were performed for both increasing and decreasing temperature cycles at 5ºC increments from 30ºC to 165ºC. Figure 4-15 and Figure 4-17 show the results for the increasing and decreasing temperature cycles, respectively. It can be observed that there is an initial modulus which relaxes over time. Figure 4-16 and Figure 4-18 show the isochronal cross-sections of the stress relaxation results. For the isochronals, the relaxation modulus is plotted as a function of temperature for a given value of time.

From the stress relaxation results it can be observed that the change in modulus due to a change in temperature is much greater than the change in modulus due to holding for an amount of time. This suggests that Twintex® behaves much more thermo-elastic than thermo-viscoelastic. In the short time scales of roll forming, these results suggest that any viscoelastic effect will have a small impact on the modulus development. This trend is consistent with the small phase lag angle as seen in the DMA testing in Section 4.4.

In addition to the viscous effect, Figure 4-18 shows the presence of a small but meaningful modulus at temperatures above the crystallization temperature range. For a decreasing thermal cycle, it was previously expected that the modulus was negligible before the crystallization process. However, these results suggest that the pre-crystallization, amorphous, supercooled matrix material begins to develop a significant modulus when cooled to temperatures below its equilibrium melting temperature. A pre-crystallization modulus development can have an effect on the spring-in angle predictions as described in Section 2.3.1.4 . Two external sources could have caused this small modulus. First, it is possible that in the experiment, the sample did not completely melt before the cooling procedure started. This could leave some residual, pre-melt modulus. Second, due to the very slow cooling rate, crystallization in the sample would have started much earlier than for the fast cooling rate used in a real roll forming process. It may be that some crystallization has started leading to the apparent modulus. At this time, these results are considered preliminary and it remains for future work to investigate the pre-crystallization modulus development of the matrix material more closely.

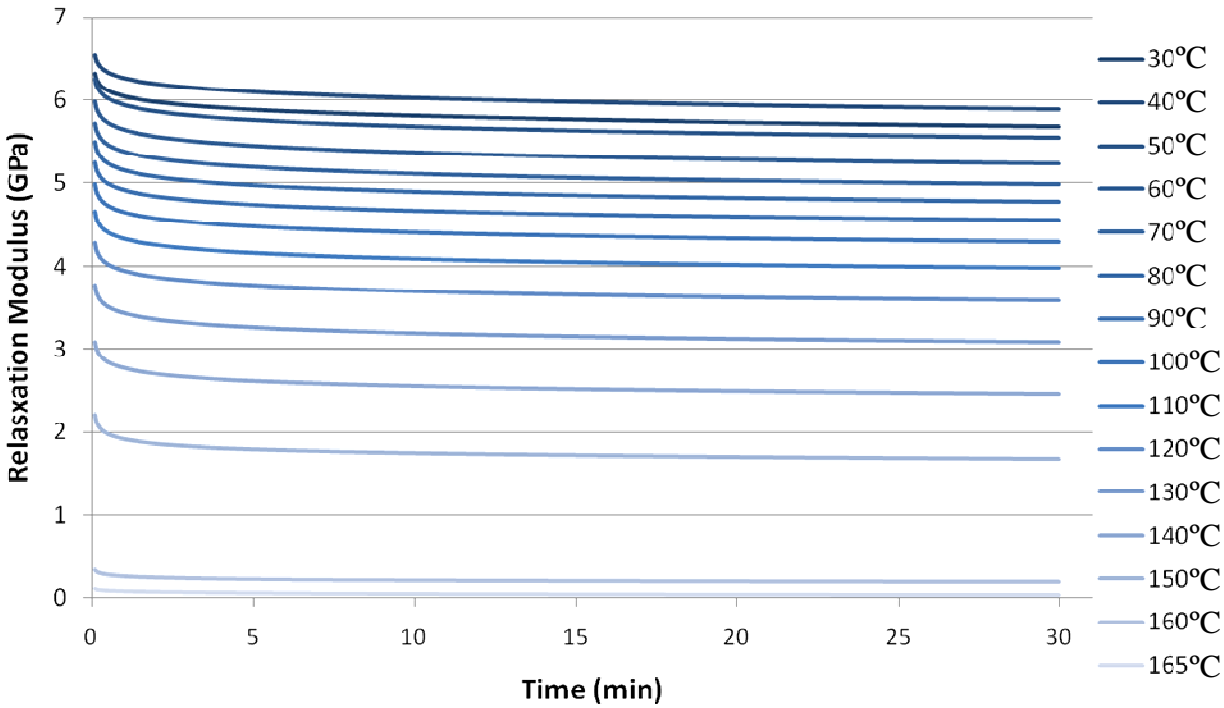

Figure 4-15 Stress relaxation results: three point bending, increasing temperature

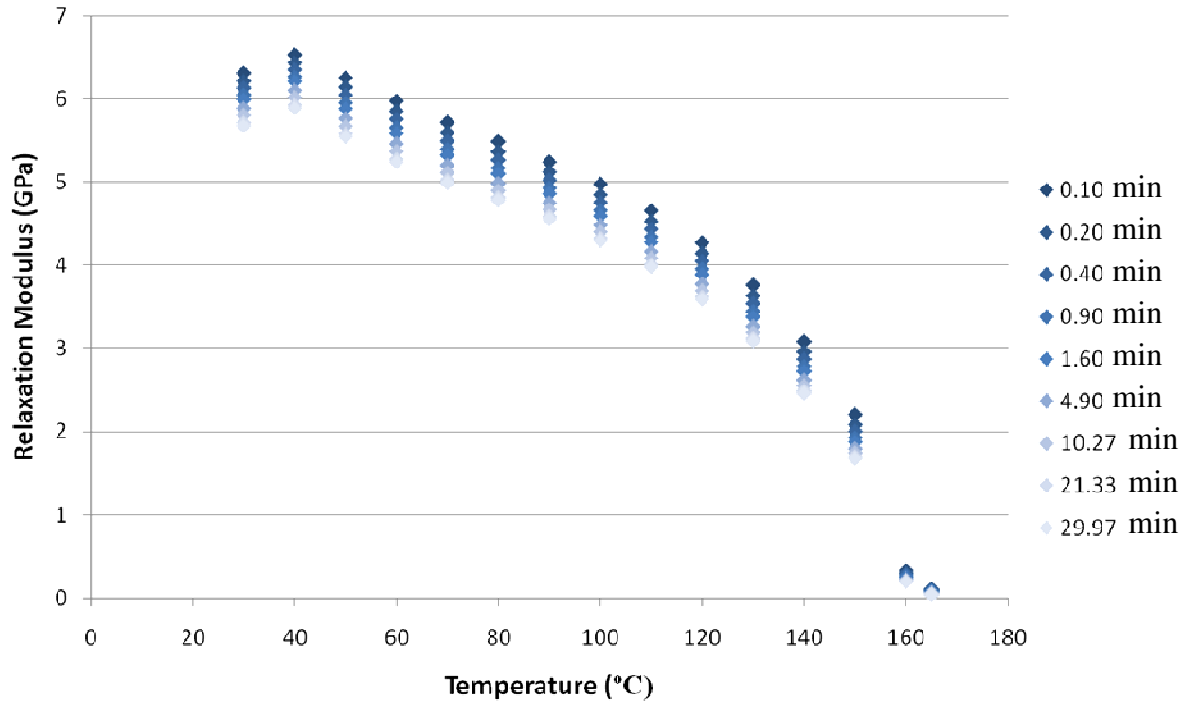

Figure 4-16 Stress relaxation isochronals: three point bending, increasing temperature

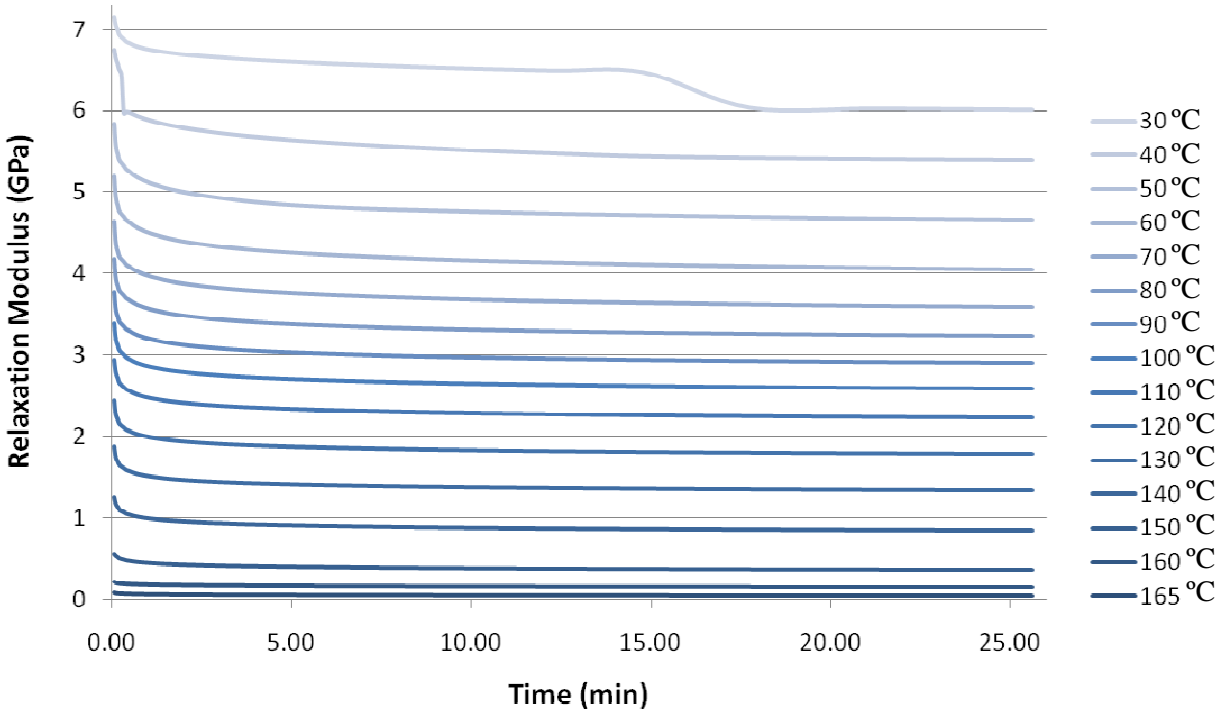

Figure 4-17 Stress relaxation results: three point bending, decreasing temperature

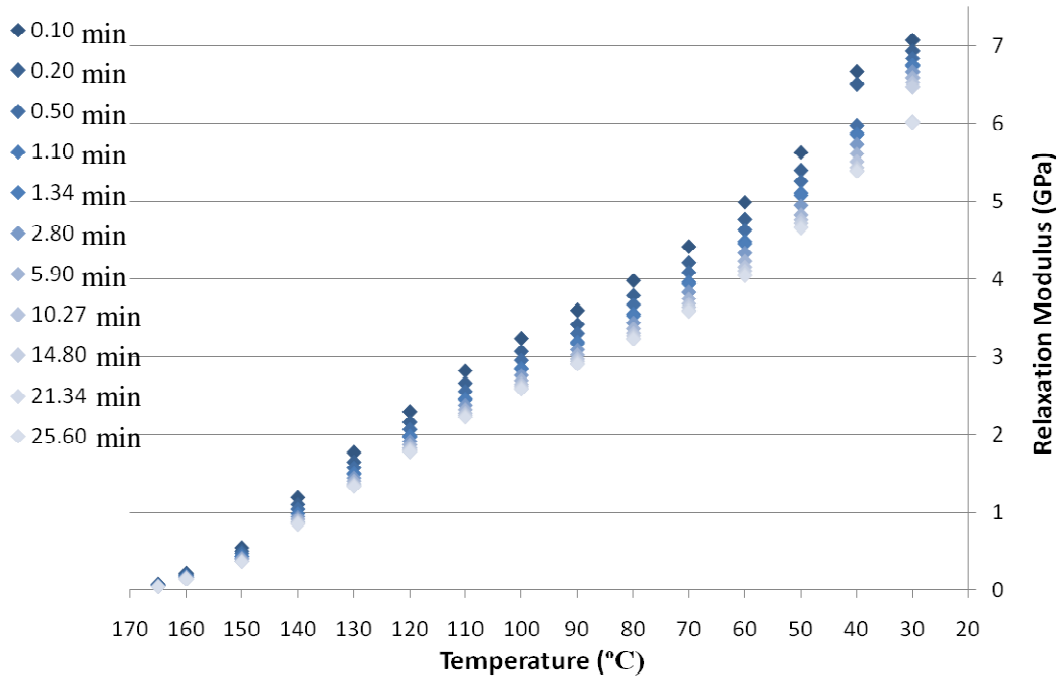

Figure 4-18 Stress relaxation isochronals: three point bending, decreasing temperature

Overall, the results of DMA and stress relaxation testing have revealed the complex thermal mechanical behaviour of Twintex®. In general, both experiments have shown that Twintex® behaves much more thermo-elastically than thermo-viscoelastically and that, particularly in the time scales of roll forming, the viscous component can likely be neglected. A complete characterization of the thermoviscoelastic behaviour of Twintex® is planned to be completed in the future since it appears to be more applicable to other manufacturing methods than roll forming. Nonetheless, in Sections 6.3 and 6.4, a hypothetical viscoelastic model will be adopted with the purpose of demonstrating how its inclusion can affect the FE modeling results.

5 Process Characterization of Roll Forming

5.1 Geometry of Example Case

The geometry of the example case used in this study is based on a previously developed roll forming machine at AS Composites Inc. The machine arrangement consists of an upper and lower convection oven, two pairs of compaction rollers and two pairs of forming rollers, similar to Figure 2-6 and Figure 5-1. The machine is designed to form two layers of 44 oz/yd^2 Twintex® into V-shaped channels. The fibre orientations for the warp and weft fibres in the woven Twintex® laminates are 0º and 90º respectively, relative to the longitudinal axis of the forming line. The initial laminate width is 100 mm. The compaction rollers are 450 mm in diameter, 100 mm wide and are spaced at 500 mm apart, based on their centre lines. The geometry of the male and female V-shaped forming rollers are as shown in Figure 5-2 and Figure 5-3, respectively. The rollers are arranged such that the roller gap (distance between the upper and lower roller) is half of what is given in Table 2-1 (since Table 2-1 is for a four layer laminate), so that a low void content in the final product can be achieved. The line speed is 0.5m/min.

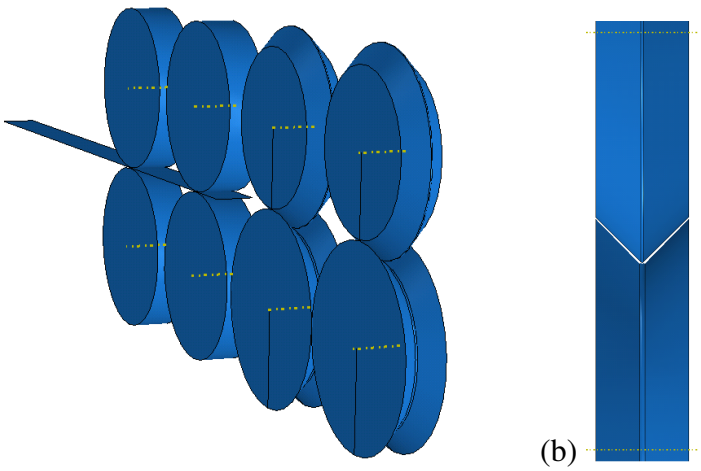

(a) (b)

Figure 5-1 (a) 3D Geometry of a roll forming simulation (b) end view of 90^o forming rollers

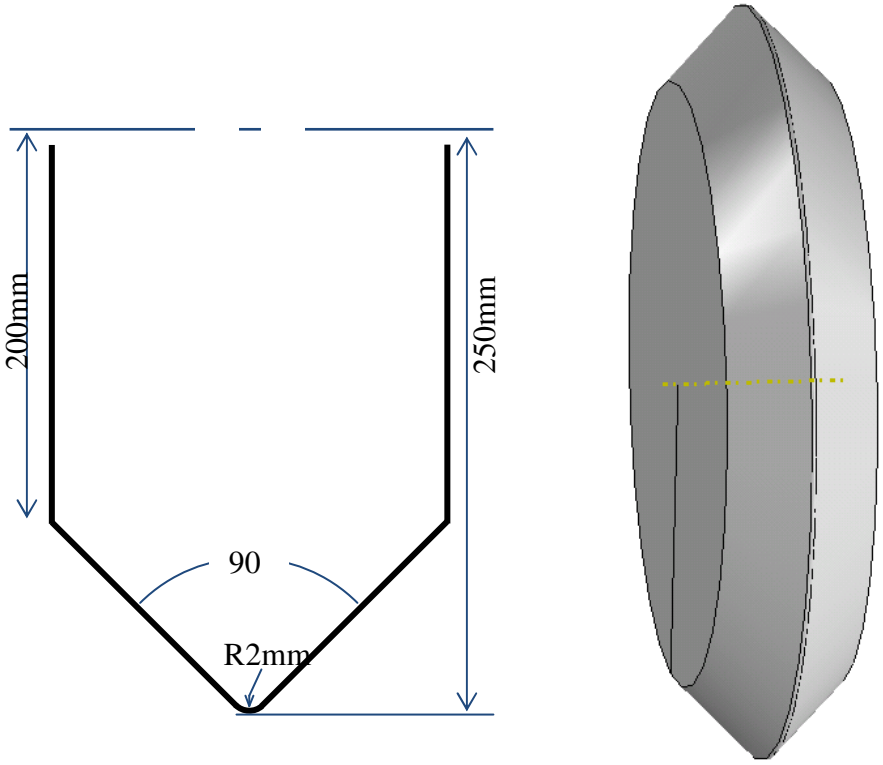

Figure 5-2 Geometry of 90° V-shape male forming roller

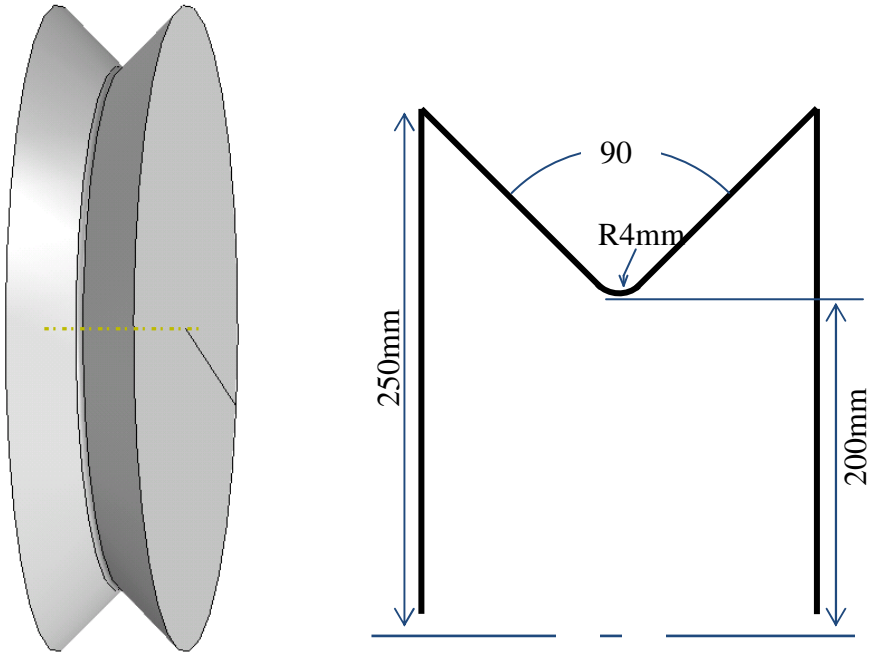

Figure 5-3 Geometry of 90° V-shape female forming roller

5.2 Thermal Cycle

A typical thermal cycle used for the roll forming process is shown in Figure 2-7. As the laminate passes through the oven, it is heated above it melting temperature. Then, as the laminate passes through the pairs of rollers, it cools below its crystallization temperature so that at the exit of the last roller, the material is consolidated. For the example case described in Section 5.1, previous trial and error optimization work performed by AS Composites have identified limits to the thermal processing window in order to produce high quality roll formed components. These limits are given as an average temperature range of the laminate at each forming stage. Figure 5-4 shows the temperature limits at each stage in red as well as a curve fit through the given temperature limits.

Remark: The imposed thermal cycle for DSC testing in Section 4.3; the ABAQUS models to be presented in Chapter 6; and the stamp forming experiments in the next section are all based on the thermal cycle shown in Figure 5-4, since it is the best approximation of an optimized thermal cycle for the example case under study. In Section 6.2.7 , a sensitivity analysis will be performed where the thermal cycle is shifted to the upper and lower limits of the given temperature ranges to investigate the effect of the thermal cycle on spring-in.

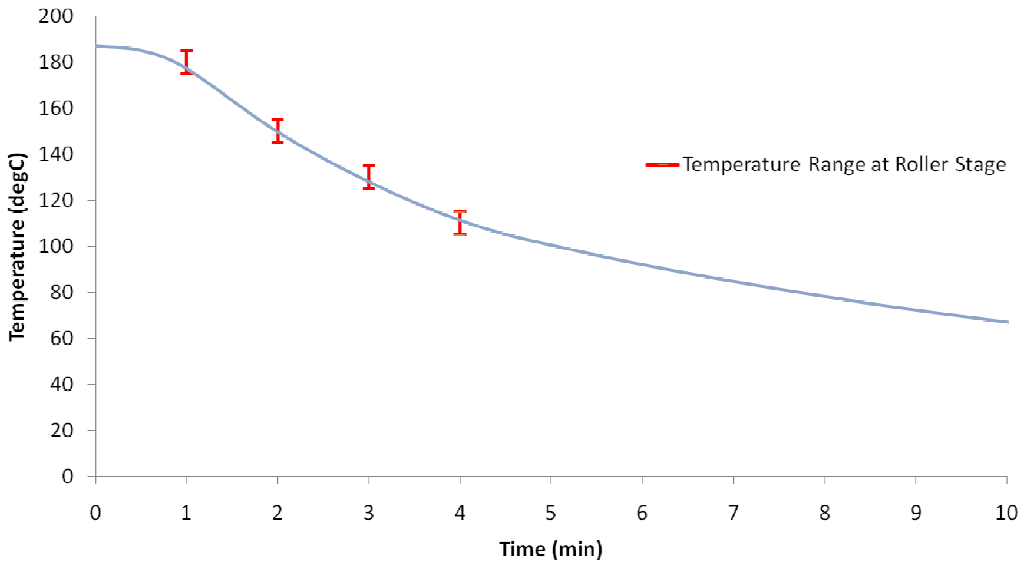

Figure 5-4 Roll forming thermal cycle for V-shaped parts (surface temperatures shown)

5.3 Spring-in Measurements

The spring-in angle was measured on Twintex® samples formed into a 90° V-shape. Unfortunately, at the time of this study, there were no V-shaped rollers available to perform full scale roll forming experiments. Instead, as the best approximation of roll forming, stamp forming experiments were performed with a V-shaped stamping die. The equivalencies between roll forming and stamp forming are used to observe the spring-in behaviour in the test samples.

Stamp forming tests were performed using a MTS fatigue test frame with a 250 kN load cell. A fatigue test frame was used so that a high tool closing and opening rate could be achieved in order to simulate the quick entrance and exit from a pair of roll forming rollers. In the stamp forming process, a pre-consolidated two layer plate of Twintex® was heated in an oven until it was above the melting temperature of the matrix. The sample was then quickly transferred by hand to a pair of stamp forming tools, which close on the sample and hold until it cools below its

crystallisation temperature. Figure 5-5 shows the stamp forming arrangement that was used. An oven is located very close to the stamp forming frame to allow for a quick transfer of the sample from the oven to the stamping tool. Figure 5-6 shows the 90^{o} V-shaped stamp forming tools. The corner radiuses of the male and female tools are 2 mm and 4 mm, respectively. Samples were pre-consolidated into flat plates using a compression moulding process. Figure 5-7 shows these samples prior to forming, which were rectangular at 250 mm by 100 mm. Two thermocouples were inserted into the samples during the compression moulding process. One thermocouple was placed between the two Twintex® ply's so that it is at 50% through the laminate thickness. The other thermocouple was inserted underneath one bundle of the top Twintex® ply's weave, which locates it at 25% through the laminate thickness.

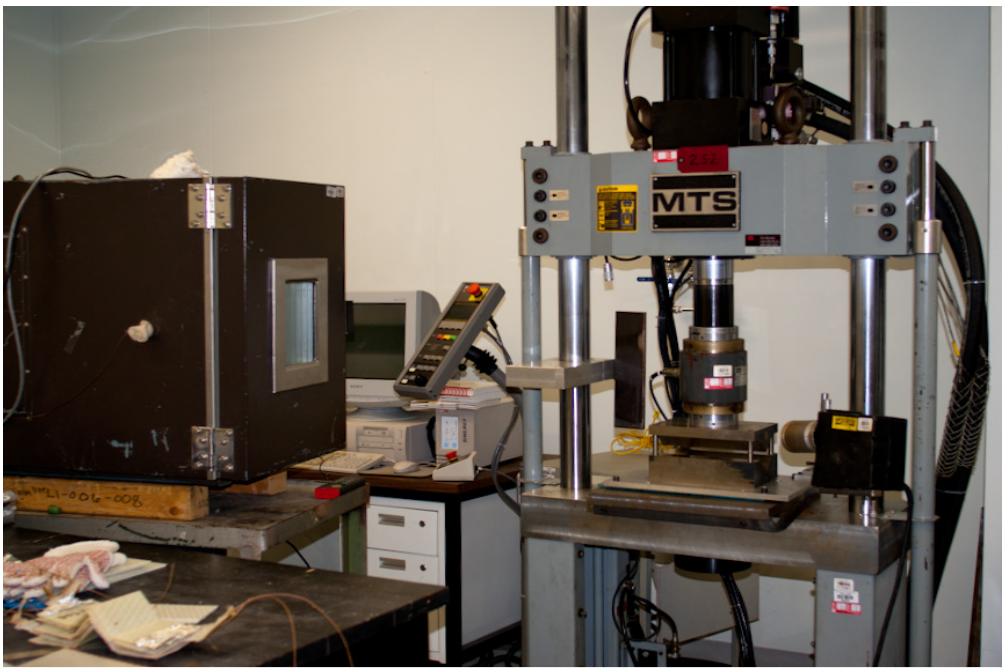

Figure 5-5 Stamp forming arangement

Figure 5-6 Stamp forming tools

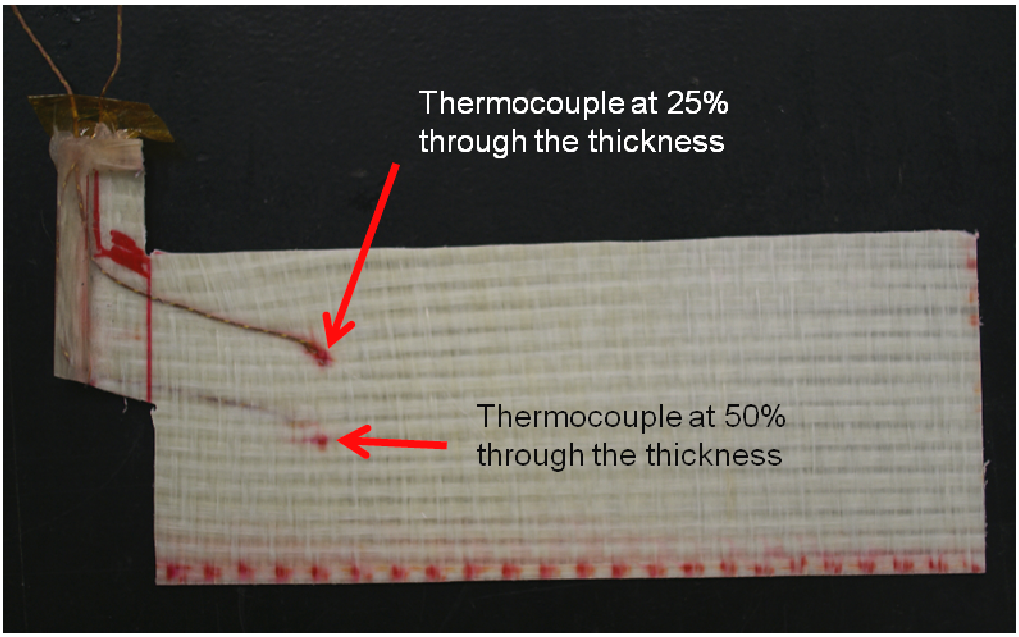

Figure 5-7 Stamp forming sample, pre-consolidated prior to forming

The stamp forming process was developed in a way that the treatment of the laminate is as close to the example case roll forming process as possible. Namely, in order for the stamp forming experiment to simulate the roll forming process, it was important that crystallization of the matrix happens at the correct temperature. If the cooling rate is too fast, crystallization will occur at a lower temperature and the driving force for spring-in, namely the difference between room temperature and the crystallization temperature, will be reduced. If the cooling rate is too slow, crystallization will occur at a higher temperature and the driving force for spring-in will be greater. The challenge was that in stamp forming, when the laminate comes into contact with the room temperature tools, it cools very quickly. In roll forming, only a thin cross section of the laminate is in contact with the forming rollers at a given time, thus the cooling rate of the laminate is much slower compared with stamp forming. Accordingly, the cooling rate of the sample in the stamp forming experiments was controlled so that it was as close as possible to the cooling rate of the roll forming process. Also, the hold time of the stamp forming tools was reduced so that the tools are only in contact with the laminate for a very short period of time.

Figure 5-8 shows the thermocouple readings of the stamp forming sample along with the target roll forming thermal cycle. The cooling rate of the sample and that of the target are the same up to the point at which the sample enters the stamping press. Since the cooling rates are the same for the period between cooling below the melting temperature and close to the crystallization temperature, the crystallization temperature for the two cycles should be as equal as possible. In order to achieve this matched cooling cycle, the following process was developed after several trials:

- Heat sample in the oven to 190°C
- Open the oven door to cool slowly at roll forming cooling rate
- Transfer the sample to the press at 140°C
- Start the press immediately
- Hold for 3 seconds before opening
- Remove the sample from the press and cool in air to room temperature

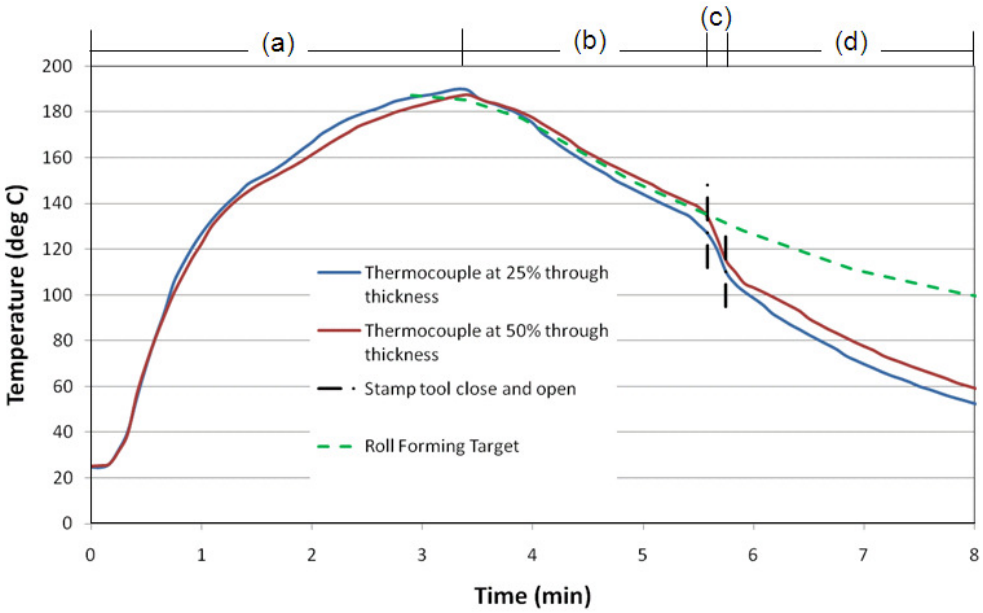

Figure 5-8 Stamp forming temperature cycle with roll forming target cycle. (a) Heating in the oven, (b) Cooling rate following target, (c) Stamping tool close and open, (d) Cooling to room temperature

As shown in Figure 5-8, there is an increased cooling rate when the sample enters the stamp forming tools. The degree of this increased rate was minimized by limiting the hold time of the tools. Figure 5-9 shows the displacement of the male stamp forming tool over time. The female tool is fixed. The tool closes to a 5 mm gap at a rate of 23 mm/min, then to a gap of 2.5 mm at a rate of 3.5 mm/min and, finally, to a gap of 1.9 mm at a rate of 1 mm/min. During the initial fast closing rate, the laminate is easily formed over the tool surfaces. The second and third

closing rates are slower since the laminate is being compressed and time is given for the matrix to diffuse within the laminate. A faster closing rate during the compression stage can result in fibre movement. The tool is held at a gap of 1.9 mm for 3 seconds before releasing quickly.

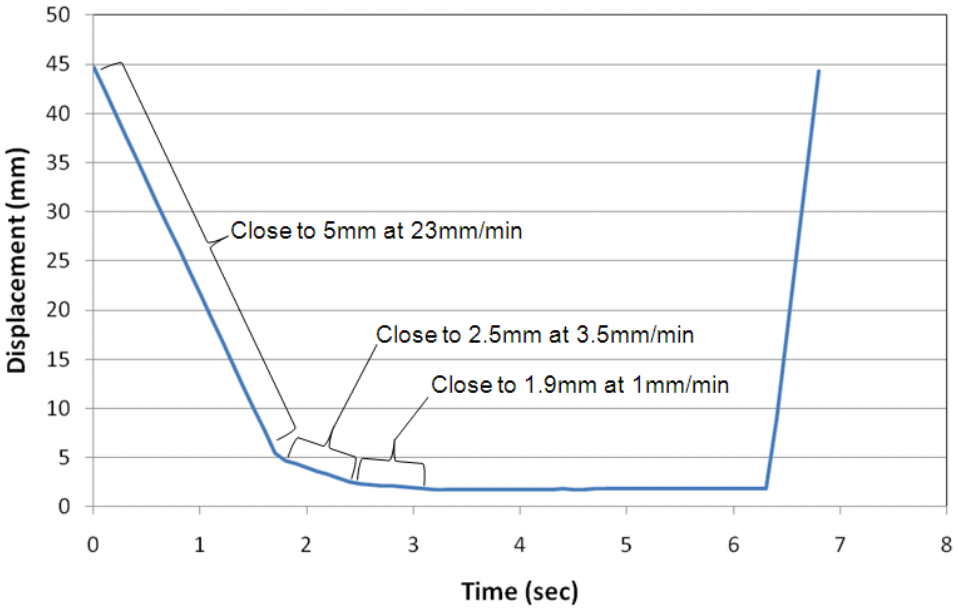

Figure 5-9 Displacement of stamp forming tool

In the roll forming process, crystallization happens between the two sets of forming rollers while the laminate is constrained to a V shape. Thus, in order for the stamp forming experiments to simulate roll forming, it is crucial that crystallization happens while the laminate is constrained within the stamping tools. If crystallization begins before the laminate is formed over the stamp forming tools, there will be elastic and potentially plastic deformation of the laminate. This can damage the laminate and will lead to a spring-back due to the elastic return of the material. If crystallization does not begin until after the tools release from the laminate, the laminate will crystallize without any applied pressure. Typically, this will also lead to a spring-back-like deformation, since the laminate will not be completely conformed over the mould. It is

a significant challenge, in these equivalent stamp forming experiments, to ensure that crystallization occurs while the laminate is constrained in the tool but, at the same time that the tool is not in contact with the laminate for a long period of time so that the cooling does not deviate significantly from the target. Since a deviation of the crystallization point in either direction will lead to a spring-back-like deformation, only samples with a large spring-in angle should be considered as successful experiments and a close representation of the roll forming process.

Figure 5-10 shows the stamp forming sample after forming into a V-shape. The angle of the V-shape was measured using an OGP Smartscope Flash optical CMM machine. The angle was taken by measuring several points on each face and fitting two flat surfaces from which the included angle can be found. Table 5-1 lists the angles of each sample.

Table 5-1 Spring-in angles of stamping samples

Sample No.	Spring-in Angle
1	2.12°
2	1.87°
3	1.36°
4	1.33°

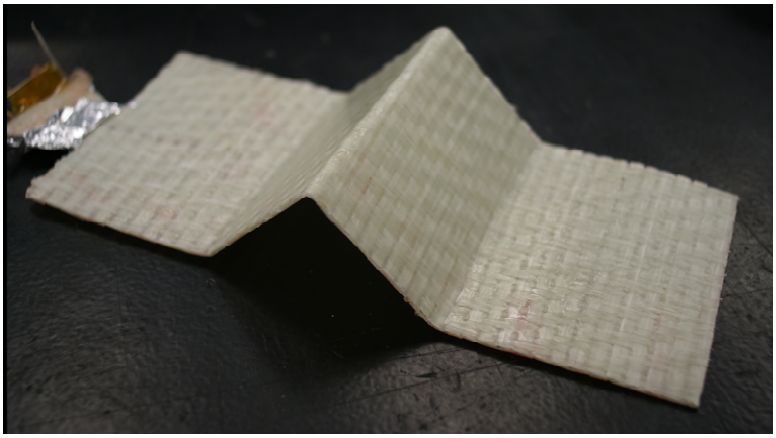

Figure 5-10 Stamp forming sample after forming a V-shape

6 Modeling Approaches and Results

A finite element simulation of the roll forming process described in Chapter 5 was implemented in the commercial finite element package ABAQUS 6.9.2 CAE. In an effort to find the best modeling approach, a large number of different models were investigated during this study. Three of these models are described in detail in the following sections. All of the models share what was found to be the best geometry and boundary conditions to simulate roll forming of a V-shaped Twintex® channel. They differ in their constitutive model and the underlying assumptions that govern the analysis. Model 1 (Section 6.2) assumes that the effect of viscoelasticity can be ignored for the case of roll forming. In roll forming, crystallization of the matrix material occurs around the final set of forming rollers. The laminate is, therefore, only in contact with the forming rollers for a short period of time before it is released and allowed to deform freely. In addition, with a high production line speed and a fast cooling rate, it is not expected that the stress relaxation of constrained components mechanism (described in Section 2.3.1.4) will have a significant effect on spring-in angle predictions. By ignoring the effect of viscoelasticity, Model 1 can save significant computational time. In order to check this assumption, Model 2 (Section 6.3) includes a viscoelastic constitutive material model. The effect of including viscoelasticity in the constitutive material model is then analysed. It is expected that for other manufacturing methods, such as compression moulding or vacuum bagging, where the laminate is in contact with the forming mould for a longer period of time and the cooling rate is slow, viscoelasticity will have a more significant impact on the spring-in angle prediction and the increased computational cost is unavoidable. Model 3 (Section 6.4) presents a decomposition of the laminate into subdomains that represent the fibres and matrix constituents individually. It

investigates the effect of the viscoelastic stress relaxation of internal residual stresses (described in Section 2.3.1.7).

6.1 Analysis Type

A complete process simulation model of any manufacturing process would involve two distinct analyses: a heat transfer analysis followed by a mechanical analysis. A heat transfer analysis can be used to simulate the development and change of temperature during the manufacturing process. In this analysis, each component of the manufacturing process must be modeled. For roll forming, this would include as a minimum: the laminate, ovens, forming rollers and surrounding airflow. Thermal properties (thermal conductivity, heat capacity, etc.) are needed for each component of the system. The heat transfer analysis would then be used to develop temperature values for each node at each time increment. This thermal cycle is used as an input to the mechanical analysis which finds stress and displacement values based on boundary conditions. Thermal stresses and/or displacements are calculated in the mechanical analysis using thermal expansion properties. This approach is the most general and if given all required material properties, it can represent the most complete simulation model.

Alternatively, the approach used in this study is to eliminate the heat transfer analysis step described above by defining the thermal cycle directly through boundary conditions and prescribed constraints. The thermal cycle is based on measurements from the actual roll forming process as described in Section 5.2. By eliminating the heat transfer analysis, uncertainties in thermal properties and in the analysis itself are avoided. In this approach, the imposed temperature conditions can potentially be a more accurate representation of the real

manufacturing process since they are based on direct measurements. The disadvantage of this approach is that if any changes are made to the manufacturing process or if there is interest in modeling a different process, a new set of process characterization measurements are required.

6.2 Model 1: Using Elastic Mechanical Properties

6.2.1 Geometry

In order to save computational time, a two dimensional approximation of the roll forming machine described in Section 5.1 is established. Figure 5-1 shows the three dimensional geometry of the forming rollers and the laminate. A model including this 3D geometry was defined in ABAQUS with a simple isotropic and linear elastic material model for the laminate. With simple contact conditions and boundary conditions applied, the runtime of the 3D model was on the order of 10 hours. A 2D approximation can be used to significantly reduce this run time, although with some inherent simplifications. The 2D model considers a section of the laminate transverse to the rolling direction and follows it as it passes through the roll forming machine. Figure 6-1 shows the 2D geometry with a cross section of the laminate and two rigid body wires to represent the forming rollers. The desired V-shape is rotated 45^{o} to an L-shape for the ease of defining the model within the global x,y coordinates of the work space.

The initial shape of the laminate in Figure 6-1 is the deformed shape of the laminate draped over the forming rollers. When the matrix is heated above its melting temperature, the laminate behaves like a deformable fabric. As the fabric is deformed over the forming moulds, no back stresses or strains develop. The stress and strain history of the laminate begins as the matrix crystallises. The initial shape is then the shape of the laminate as the matrix crystallises

since it is the difference between this shape and the final shape that will define spring-in. The 2D model is, therefore, valid from the instant before matrix crystallization to the end of the process or room temperature.

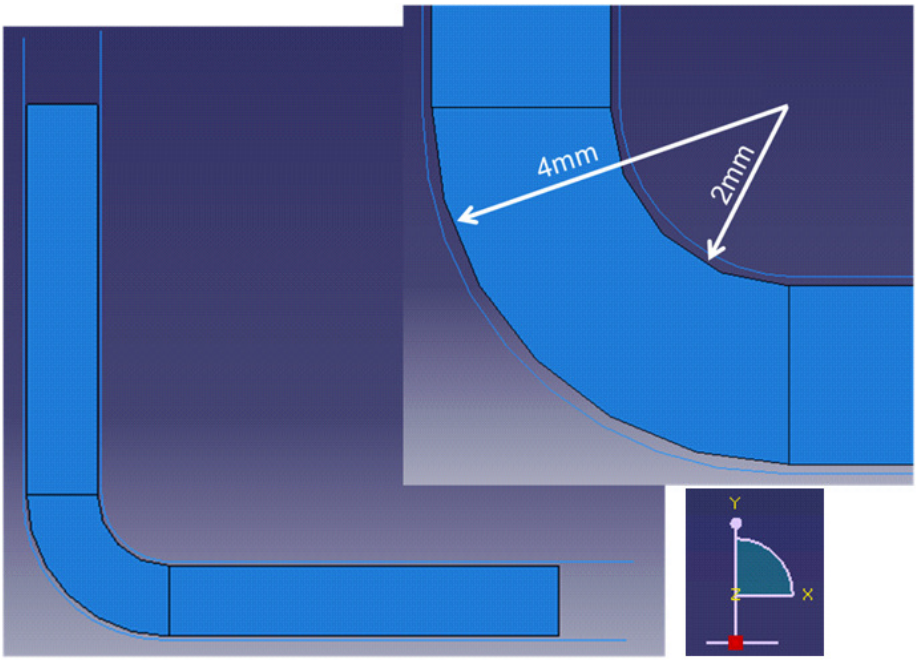

Figure 6-1 2D FE model geometry showing the cross section of the laminate; upper and lower rigid body surfaces represent the forming rollers

A 2D analysis is very applicable to the roll forming process. This is because once the process reaches a steady state line speed, a conversion can be made between distance along the roll forming line and the analysis time. Temperatures also reach a steady state condition where the temperature at any position along the production line is constant. The temperature cycle can then be defined as a function of analysis time and correlated to any position along the production line (see Figure 2-7). Section 6.2.3.1 describes the defined thermal cycle for the analysis.

In order to simulate the laminate passing through a pair of forming rollers in two dimensions, two analytical rigid wires are defined: one above and one below the laminate. Figure 6-1 shows these analytical rigid wires. Forming rollers are typically made of high strength steel with stiffness significantly higher than the laminate, particularly at forming temperatures. It is assumed that at the forming pressure, the laminate is not able to deform the forming rollers. To simulate a cross section of the laminate as it passes through a pair of rollers, the analytical rigid wires are closed onto the laminate, held for the contact duration, and then released from the laminate. This modeling procedure mimics the equivalencies between the roll forming process and stamp forming, as described in Section 2.2.4 . In the present model, the analytical rigid wires are closed onto the laminate at the point in the analysis where the laminate enters the first pair of forming rollers. They are held on the laminate until the point at which the laminate exits the second pair of forming rollers. Figure 5-1 shows a 3D rendering of the roll forming machine with two forming roller stages. This approach will restrict any deformation of the laminate for the time period between the entrance of the first forming roller pair and the exit of the last forming roller pair. In the real process, between the two forming roller stages, the laminate is free from any contact. It is, however, not free to deform, tension in the laminate in the rolling direction maintains a V-shape between the two forming roller stages with some sag or deformation due to the laminate's own mass. This deformation between the forming roller stages cannot be captured with the 2D model as currently described. It is believed that this simplification would not have a significant impact on the spring-in angle predictions. Since crystallization of the matrix occurs around the last forming roller stage, crystallization happens when the laminate is in contact with the final forming rollers and constrained to the 90^{o} V-shape.

6.2.2 Material Properties

6.2.2.1 Crystallization Kinetics

In order to model the manufacturing process of a thermoplastic composite, the model must be able to accurately describe the change in structure of the matrix material from the melt through crystallization. Section 4.3 described how the DSC machine was used to characterize the crystallization of Twintex® samples subjected to the roll forming thermal cycle. In order to model the change of the material microstructure, a new state variable is defined for the relative crystallinity (RC). The relative crystallinity is defined as equal to zero when the matrix material is melted and equal to one when the matrix material has completed crystallization. Values between zero and one describe the progression of the crystallization process. Figure 4-10 shows the relative crystallinity as a function of temperature as found by DSC testing of a Twintex® sample given the roll forming thermal cycle in Figure 4-7. In ABAQUS, the relevant material properties are defined twice as shown in Table 6-1. At a RC of zero, very low mechanical properties are defined. When the matrix has been melted, the stiffness of the laminate is essentially zero. A very low stiffness is used in place of zero so that a numerical solution can converge. At a RC of one, the fully crystallized properties are defined as found through mechanical testing of fully consolidated samples (see Chapter 4). The transition from a RC of zero to one is defined in FORTRAN with a USDFLD user defined subroutine. The subroutine is shown in Figure 6-2. The S-curve in Figure 4-10 is fit by Equation 6-1:

$$RC = (-85.1731 - 12.7484T - 3.67281T^2 - 66.37631T^3 + 529.849T^4 - 13.0083T^5 + 0.106611T^6 - 0.00029136T^7)/(-0.0146362 + 9.71833T + 456.268T^2 + 13578.7T^3 - 232.956T^4 + T^5) \quad \text{Equation 6-1}$$

Thermal expansion properties are defined in a UEXPAN user subroutine in FORTRAN so that the through thickness thermal expansion can be a function of both temperature and RC. When the RC is zero, the through thickness coefficient of thermal expansion is zero. When the RC is one, the through thickness coefficient of thermal expansion is equal to the temperature dependant value found from TMA testing (Section 4.2) as follows:

$$Alpha_{TT} = -1.445894 \times 10^{-8}T^2 + 5.063871 \times 10^{-6}T - 5.562424 \times 10^{-5} \quad \text{Equation 6-2}$$

Table 6-1 Through thickness material properties as a function of relative crystallinity

Young's Modulus (MPa)	**Coefficient of Thermal Expansion (/°C)**	**RC**
10	0	0
1500	$Alpha_{TT}$	1

```
      SUBROUTINE USDFLD(FIELD,STATEV,PNEWDT,DIRECT,T,CELENT,TIME,DTIME,
     1 CMNAME,ORNAME,NFIELD,NSTATV,NOEL,NPT,LAYER,KSPT,KSTEP,KINC,
     2 NDI,nshr,coord,jmac,jmtyp,matlayo,laccflg)

      INCLUDE 'ABA_PARAM.INC'
      CHARACTER*80 CMNAME,ORNAME
      CHARACTER*3  FLGRAY(15)
      DIMENSION FIELD(NFIELD),STATEV(NSTATV),DIRECT(3,3),T(3,3),TIME(2),
     * coord(*),jmac(*),jmtyp(*)
      DIMENSION ARRAY(15),JARRAY(15)

      call getvrm('TEMP',array,jarray,flgray,jrcd,
     1     jmac, jmtyp, matlayo, laccflg)
      TEMP = array(1)

      Crystallization Development:

      STARTTEMP = 126.07
      FINISHTEMP = 110.57

      SCURVE = (-85.1731D0-12.7484D0*TEMP-3.67281D0*TEMP*TEMP-66.3763D0*
     1TEMP*TEMP*TEMP+529.849D0*TEMP*TEMP*TEMP*TEMP-13.0083D0*TEMP*TEMP*
     2TEMP*TEMP*TEMP+0.106611D0*TEMP*TEMP*TEMP*TEMP*TEMP*TEMP-
     30.00029136D0*TEMP*TEMP*TEMP*TEMP*TEMP*TEMP*TEMP)/(-0.0146362D0+
     49.71833D0*TEMP+456.268D0*TEMP*TEMP+13578.7D0*TEMP*TEMP*TEMP-
     5232.956D0*TEMP*TEMP*TEMP*TEMP+TEMP*TEMP*TEMP*TEMP*TEMP)

      FIELD(1)=0.D0
      IF(TEMP.LT.STARTTEMP) FIELD(1)=SCURVE
      IF(TEMP.LT.FINISHTEMP) FIELD(1)=1

      STATEV(3)=FIELD(1)

      RETURN
      END

      SUBROUTINE UEXPAN(EXPAN,DEXPANDT,TEMP,TIME,DTIME,PREDEF,
     1 DPRED,STATEV,CMNAME,NSTATV,NOEL)
      INCLUDE 'ABA_PARAM.INC'
      CHARACTER*80 CMNAME
      DIMENSION EXPAN(*),DEXPANDT(*),TEMP(2),TIME(2),PREDEF(*),
     1 DPRED(*),STATEV(NSTATV)

      Thermal Expansion:

      ALPHA=-1.445894D-8*TEMP(1)*TEMP(1)+5.063871D-6*TEMP(1)-5.562424D-5

      ALPHATT=ALPHA*STATEV(3)
      ALPHAIP=7.29D-6

      STATEV(1)=ALPHAIP
      STATEV(2)=ALPHATT
      EXPAN(1)=ALPHAIP*TEMP(2)
      EXPAN(2)=ALPHATT*TEMP(2)
      EXPAN(3)=ALPHAIP*TEMP(2)


      RETURN
      END
```

Figure 6-2 USDFLD and UEXPAN user subroutines written in FORTRAN

6.2.3 Boundary Conditions

6.2.3.1 Thermal Cycle

The thermal cycle is based on the measurements described in Section 5.2. Figure 5-4 shows the temperature of the laminate as a function of analysis time. Based on measurements of the core and surface temperature during forming experiments, shown in Section 5.3, there is a small thermal gradient through the thickness of the laminate. As the laminate is heated, the surface temperature will be higher than the core temperature. Then, as the laminate cools, the thermal profile changes so that the surface temperature is lower than the core temperature. This through thickness thermal gradient is a result of the direction of heat flow into or out of the laminate.

The above thermal cycle is defined in the ABAQUS model to reflect this through thickness temperature gradient. Upon cooling, the surface temperature is taken as 98% of the core temperature. Figure 6-3 shows the through thickness temperature distribution for the heating and cooling parts of the cycle respectively. The thermal gradients are applied over the thermal cycle as shown in Figure 6-4.

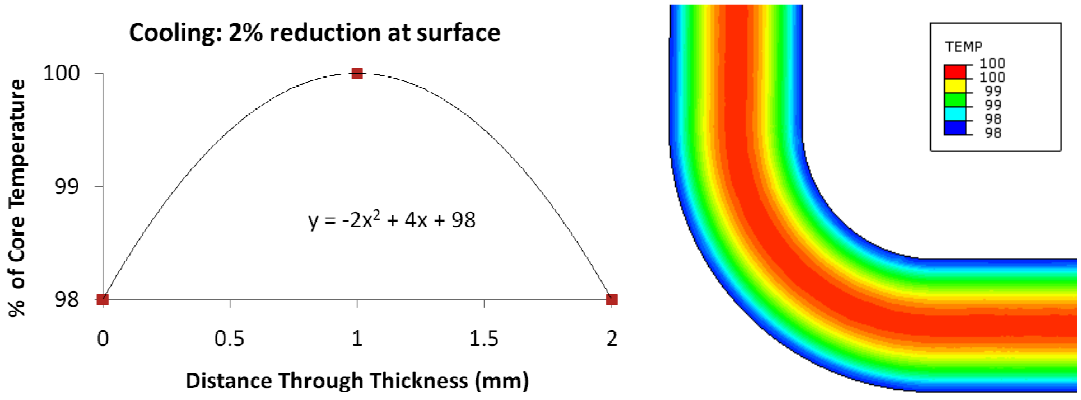

Figure 6-3 Temperature distribution through thickness relative to core, during cooling

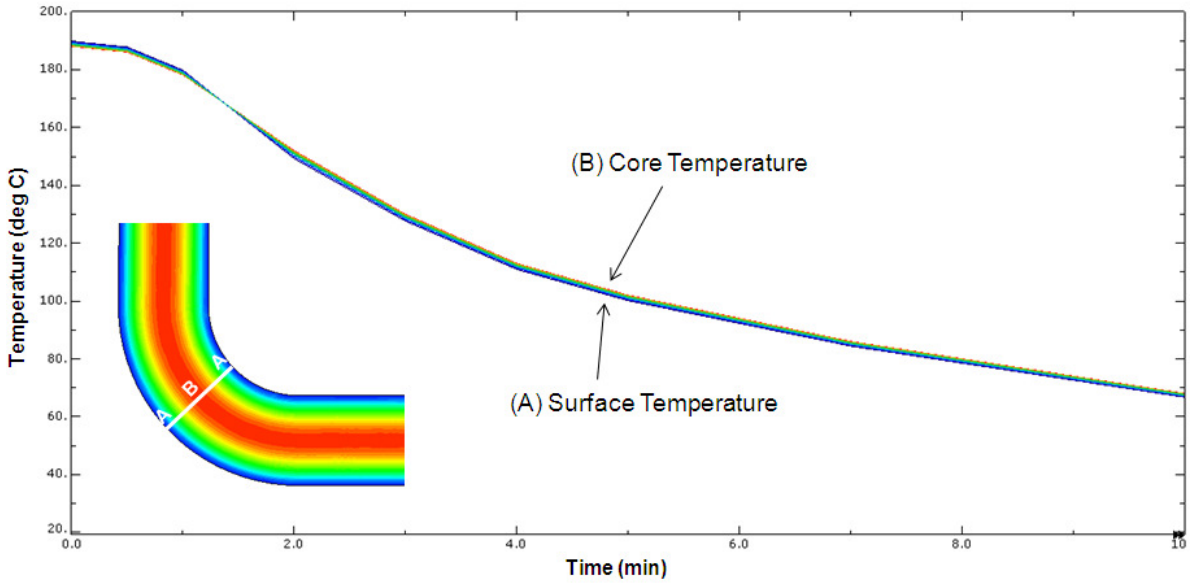

Figure 6-4 Predefined thermal cycle for the simulation model

6.2.4 Analysis Steps

The simulation model contains three distinct analysis steps. The steps are shown in Figure 6-5 to Figure 6-9. In the initial condition, the laminate is at its maximum temperature, corresponding to a point in the process line where the laminate exits the ovens. At this point, the surface temperature is higher than the core temperature. In the first analysis step, the laminate begins to cool and the thermal profile through the thickness switches so that the core is at a higher temperature than the surface. At the end of step 1, the rollers close on the laminate. In step 2, the rollers are held on the laminate for the contact duration. At the end of step 2, the rollers begin to release from the laminate. Finally in step 3, the laminate is free to deform as it cools to a uniform room temperature.

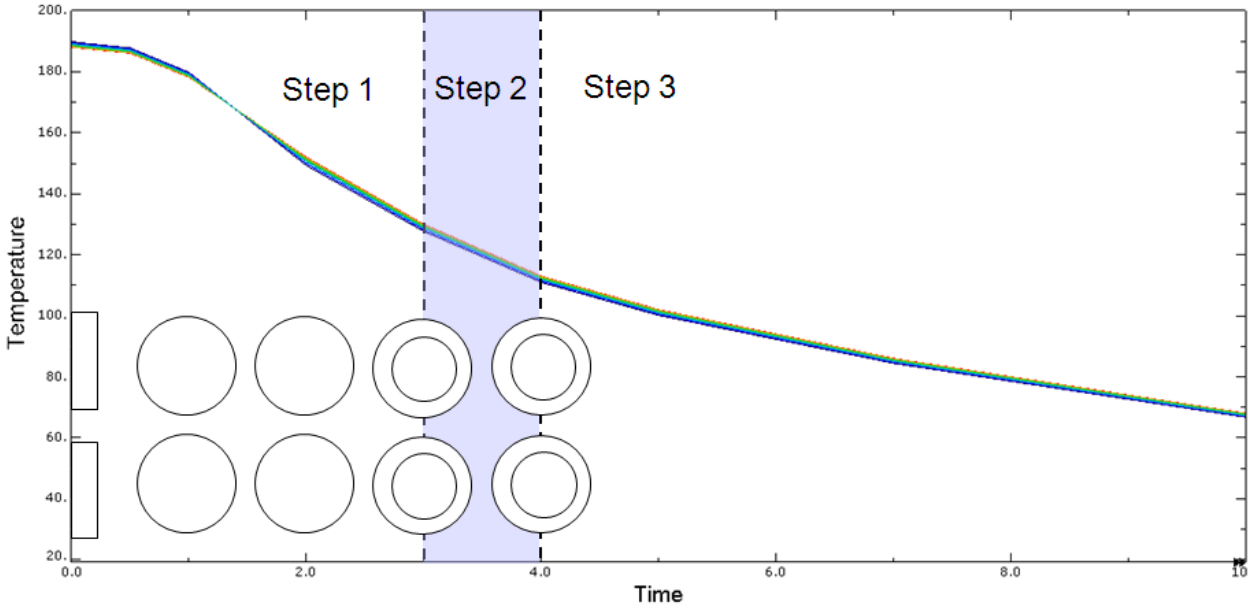

Figure 6-5 Analysis steps of the FE model

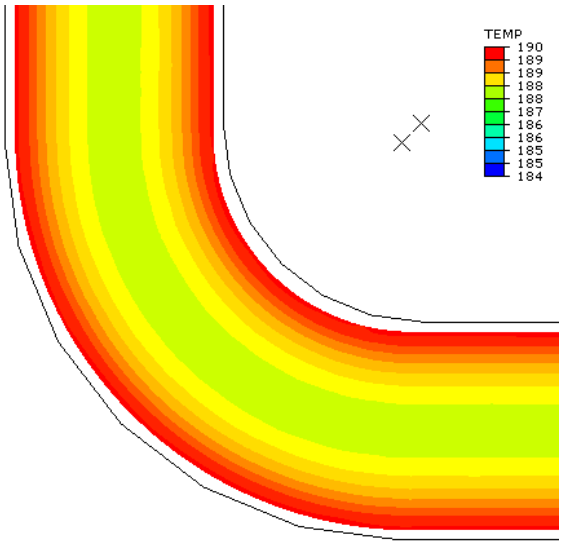

Figure 6-6 Corner section at initial condition: surface at higher temperature than core and no contact between rollers and laminate

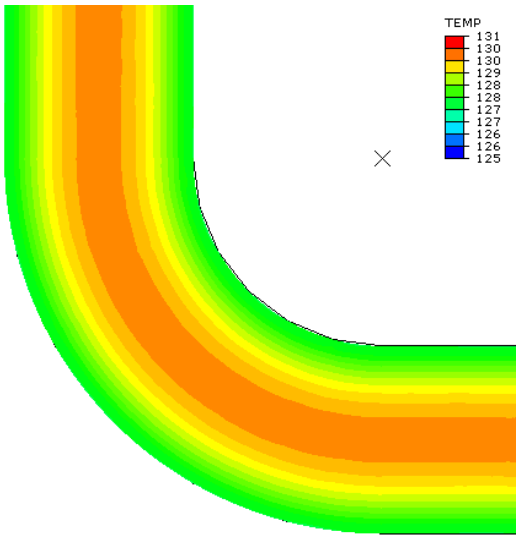

Figure 6-7 Corner section at the end of Step 1: surface is at a lower temperture than the core and rollers have closed on to the lamiante

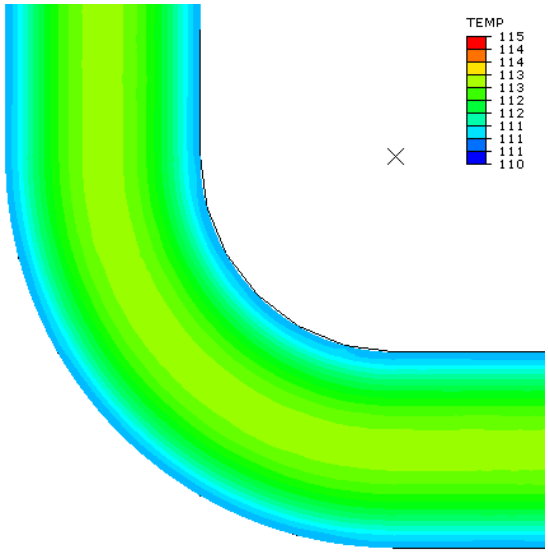

Figure 6-8 Corner section at the end of Step 2: end of the hold time, rollers about to release from the laminate

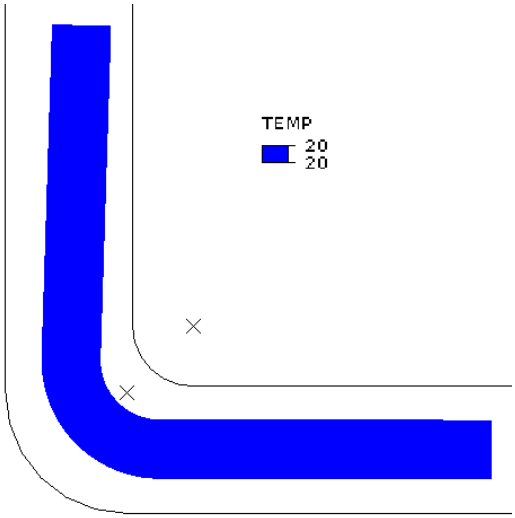

Figure 6-9 Whole model at the end of Step 3 and final condition: laminate is at 20°C, rollers are released from laminate.

6.2.5 Mesh

Plain stress elements are selected for the 2D mesh despite a geometry that would typically suggest using a plain strain condition (since the third direction is very long). The plain stress condition ensures that the deformations in the final condition are calculated with zero mechanical stress in all directions, given the load-free state. Equation 6-3, 6-4 and 6-5 are derived from the constitutive equation for an orthotropic material including orthotropic thermal expansion. Equation 6-3 shows how if plain strain conditions were used, and ε_{33} is set to zero, there would be an amount of stress in the third direction ($\sigma_{33} = -\alpha_3 \Delta T E_3$). Equation 6-4 and 6-5 shows how if σ_{33} is not zero, it can influence the in plane deformation. By assuming plain stress conditions, the stress in the third direction is forced to be zero and any deformation is a result of in plane thermal strains only.

$$\sigma_{33} = E_3(\varepsilon_{33} - \alpha_3 \Delta T) \qquad \text{Equation 6-3}$$

$$\varepsilon_{11} = \frac{\sigma_{11}}{E_1} - \frac{\nu_{12}\sigma_{22}}{E_2} - \frac{\nu_{13}\boldsymbol{\sigma_{33}}}{E_3} + \alpha_1 \Delta T \qquad \text{Equation 6-4}$$

$$\varepsilon_{22} = \frac{\sigma_{22}}{E_2} - \frac{\nu_{12}\sigma_{11}}{E_1} - \frac{\nu_{23}\boldsymbol{\sigma_{33}}}{E_3} + \alpha_2 \Delta T \qquad \text{Equation 6-5}$$

Here, indices 1 and 3 are taken to be the fibre directions and 2 to be the through thickness direction of the laminate. The 1-2 plane is the cross section used in the 2D analysis.

A mesh convergence study was performed to find an appropriate mesh size and element type. Four different element types were selected including, by ABAQUS naming conventions: CPS4, CPS4R, CPS8 and CPS8R. Each element type is described as follows:

CPS4: 4-node bilinear plane stress quadrilateral

CPS4R: 4-node bilinear plane stress quadrilateral, reduced integration

CPS8: 8-node biquadratic plane stress quadrilateral

CPS8R: 8-node biquadratic plane stress quadrilateral, reduced integration

The mesh was generated by defining the number of elements through the thickness of the laminate and then sweeping the elements along the fibre direction. The mesh convergence study started with 2 elements through the thickness and continuously increased the number of elements until convergence of the spring-in angle was found. Table 6-2 and Figure 6-10 show the results of this convergence study.

Table 6-2 Mesh convergence study for plain stress quadrilateral elements

Element Type:		**CPS4**		**CPS4R**		**CPS8**		**CPS8R**	
Number of elements through the thickness	**Total number of elements**	**Angle**	**Run time (min)**	**Angle**	**Run time (min)**	**Angle**	**Run time (min)**	**Angle**	**Run time (min)**
2	**52**	1.1880	0.65	1.6921	0.65	1.7405	0.85	1.7448	0.82
5	**340**	1.6673	0.92	1.7381	0.77	1.7449	1.85	1.7450	0.98
10	**1340**	1.7205	1.68	1.7435	1.52	1.7427	3.42	1.7450	2.98
15	**3030**	1.7351	4.65	1.7443	2.62	1.7427	9.05	1.7449	7.22
20	**5340**	1.7394	7.77	1.7424	3.50	1.7427	16.10	1.7448	11.03
30	**12000**	1.7402	8.62	1.7448	9.02	1.7427	26.53	1.7449	26.25
40	**21440**	1.7413	21.80	1.7426	11.43	1.7427	38.24	1.7437	35.35

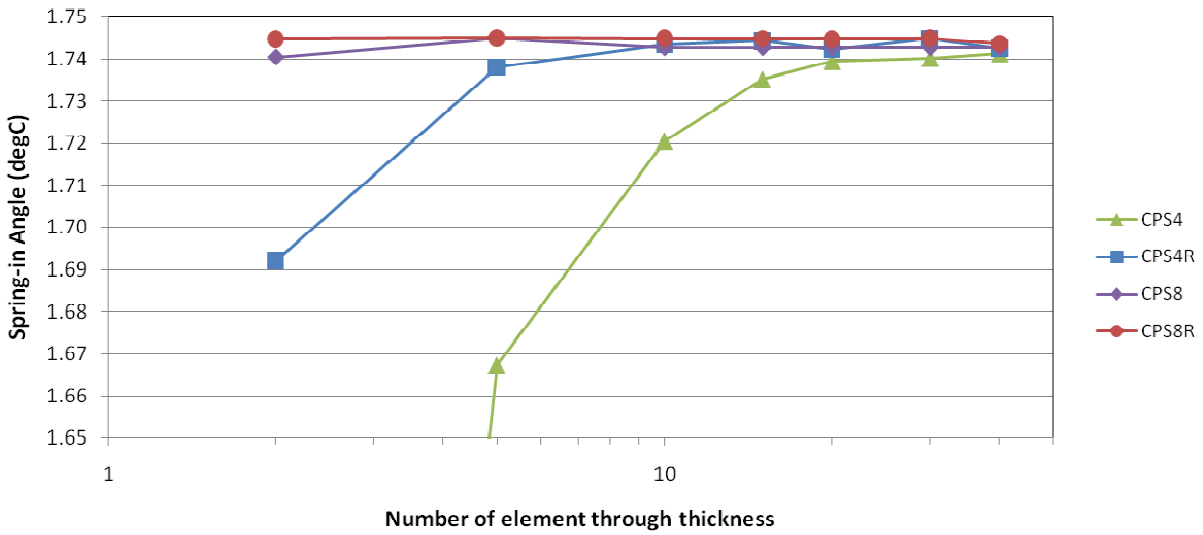

Figure 6-10 Mesh convergence study for plain stress quadrilateral elements

Elements CPS8 and CPS8R showed very good convergence at a low number of elements. Elements CPS4 and CPS4R showed some convergence but continued to fluctuate depending on the number of elements. Therefore, CPS8R elements were selected in the analysis since they show very good convergence and short analysis times. A distribution of 10 elements through the thickness with a total of 1340 elements is selected as shown in Figure 6-11.

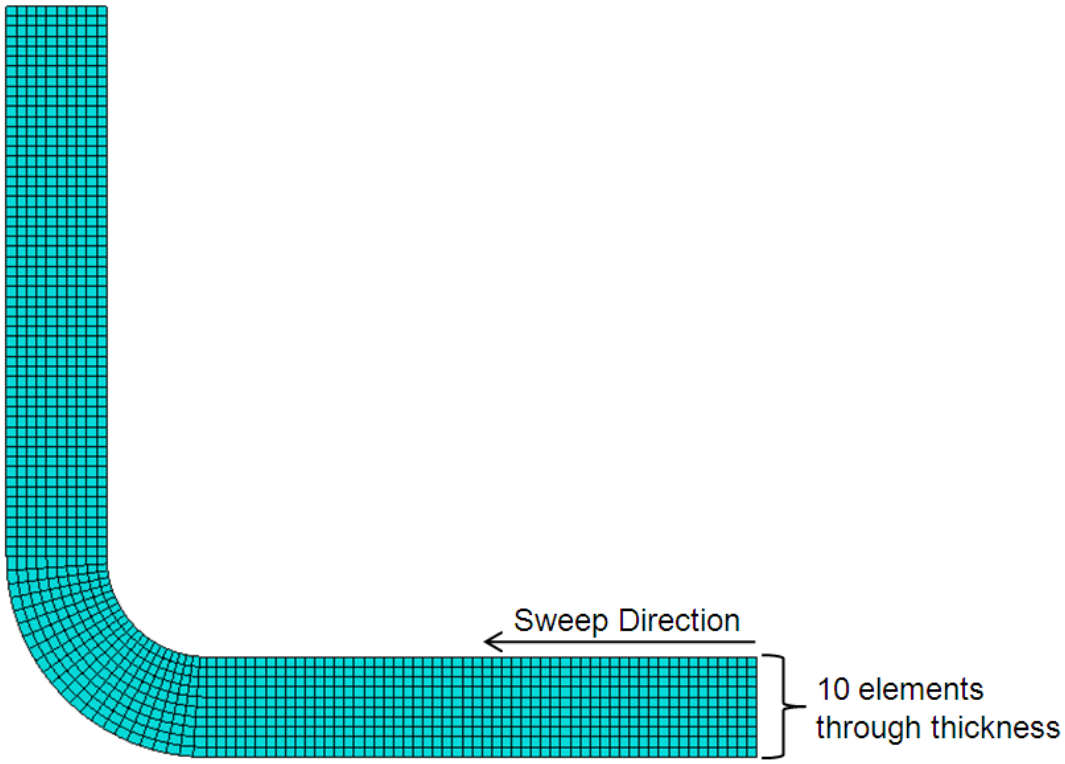

Figure 6-11 Selected mesh distribution of the layup cross section with 1340 CPS8R elements

6.2.6 Results

The simulation model results are summarized in Figure 6-12 and Figure 6-13. Figure 6-12 shows how the relative crystallinity develops over time. Due to the thermal gradient present through the thickness of the laminate, crystallization starts at the surface and progresses towards the core. It is interesting to note where the crystallization process occurs relative to the forming rollers (shown in Figure 6-12). The thermal cycle and roll forming set-up that were used to define the current model were based on previous trial and error iterations at AS Composites to produce high quality final parts. The simulation model shows that these trial and error iterations were indeed successful at positioning crystallization at the ideal point in the process line. Figure 6-12 shows that no crystallization occurs before the laminate enters the first forming stage. This allows the laminate to be deformed freely from a flat state in the compaction rollers to a V-shape

in the forming roller. If any crystallization did occur before the first forming roller, the deformation would induce elastic and potentially plastic deformations that could damage the quality of the final part. Also, Figure 6-12 shows that the crystallization transition is very close to complete at the exit of the last forming stage. The surface of the laminate and the majority of the thickness are at a relative crystallinity of 1, while the core is at a relative crystallinity of 0.96 at the exit point. If the majority of the crystallization transition occurred after the exit of the last forming stage, the formed laminate would fall open under its own weight and crystallize while not under pressure. This could also appear to be a spring-back like deformation. Therefore, the simulation model confirms that the crystallization transition occurs during an optimum period in the process line (i.e. almost entirely between the two forming roller stages).

Figure 6-13 shows the spring-in development over time in the process. There is no spring-in until the exit of the laminate from the last forming stage. Since the majority of the crystallization transition occurs before this stage, there is an initial instantaneous elastic spring-in deformation at the exit due to the release of contact stresses from the tool. Figure 6-14 shows the stress distribution in the fibre direction at the instant before the laminate exits the last set of forming rollers. As expected, there are tensile tresses on the inside radius and compressive stresses on the outside radius due to the forming rollers constraining the laminate from springing in. The stresses are very small since crystallization occurs very close to the exit of the last forming roller. After exiting the forming rollers, the laminate is allowed to deform freely and the stresses reduce to zero. The initial elastic spring-in at the exit of the forming rollers is small at only 0.05^{o}. As the laminate cools to the room temperature, the spring-in angle increases until its final (room temperature) value of 1.74^{o}, shown in Figure 6-13.

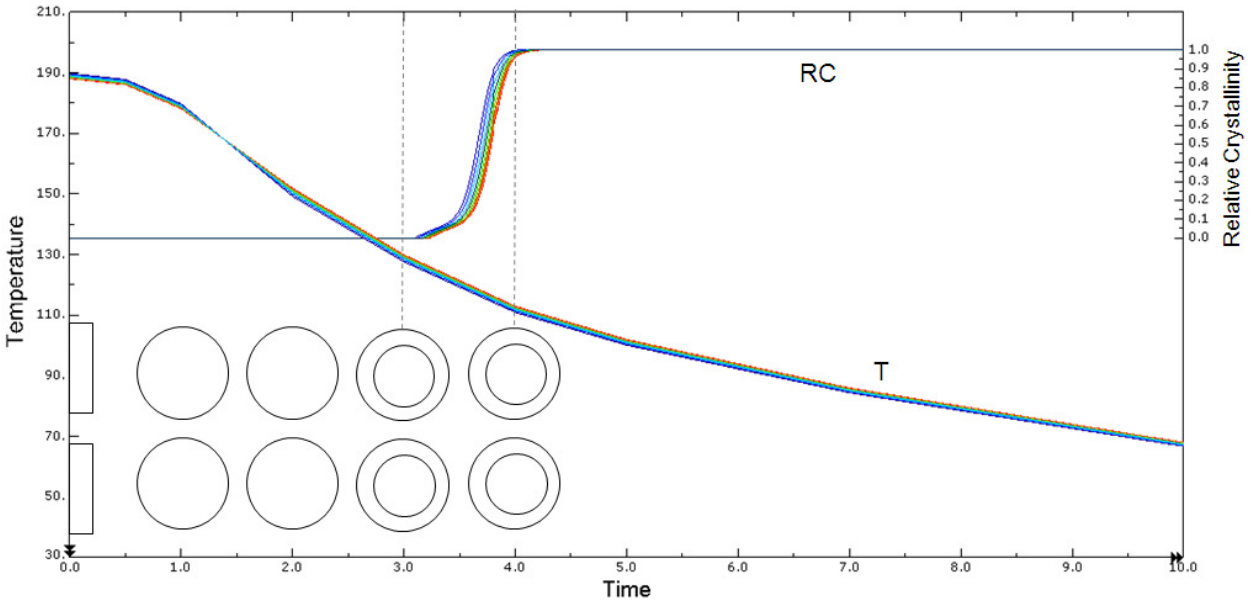

Figure 6-12 The temperature and RC variations with time during the roll forming process; the majority of the matrix crystallization occurs between the forming stages; at the exit roll, the RC is almost equal to one for the entire laminate

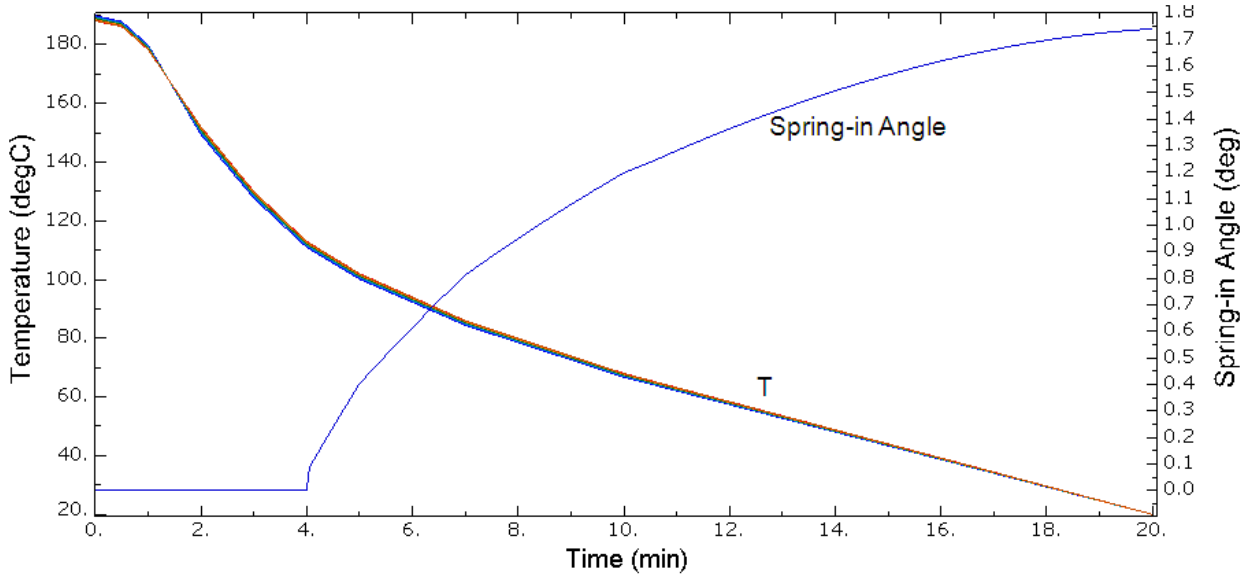

Figure 6-13 Spring-in angle development

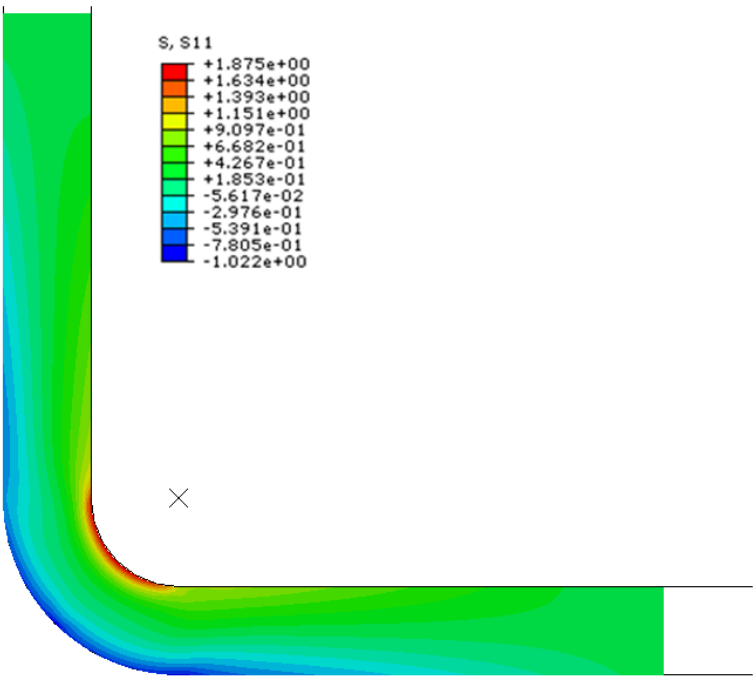

Figure 6-14 Fibre direction stress distribution at the instant before exiting the last forming rollers

6.2.7 Sensitivity Analysis

A sensitivity analysis was performed on Model 1 in order to identify the input factors that have the greatest effect on the spring-in angle prediction. Six factors were chosen as the relevant input parameters. These factors are: the relative crystallinity, the through thickness coefficient of thermal expansion, the thermal cycle, the corner inner radius, the laminate thickness and the Young's modulus. High and low values were selected for each factor and a 2^6 full factorial design of experiments analysis was conducted. High and low values for the relative crystallinity (RC) were also taken as a plus or minus two degree shift of the RC S-curve as shown in Figure 6-15. For the through thickness coefficient of thermal expansion, high and low values were taken as the maximum and minimum sample results from the TMA testing (described in Section 4.2) and are shown in Figure 6-16. High and low values for the thermal cycle were taken from the bounding limits defined by AS Composites Inc. as the processing window for high quality parts.

These limits are shown in Figure 5-4 and the high and low values shown in Figure 6-17. High and low values for the corner radius and laminate thickness were selected to be 2mm and 3mm. Finally, high and low values for the Young's modulus were also taken as the maximum and minimum sample values from tensile testing as described in Section 4.1. The selected high and low values for all of the factors are summarized in Table 6-3.

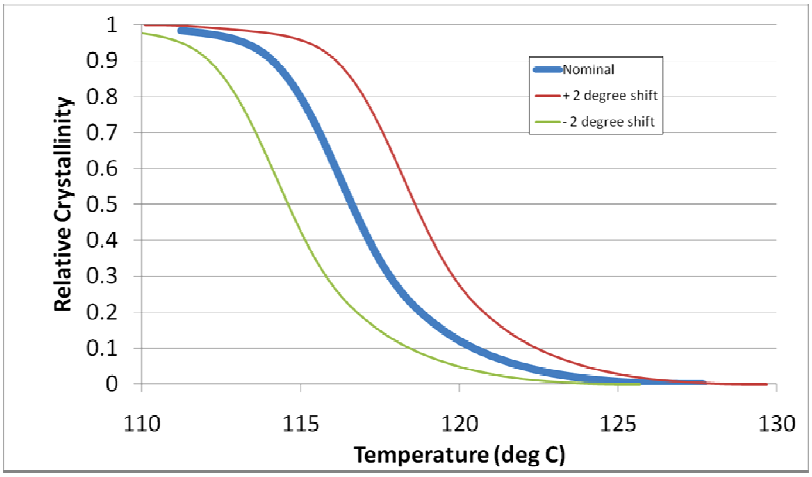

Figure 6-15 High and low values of relative crystallinity

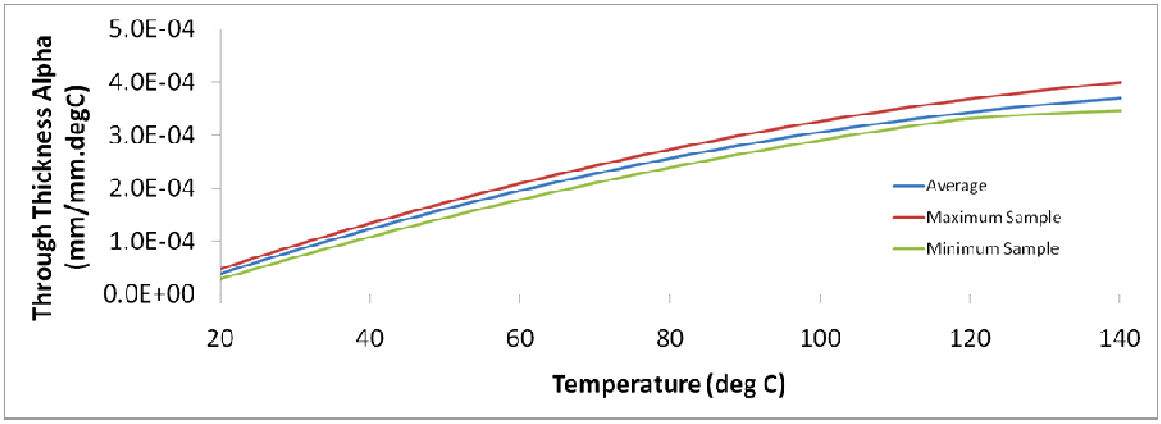

Figure 6-16 High and low values of the through thickness coefficient of thermal expansion

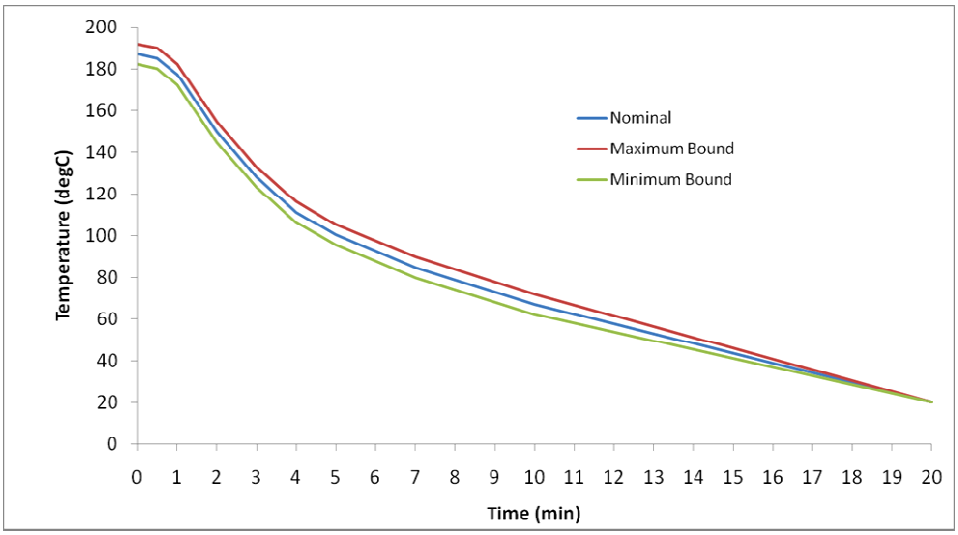

Figure 6-17 High and low values of the thermal cycle

Table 6-3 High and low values for sensitivity analysis

Label	Factor	High (+)	Low (-)
A	Relative crystallinity	+2 °C	-2 °C
B	Through thickness coefficient of thermal expansion	max data	min data
C	Thermal cycle	+5 °C	-5 °C
D	Young's Modulus	max data	min data
E	Thickness	3mm	2mm
F	Radius	3mm	2mm

The results of the 2^6 full factorial analysis are shown in Table 6-4 where the final, room temperature spring-in angle is calculated from the corresponding FE model for each combination of the factors. For a general factor 'Z', the effect estimate, sum of squares and percent contribution of each main factor can be found by Equation 6-6, 6-7 and 6-8 respectively and are shown in Table 6-5.

$$effect(Z) = \bar{y}_{Z+} - \bar{y}_{Z-} \qquad \text{Equation 6-6}$$

where $\bar{y}_{Z+}$and $\bar{y}_{Z-}$ are the average response when factor Z is high or low respectively.

$$SS_Z = b\sum_{i=1}^{a}(\bar{y}_{Z_i} - \bar{\bar{y}})^2 \qquad \text{Equation 6-7}$$

where a=2 is the number of levels of Z and b=32 is the number of replicates at each level.

$$\%\, Contribution = {SS_Z}/{SS_T} \qquad \text{Equation 6-8}$$

where SS_T is the total sum of squares.

Table 6-4 Results of a 2^6 full factorial design-of-experiments analysis

experiment #	A	B	C	D	E	F	Angle (deg)
1	-	-	-	-	-	-	1.5492
2	+	-	-	-	-	-	1.6654
3	-	+	-	-	-	-	1.8100
4	+	+	-	-	-	-	1.9414
5	-	-	+	-	-	-	1.5437
6	+	-	+	-	-	-	1.6610
7	-	+	+	-	-	-	1.8045
8	+	+	+	-	-	-	1.9370
9	-	-	-	+	-	-	1.5492
10	+	-	-	+	-	-	1.6654
11	-	+	-	+	-	-	1.8100
12	+	+	-	+	-	-	1.9414
13	-	-	+	+	-	-	1.5437
14	+	-	+	+	-	-	1.6610
15	-	+	+	+	-	-	1.8045
16	+	+	+	+	-	-	1.9370
17	-	-	-	-	+	-	1.5493
18	+	-	-	-	+	-	1.6655
19	-	+	-	-	+	-	1.8101
20	+	+	-	-	+	-	1.9415
21	-	-	+	-	+	-	1.5437
22	+	-	+	-	+	-	1.6611
23	-	+	+	-	+	-	1.8045
24	+	+	+	-	+	-	1.9371
25	-	-	-	+	+	-	1.5493
26	+	-	-	+	+	-	1.6655
27	-	+	-	+	+	-	1.8101
28	+	+	-	+	+	-	1.9415
29	-	-	+	+	+	-	1.5437
30	+	-	+	+	+	-	1.6611
31	-	+	+	+	+	-	1.8045
32	+	+	+	+	+	-	1.9371

experiment #	A	B	C	D	E	F	Angle (deg)
33	-	-	-	-	-	+	1.5498
34	+	-	-	-	-	+	1.6661
35	-	+	-	-	-	+	1.8108
36	+	+	-	-	-	+	1.9421
37	-	-	+	-	-	+	1.5443
38	+	-	+	-	-	+	1.6617
39	-	+	+	-	-	+	1.8052
40	+	+	+	-	-	+	1.9378
41	-	-	-	+	-	+	1.5498
42	+	-	-	+	-	+	1.6661
43	-	+	-	+	-	+	1.8108
44	+	+	-	+	-	+	1.9421
45	-	-	+	+	-	+	1.5443
46	+	-	+	+	-	+	1.6617
47	-	+	+	+	-	+	1.8052
48	+	+	+	+	-	+	1.9378
49	-	-	-	-	+	+	1.5496
50	+	-	-	-	+	+	1.6658
51	-	+	-	-	+	+	1.8105
52	+	+	-	-	+	+	1.9418
53	-	-	+	-	+	+	1.5440
54	+	-	+	-	+	+	1.6614
55	-	+	+	-	+	+	1.8049
56	+	+	+	-	+	+	1.9374
57	-	-	-	+	+	+	1.5496
58	+	-	-	+	+	+	1.6658
59	-	+	-	+	+	+	1.8105
60	+	+	-	+	+	+	1.9418
61	-	-	+	+	+	+	1.5440
62	+	-	+	+	+	+	1.6614
63	-	+	+	+	+	+	1.8049
64	+	+	+	+	+	+	1.9374

Table 6-5 Effect, sum of squares and percent contribution of each factor

Label	Factor	Effect	Sum of Squares	% Contribution
A	Relative crystallinity	0.1244	0.248	17.67
B	Through thickness coefficient of thermal expansion	0.2684	1.153	82.30
C	Thermal cycle	-0.0050	3.98E-04	2.84E-02
D	Young's Modulus	0.0000	3.16E-30	2.25E-28
E	Thickness	-0.0001	1.64E-07	1.17E-05
F	Radius	0.0005	4.04E-06	2.89E-04

It can be seen from Table 6-5 that the relative crystallinity and the through thickness coefficient of thermal expansion have significantly higher effect on the spring-in angle than the other factors. This was expected to be the case for the elastic model since it is the anisotropic thermal properties as well as the difference between the crystallization temperature and room temperature that are the primary driver for spring-in (see Section 2.3.1.1). The thermal cycle has very little effect on the final spring-in value in this case because we have defined the relative crystallinity to be a direct function of temperature. While a shift of the thermal cycle will affect when crystallization occurs, it will not change the overall temperature difference between the crystallization temperature and room temperature. However, a change in the slope of the thermal cycle, i.e. a change in the cooling rate, will affect the crystallization temperature and, therefore, the spring-in. Further DSC tests would be needed to characterize the effect of different cooling rates.

The effect of the relative crystallinity and through thickness coefficient of thermal expansion is shown in Figure 6-18, including the intermediate nominal levels of each factor. It

can be seen that, by varying the relative crystallinity and/or the through thickness coefficient of thermal expansion within the selected margin, the spring-in value can vary significantly: from 1.54° to 1.94°. The predicted spring-in angle from Model 1, with elastic mechanical properties is, therefore, found to be: 1.74° ± 0.20°.

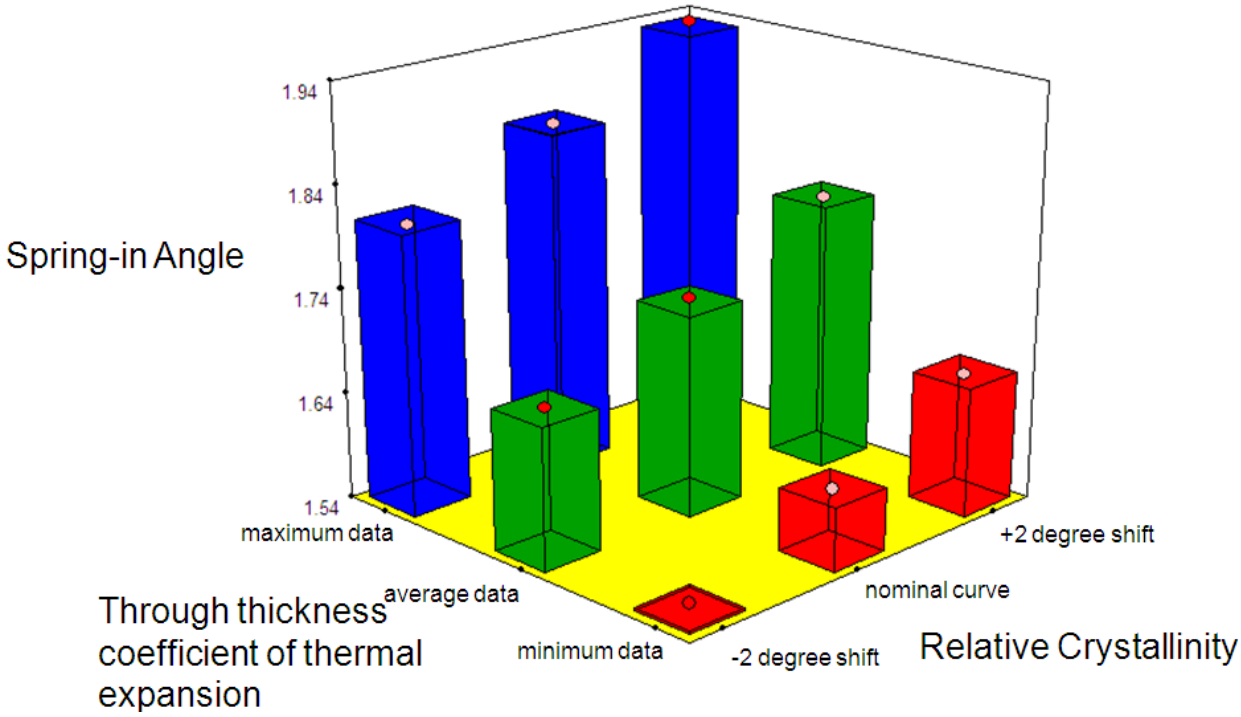

Figure 6-18 Effect of the relative crystallinity and the through thickness coeficient of thermal expansion on the spring-in angle prediction

6.2.8 Summary

A finite element model of the roll forming process was developed using orthotropic, elastic mechanical and thermal properties (Model 1). In order to model the crystallization process, a new state variable was defined based on DSC testing. With this state variable, the material properties were defined twice in ABAQUS: once for properties of the melted matrix and once for properties of the crystallized matrix. The state variable was then used to describe the

change of properties during crystallization. The model geometry and boundary conditions are defined to be specific to a roll forming process, however, they can easily be extended to other manufacturing processes, such as compression moulding, vacuum bagging or stamping. It was found that for the roll forming case, since crystallization happens very close to the exit of the last forming roller, there are only small internal stresses that develop due to constraining the laminate. The initial elastic spring-in was also very small. For roll forming the majority of the spring-in angle develops after the laminate exits the last forming roll and is free to deform. Because of this lack of mechanical constraint, the predicted spring-in angle is very close to what is given by O'Neill's equation (Equation 2-3). A sensitivity analysis was performed on Model 1 revealed that the two dominating factors that affect the final spring-in angle are the relative crystallinity and the through thickness coefficient of thermal expansion. Since a change to the relative crystallinity is equivalent to changing the crystallization start temperature, the dominating factors found in the sensitivity analysis are the same as the factors in O'Neill's equation. This equivalency between the model and O'Neill's equation is expected for the case where elastic orthotropic material properties are used, since the underlying mechanisms are the same. The second order mechanisms must now be considered, described in Section 2.3.1 , specifically, the inclusion of a time dependant viscoelastic material model.

6.3 Model 2: Using Viscoelastic Mechanical Properties

The geometry and boundary conditions used for Model 2 are the same as those described for Model 1 in Section 6.2. Model 2, however, incorporates a viscoelastic material model in order to capture the stress relaxation mechanism described in Section 2.3.1.4 . For this mechanism, stresses that develop due to the constraint of the laminate in the rollers are allowed

to relax over time. For Model 1, the stress distribution at the instant before the laminate exits the last forming rollers is shown in Figure 6-14. With a viscoelastic material model and given a sufficient amount of time, these stresses would relax and the final spring-in angle would be reduced. Model 2 incorporates a viscoelastic material model to investigate whether or not this viscoelastic stress relaxation mechanism will have a significant effect on the final spring-in angle.

In order for this mechanism to be captured by the model, a coupled thermal-stress analysis is performed. In the elastic model (Model 1), the thermal and mechanical solutions are found sequentially. Strains are calculated based on the imposed thermal boundary conditions and the material thermal expansion properties only. Stresses are then found in a later step using the specified modulus values. By performing a coupled thermal-stress analysis for the viscoelastic model (Model 2), the thermal and mechanical solutions are found simultaneously. Therefore, at each integration point, stresses, strains and temperatures are solved for together and a changing level of stress (due to the viscoelastic material model) can affect the strains and ultimately the spring-in angle. Model 2 uses the same mesh distribution as described in Section 6.2.5 but with CPS8RT elements, as described below.

CPS8RT: 8-node plane stress thermally coupled quadrilateral, biquadratic displacement, bilinear temperature, reduced integration.

6.3.1 Material Properties

A complete thermoviscoelastic material model for Twintex® has not yet been developed in the literature. Further material testing of Twintex® and a full characterization of its viscoelastic properties is planned to be completed in the future by the UBC composites group. At this point, a hypothetical viscoelastic material model is used to demonstrate how the spring-in angle can change with the inclusion of a time-dependant material model. The model uses the built in viscoelastic material model in ABAQUS 6.9.2, which assumes that the dimensionless relaxation modulus is given by the prony series shown in Equation 6-9 (where $G_R(t)$ is the time dependant modulus and G_0 is the instantaneous modulus). Table 6-6 shows the selected values for direct specification of the prony series parameters.

$$G_R(t) = G_0\left[1 - \sum_{i=1}^{N} \bar{g}_i^P \left(1 - e^{-t/\tau_i}\right)\right] \qquad \text{Equation 6-9}$$

Table 6-6 Prony series coeficients for a hypothetical viscoelastic material model

$\bar{g}_i^P$	$\bar{k}_i^P$	τ_i	N
0.9	0	0.9	1

6.3.2 Results and Discussion

Including a viscoelastic material model showed very little effect on the final spring-in value for the given roll forming boundary conditions. This result was expected due to the very short time that the laminate is in contact with the forming rollers after crystallization. The stress build up due to the laminate being constrained by the forming rollers is very small. Figure 6-14 shows that the maximum stress in the laminate is less than 2 MPa and acts for a very short period

of time. Table 6-7 and Figure 6-19 show the very similar spring-in angles from the elastic and viscoelastic models. To check that the model is working correctly and to demonstrate the mechanism, a modified model was run where the hold time of the forming roller is artificially extended so that it constrains the laminate for a very long time and higher stresses build up. Table 6-7 and Figure 6-19 also show the results of the modified model, which has a final spring-in angle 0.27^{o} less than the unmodified models. This modified viscoelastic model shows how the viscoelastic stress relaxation mechanism can affect the spring-in angle for manufacturing processes, such as compression moulding, vacuum bagging or stamping, where the hold time is long. For roll forming, it appears that it is not necessary to include a macro level viscoelastic material model in the spring-in angle prediction. However, this conclusion will be revisited when a viscoelastic material model is available for Twintex®.

Table 6-7 Spring-in angle comparison for elastic and viscoelastic material models with a normal or extended hold period.

Model	Spring-in Angle
Elastic material properties (Model 1)	1.744^{o}
Viscoelastic material properties (Model 2)	1.742^{o}
Viscoelastic material properties with extended hold	1.470^{o}

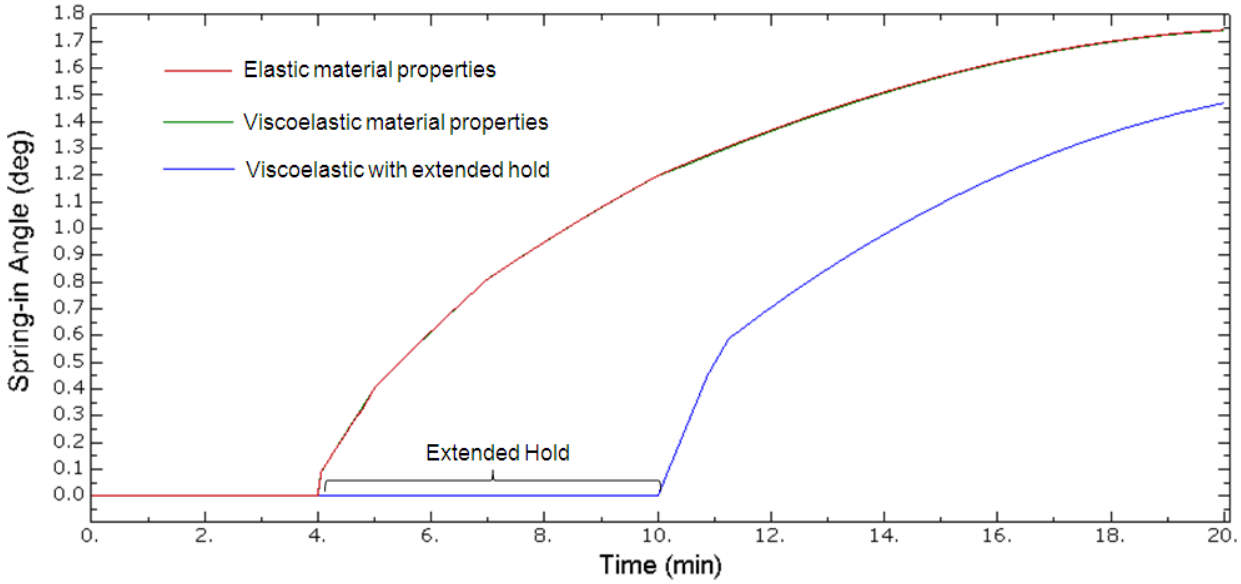

Figure 6-19 Spring-in angle comparison for the elastic and viscoelastic material models with a normal and extended hold period.

6.4 Model 3: Pseudo Meso-Level Decomposition

The geometry and boundary conditions used for Model 3 are the same as those described for Model 1 and Model 2 in Sections 6.2 and 6.3, respectively. Model 3, however, incorporates a decomposition of the laminate cross-section into subdomains that represent the behaviour of the fibres and matrix individually. This is referred to as a pseudo meso-level decomposition, since a true meso-level decomposition would model the fibres and matrix exactly, whereas this study uses subdomains that represent their equivalent behaviour. This decomposition will demonstrate the effect of viscoelastic relaxations of internal residual stresses on the spring-in angle. For this mechanism, described in Section 2.3.1.7 , the model is modified so that the different internal stresses present in the fibres and matrix constituents of the composite are identified uniquely. Figure 6-20 shows how the cross section of the laminate is modified so that each ply of the laminate is modeled with three subdomains: a center subdomain with orthotropic elastic material properties to represent the behaviour of the fibres and two surrounding subdomains with

isotropic viscoelastic material properties to represent the behaviour of the matrix. The size of each subdomain is defined to be consistent with the weight percent of fibres in Twintex® (60wt% fibres). The mesh and element type are the same as for Model 2 with 1340 CPS8RT elements.

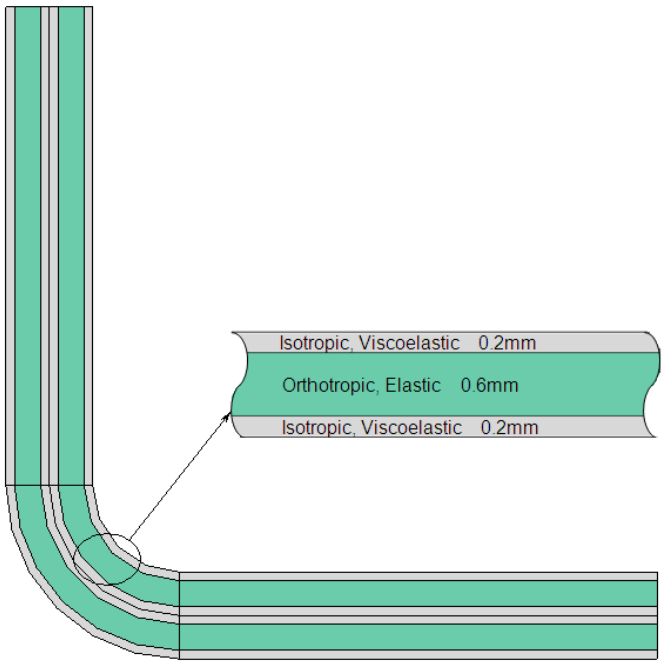

Figure 6-20 Decomposition of the laminate cross section into subdomains representing the behaviour of the fibre and matrix constituents

6.4.1 Results and Discussion

Figure 6-21 shows the residual stress distribution in the in-plane direction (fibre direction). The through thickness stress is uniformly equal to zero since the thermal expansion of each subdomain is unrestricted by adjacent subdomains in this direction. The stress in the in-plane direction is compressive in the fibre subdomains and tensile in the matrix subdomains. The stress magnitudes in the two subdomains are equal and opposite.

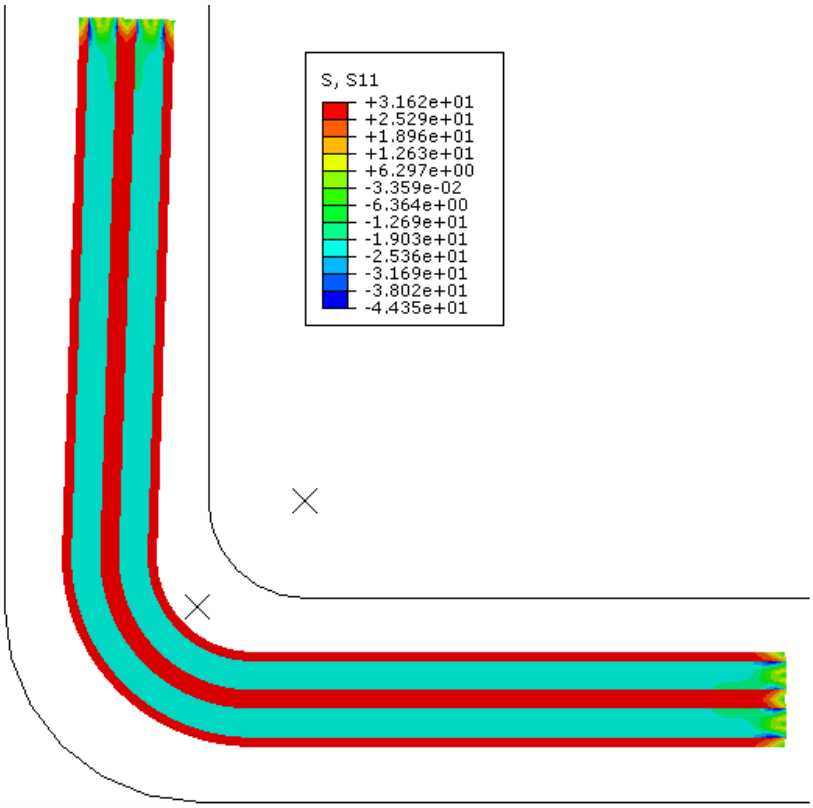

Figure 6-21 In-plane (fibre direction) residual stress distribution at room temperature

Figure 6-22 shows how including the pseudo meso-level decomposition along with a viscoelastic material model for the matrix subdomains can lead to an increased spring-in angle. The spring-in angle for Model 3 is 1.895°, a 0.15° increase over the elastic model. For the purpose of predicting spring-in angles for roll forming Twintex®, including this decomposition may not have a significant effect on the angle prediction. However, it should be noted again that Model 3 was performed with a hypothetical viscoelastic material model and the analysis should be revisited once a complete viscoelastic material model for Twintex® is available.

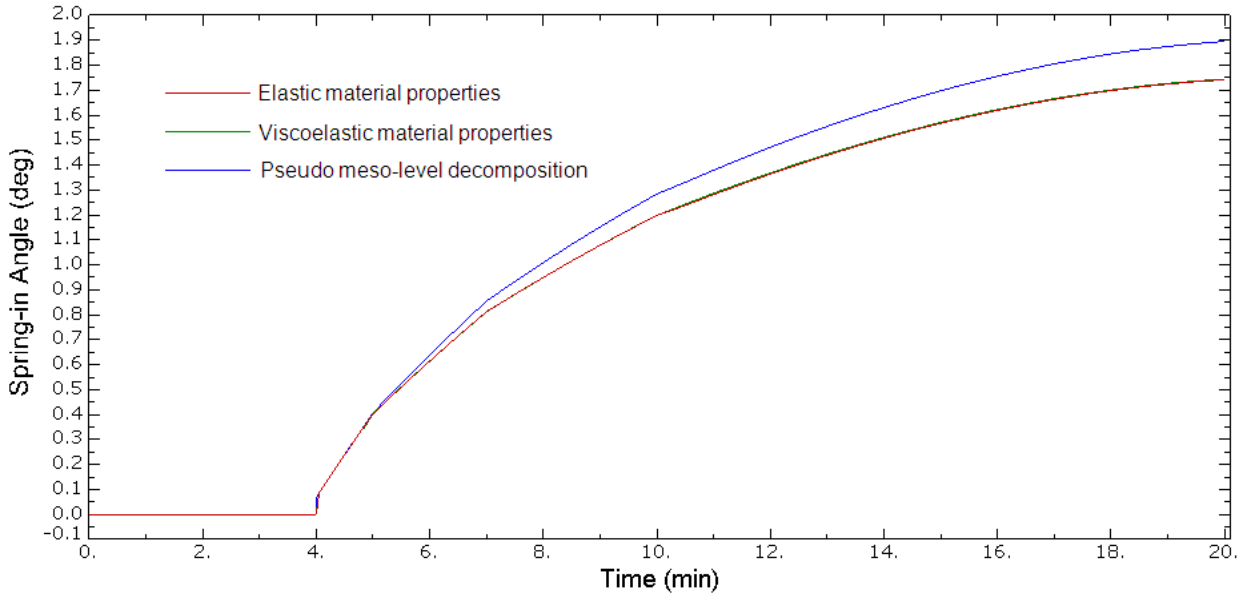

Figure 6-22 Spring-in angle comparison for Model 1 (elastic material properties), Model 2 (viscoelastic material properties), and Model 3 (pseudo meso-level decomposition)

7 Conclusions and Recommendations

The objective of this study was to describe the fundamental mechanisms that lead to spring-in deformations and to investigate a methodology to predict spring-in deformations in thermoplastic matrix composites produced by a roll forming manufacturing technique. A finite element based model of the manufacturing process was developed, which can be used to capture many of the different mechanisms that lead to spring-in. These mechanisms include: anisotropic thermal properties, asymmetric thermal gradients, local matrix rich regions, pre-crystallization modulus development, crystallization shrinkage, stress relaxation of constrained components, and viscoelastic relaxation of internal stresses. It was found that, depending on the manufacturing process, only some of the mechanisms may have a significant affect. For roll forming, the primary driving force for spring-in remains the anisotropy of thermal properties. This mechanism can be adequately predicted by O'Neil's equation as long as the layup is balanced and symmetric (orthotropic). Asymmetric thermal gradients should not have a significant effect on the spring-in angle in roll forming as long as the manufacture adequately controls the process parameters such that heat transfer above and below the laminate are equal. This level of control is an ongoing challenge for manufactures. Similarly, the process should be optimized such that there is no matrix pooling in the corner sections of the laminate. Matrix pooling can significantly increase the spring-in angle and should be monitored and controlled as closely as possible. A small, but potentially meaningful, pre-crystallization modulus development has been observed in some stress relaxation testing. Future work will investigate the presence and impact of this early modulus as well as its relation to crystallization shrinkage. Next, the viscoelastic stress relaxation mechanisms were investigated with subsequent finite element models. It was found that, since crystallization occurs very close to the exit of the last

forming roller, there is very little stress built up due to constrain of the laminate by the tooling. The laminate was quickly released and allowed to cool to room temperature unconstrained. Although this conclusion needs to be revisited with a complete viscoelastic material model for Twintex®, it is expected that for roll forming, stress relaxation of constrained components should not have a significant effect on the spring-in deformation. This mechanism is much more likely to have a significant effect for other manufacturing processes, such as compression moulding, vacuum bagging and stamping, where the amount of time in contact with the mould is much longer. Finally, viscoelastic stress relaxations of internal residual stresses were found to affect the spring-in angle for roll forming. The effect, with a hypothetical viscoelastic model, was found to be small (an increase of 0.1^{o} to 0.2^{o}). The magnitude of this effect should also be re-examined once a complete viscoelastic material model is available.

The manufacturing process model developed in this study can also be used to optimize the manufacturing process. For roll forming of a thermoplastic matrix composite, such as Twintex®, it is important that crystallization of the matrix material occurs at the appropriate point along the process line. The finite element model confirmed that previous trial and error optimization work of the roll forming processing parameters was successful in positioning the crystallization point to be just before the exit of the last forming roller stage. Future optimizations can make use of this finite element model to reduce the trial and error optimization time of a new product. By developing a crystallization kinetics model for Twintex® and a thermal model of the manufacturing process, the method demonstrated in this study can be used to predict the crystallization point and process parameters, which can be optimized, such that crystallization occurs at the optimal position in the process line.

Spring-in variations seen in practice and in the literature are likely the result of a combination of additional factors. Being based on a commodity polymer, Twintex® can be expected to have some variation in the material properties from batch to batch. Most significantly, differences in the thermal expansion coefficient or the weight percent fibres in different material batches will have the largest affect on the spring-in angle. It can also be difficult to control variations in the manufacturing process particularly as the rollers slowly heat as the machine operates. Most significantly, if the thermal cycle changes, such that the cooling rate increases or decreases, this will affect the crystallization temperature. Any change in the crystallization temperature will affect the spring-in angle by changing the magnitude of the temperature difference in O'Neils equation. However, the biggest variations seen in the previously measured spring-in values are likely due to the crystallization point being outside of the optimal position in the manufacturing line. If crystallization occurs too early, the laminate can spring back due to an elastic return. If crystallization occurs too late, the laminate can also appear to spring back due to crystallization occurring outside of the application of pressure and the laminate being allowed to fall open under its own weight. In this study, it was shown that O'Neils equation can give a reasonable prediction of the spring-in angle as long as the process is properly optimized, such that the crystallization point is well understood.

For roll forming, the recommendation moving forward is to use a crystallization kinetics model as well as the finite element model presented in this study to optimize the process so that crystallization occurs at the optimal location in the process line. Once the process has been optimized, O'Neils equation, or an orthotropic thermoelastic finite element model, should give

an acceptable prediction of the spring–in angle. For other manufacturing processes, such as compression moulding, vacuum bagging or stamping, a thermoviscoelastic material model would be required to arrive at accurate spring-in angle predictions.

While the current project has developed the methodology for making spring-in angle predictions for roll forming, future projects within the composites group at UBC will focus on: developing complete crystallization kinetics models for Twintex®, developing a heat transfer model of the roll forming process, developing a thermoviscoelastic material model for Twintex® and validating the prediction with full scale experiments. Finally, it is recommended that the techniques developed in this study are extended to include other manufacturing processes for thermoplastic matrix composites.

Bibliography

Advani, S. G., & Sozer, M. E. (2003). *Process Modeling in Composites Manufacturing*. New York: Marcel Dekker Inc.

Alsamhan, A., Pillinger, I., & Hartely, P. (2004). The development of real time re-meshing technique for simulating cold-roll-forming using FE methods. *Journal of Materials Processing Technology , 147*, 1-9.

Arafath, A., Vaziri, R., & Poursartip, A. (2008). Closed-form solution for process-induced stresses and deformation of a composite part cured on a solid tool: Part I – Flat geometries. *Composites: Part A 39 (2008) 1106–1117 , 39*, 1106–1117.

Barnes, J. A., Byerly, G., LeBouton, M. C., & Zahlan, N. (1991). Dimensional stability effects in thermoplastic composites - towards a predictive capability. *Composites Manufacturing , Vol 2 No 314*, 171-178.

Borazghi, H., Boucher, D. T., Denault, J., & Fisa, B. (2008). Continuous Consolidation of Polypropylene/Glass Fibre Commingled Fabric. *Polymers & Polymer Composites vol.16 no.1 , 16*.

Dykes, R. J., Mander, S. J., & Bhattacharyya, D. (2000). Roll forming continuous fibre-reinforced thermoplastic sheets: experimental analysis. *Composites: Part A , 31*, 1395-1407.

Fernlund, G., & Poursartip, A. (2003). Finite element based prediction of process-induced deformation of autoclaved composite structures using 2D process analysis and 3D structural analysis. *Composite Structures , 62*, 223-234.

Fernlund, G., Poursartip, A., Twigg, G., & Albert, C. (2003). Efficient Modelling Techniques for Predicting Processing Residual Stress and Deformation in Composite Parts. *SAMPE* .

Friedrich, K., & Hou, M. (1998). On Stamp Forming of Curved and Flexible Geometry Components from Continuous Glass Fibre/Polypropylene Composites. *Composites Part A* , 217-226.

Furlund, G., Slesinger, N., & Poursartip, A. (2010). Development of a test method to validate cure kinetics models used in process simulation. *SAMPE.* Seatle.

Garstka, T., Cole, G., Irving, D., & Lyons, P. (2010). Using a High Precision Moulding Environment to Deliver 'Right first time' Tooling. *SAMPE.* Seatle.

Gilbert, & Denault, J. (2003). Evaluation of bias-extension and picture-frame test methods for the measurement of intraply shear properties of PP/glass commingled fabrics. *Composite Structures , 61*, 341-352.

Hancock, S. G. (2006). *Forming Woven Fabric Reinforced Composite Materials for Complex Shaped Components.* University of Bristol.

Hellborg, S. (January 2007). Finite Element Simulation of Roll Forming. *Linköping University* .

Holzapfel, G., & Gasser, T. (2001). A Viscoelastic model for fibre-reinforced composites at finite strains: Continuum basis, computational aspects and applications. *Computer Methods in Applied Mechanics and Engineering , 190*, 4379-4403.

Horrigan, D. P., Bhattacharyya, D., & Dykes, R. J. (1997). Numerical Analysis of Shape Fixability of Continuour Fibre Reinforced Thermoplastics. *Proceedings of ICCM-11 , iV*, 352.

Hou, M. (1997). Stamp Forming of Comtinuous Glass Fibre Reinforced Polypropylene. *Composites Part A , 28A*, 695-702.

Hou, M. (1996). Stamp Forming of Fabric-Reinforced Thermoplastic Composites. *Polymer Composites , 17* (4), 596-603.

Hou, M., & Friedrich, K. (1994). 3-D Stamp Forming of Thermoplastic Matrix Composites. *Applied Composite Materials* , 135-153.

Hou, M., & Friedrich, K. (1991). Stamp Forming of Continuous Carbon Fibre / Polypropylene Composites. *Composites Manufacturing , 2*, 3-9.

Hou, M., Friedrich, K., & Scherer, R. (1994). Optimization of Stamp Forming of Thermoplastic Composite Bends. *Composite Structures , 27*, 157-167.

Hubert, P., & Poursartip, A. (2001). A method for the direct measurement of the fibre bed compaction curve of composite prepregs. *Composites: Part A 32 , 32*, 179-187.

Hubert, P., & Vaziriv, R. (1999). A Two-dimensional Flow Model for the Process Simulation of Comples Shape Composite Laminates. *International Journal for Numerical Methods in Engineering , 44*, 1-26.

Jeonga, S. H., Leeb, S. H., Kimb, G. H., Seob, H. J., & Kimb, T. H. (2008). Computer simulation of U-channel for under-rail roll forming using rigid-plastic finite element methods. *Journal of materials processing technology , 201*, 118-122.

Johnston, A., Vaziri, R., & Poursartip, A. (2001). A Plane Strain Model for Process-Induced Deformation of Laminated Composite Structures. *Journal of Composites Materials , 35 no.16*, 1435-1465.

Kim, B., Bernet, N., Sunderland, P., & Manson, J.-A. (2002). Numerical Analysis of the Dimensional Stability of Thermoplastic Composites Using a Thermoviscoelastic Approach. *Journal of Composite Materials, Vol. 36, No. 20 , 36*, 2389-2403.

Lalit, J., & Mai, Y.-W. (1997). Stresses and Deformations Induced during Manufacturing. Part I: Theroretical Analysis of Composite Cylinders and Shells. *Journal of composite materials , 31*, 672-695.

Lalit, L. Y., & Mai, Y.-W. (1998). Spring-in study of the aileron rib manufactured from advanced thermoplastic composite. *Composites Part A , 29A*, 973-979.

Lalit, Y.-W. M., & Paton, R. (1997). Stresses and Deformations Induced during Manufacturing. Part II: A Study of the Spring-in Phenemenon. *Journal of composite materials , 31*, 696-719.

Lebrun, G., & Denault, J. (2010). Effect of annealing on the thermal expansion and residual stresses of bidirectional thermoplastic composite laminates. *Composites Part A , 41*, 101-107.

Lebrun, G., & Denault, J. (2003). Evaluation of bias-extension and picture-frame test methods for the measurement of intraply shear properties of PP/glass commingled fabrics. *Composite Structures , 61*, 341-352.

Lebrun, G., Bureau, M., & Denault, J. (2004). Thermoforming-stamping of Continuous Glass Fibre/Polypropylene Composites: Interlaminar and Tool–Laminate Shear Properties. *Journal of thermoplastic composite materials , 17*, 137-165.

Li, H., Foschi, R., Vaziri, R., Furlund, G., & Pousartip, A. (2002). Probability-Based Modelling of Composites Manufacturing and its Application to Optimal Process Design. *Journal of Composite Materials, Vol. 36, No. 16 , 36 no.16*, 1967-1991.

Lindgren, M. (2005). *Modelling and Simulation of the Roll Forming Process.* Luleå University of Technology.

Lord, S. J., & Stringer, L. G. (2009). A modelling approach for prediction residual stresses and distortions in polymer composites. *QINETIQ* .

Lynam, C., & Milani, A. (2010). A Viscoelastic Based Mechanisms for Improving Spring-in Angle Predictions in Compression Moulded Thermoplastic Matrix Composites. *ASME 2010 International Design Engineering Technical Conference & Computers and Information in Engineering Conference.* Montreal Quebec.

Mallick, P., & Ragone, J. C. (2009). the effect of process parameters on the quality of resin infused thermoplastic matrix prepregs. *QINETIQ* .

Manson, J. J. (2001). Material Phenomena controlling rapid processing of thermoplastic composites. *Composites Part A , 32*, 1045-1057.

Mase, T. G., & Mase, G. E. (1999). *Continuum Mechanics for Engineers.* (2, Ed.) London: CRC Press.

McGuinness, G., & Bradaigh, C. M. (1997). Development of rheological models for forming flows and picture frame shear testing of fabric reinforced thermoplastic sheets. *Journal of non-newtonian fluid mechanics , 73*, 1-28.

McGuinnesst, G. B., & BrBdaigh, C. M. (1998). Characterisation of thermoplastic composite melts in rhombus-shear: the picture-frame experiment. *Composites Part A , 29A*, 115-132.

Menczel, J. D., & Prime, B. P. (2009). *Thermal Analysis of Polymers - Fundamentals and Applications.* Hoboken, New Jersey: John Whiley & Sons Inc.

Milani, A. S., Nemes, J., Lebrun, G., & Bureau, M. N. (2009). A Comparative Analysis of a Modified Picture Frame Test for Characterization of Woven Fabrics. *Polymer Composites , DOI 10.1002/pc*, 1-8.

Mlekusch, B. (1999). The warpage of corners in the injection moulding of short-fibre-reinforced thermoplastics. *Composites Science and Technology , 59*, 1923-1931.

Nahie'ne, P. B. (2008). Simulations of textile composite reinforcement draping using a new semi-discrete three node ?nite element. *Composites , 39*, 999–1010.

Nallainathan, L., Liu, X. L., Chiu, W. K., & Jones, R. (2004). Modelling creep behaviour of orthotropic composites by the coincident element method. *Composite Structures , 66*, 409-413.

Nallainathan, L., Liu, X. L., Chiu, W. K., & Jones, R. (2003). Modelling Orthotropic Viscoelastic Behaviour of Composite Laminates Using a Coincident Element Method. *Polymers & Polymer Composites, , 11 no. 8*, 669-677.

Nima, & Poursartip, A. (2010). Computationally effcient pseudo-viscoelastic models for evaluation of residual stresses in thermoset polymer composites during cure. *Composites: Part A , 41*, 247–256.

Ochinero, T., & Hyer, M. (2002). Manufacturing Distortions of Curved Composite Panels. *Journal of Thermoplastic Composite Materials , 15*, 79-87.

O'Neill, J., Rogers, T., & Spencer, A. (1988). Thermally Induced Distortions in the Moulding of Laminated Channel Sections. *Mathematical Engineering in Industry , 2, no.1*, 65-72.

Own, C. S., Suer, D., Dsouza, N., & Brostow, W. (April 1998). Cowoven Polypropylene/Glass Composites With Polypropylene + Polymer Liquid Crystal Interlayers: Dynamic Mechanical and Thermal Analysis. *Polymer Composites , 19 no2*, 107-115.

Papeleux, L., & Ponthot, J.-P. (2002). Finite element simulation of springback in sheet metal forming. *Journal of Materials Processing Technology , 125-126*, 785-791.

Peng, X. Q., & Cao, J. (2005). A continuum mechanics-based non-orthogonal constitutive model for woven composite fabrics. *Composites: Part A , 36*, 859-874.

Poursartip, A., & Ferlund, G. (2010). Processing Science for Composite Structures Manufacturing. *SAMPE.*

R.Zheng, McCaffrey, N., Winch, K., Kennedy, P., & Yu, H. (1996). Predicting Warpage of Injection Moulded Fibre-Reinforced Plastics. *Journal of Thermoplastic Composite Materials , 9*, 90-106.

Radford, D., & Rennick, T. (2000). Separating Sources of Manufacturing Distortion in Laminated Composites. *Journal of Reinforced Plastics and Composites , 18*, 621-641.

Roy, R. J., Borazghi, H., & Benmokrane, B. (2005). Glass Fibre Reinforces Polypropylene Bridge Deck. *33rd Annual General Conference of the Canadian Society for Civil Engineering.* Toronto.

Russell, L. C. (2009). Anomalies, Influencing Factors, and Guidelines for DMA Testing of Fibre Reinforced Composites. *Polymer Composites , 30*, 962-969.

Saint-Gobain-Vetrotex. (2005). *Physical Properties for FEA Modeling of Twintex.* Saint-Gobain Vetrotex. Saint-Gobain Vetrotex.

Salomi, A., Garstka, T., Potter, K., Greco, A., & Maffezzoli, A. (2008). Spring-in angle as moulding distortion for thermoplastic matrix composite. *Composites Science and Technology , 68*, 3047-3054.

Shahkarami, A., & Vaziri, R. (2007). A continuum shell Finite element model for impact simulation of woven fabrics. *International Journal of Impact Engineering 34 , 34*, 104-119.

Shivakumar, G. S. (2009). A Re-examination of DMA Testing of Polymer Matrix Composites. *Journal of Reinforced Plastics and Composites , 28*, 979.

Sourabh, A. M. (2008). A thermo-mechanical viscoelastic analysis of orthotropic materials. *Composite Structures , 83*, 61-72.

Spencer, A. J., Watson, P., & Rogers, T. G. (1992). Thermoelastic Distortions in Laminated Anisotropic Tubes and Channel Sections. *Journal of Thermal Stresses , 15 no.1*, 129-141.

Spencer, A., Watson, P., & Rogers, T. (1991). Mathematical analysis of the springback effect in laminated thermoplastic channel sections. *Composites Manufacturing , 2 no.3*, 253-259.

Suemasu, H., Friedrich, K. F., & Hou, M. (1994). On Deformation of Woven Fabric-Reinforced Thermoplastic Composites During Stamp-Forming. *Composites Manufacturing , 5*, 31-39.

Sunderland, P., Yu, W., & Manson, J.-A. (2001). A Thermoviscoelastic Analysis of Process-Induced Internal Stresses in Thermoplastic Matrix Composites. *Polymer Composites , 22 no.5*, 579-592.

Tian, J., Yu, W. Y., & Zhou, C. (2007). Crystallization Behaviors of Linear and Long Chain Branched Polypropylene. *Journal of Applied Polymer Science , 104*, 3592–3600.

Trudel-Boucher, D., Fisa, B., Denault, J., & Gagnon, P. (2006). Experimental investigation of stamp forming of unconsolidated commingled E-glass/polypropylene fabrics. *Composites Science and Technology , 66*, 555-570.

Twigg, G., & Fernlund, G. (2003). An experimental method for quantifying tool–part shear interaction during composites processing. *Composites Science and Technology , 63*, 1985-2002.

Twigg, G., Poursartip, A., & Fernlund, G. (2001). Tool-Part Ineractions in Composites Processing. *SAMPE*.

Xue, P., & Cao, J. (2003). A non-orthogonal constitutive model for characterizing woven composites. *Composites: Part A , 34*, 183-193.

Zahlan, N., & O'Neill, J. M. (1989). Design and fabrication of composite components; the spring-forward phenomenon. *Composites , 20 no.1*, 77-82.